

Real-Time Estimation of Traffic Stream Density using Connected Vehicle Data

Mohammad Abdurraheem Aljamal

Dissertation submitted to the Faculty of the
Virginia Polytechnic Institute and State University
in partial fulfillment of the requirements for the degree of

Doctor of Philosophy
in
Civil Engineering

Hesham A. Rakha, Chair
Kevin Heaslip
Susan Hotel
Jianhe Du

08/25/2020

Blacksburg, Virginia

Keywords: Real-Time Estimation, Connected Vehicles, Traffic Density, Machine Learning, Kalman Filter, Particle Filter, Artificial Neural Network, Random Forest, k-Nearest

Neighbors, Level of Market Penetration Rate

Copyright ©2020, Mohammad Abdurraheem Aljamal

Real-Time Estimation of Traffic Stream Density using Connected Vehicle Data

Mohammad Abdurraheem Aljamal

(ABSTRACT)

The macroscopic measure of traffic stream density is crucial in advanced traffic management systems. However, measuring the traffic stream density in the field is difficult since it is a spatial measurement. In this dissertation, several estimation approaches are developed to estimate the traffic stream density on signalized approaches using connected vehicle (CV) data. First, the dissertation introduces a novel variable estimation interval that allows for higher estimation precision, as the updating time interval always contains a fixed number of CVs. After that, the dissertation develops model-driven approaches, such as a linear Kalman filter (KF), a linear adaptive KF (AKF), and a nonlinear Particle filter (PF), to estimate the traffic stream density using CV data only. The proposed model-driven approaches are evaluated using empirical and simulated data, the former of which were collected along a signalized approach in downtown Blacksburg, VA. Results indicate that density estimates produced by the linear KF approach are the most accurate. A sensitivity of the estimation approaches to various factors including the level of market penetration (LMP) of CVs, the initial conditions, the number of particles in the PF approach, traffic demand levels, traffic signal control methods, and vehicle length is presented. Results show that the accuracy of the density estimate increases as the LMP increases. The KF is the least sensitive to the initial traffic density estimate, while the PF is the most sensitive to the initial traffic density estimate. The results also demonstrate that the proposed estimation approaches work better at higher demand levels given that more CVs exist for the same LMP scenario. For traffic signal control methods, the results demonstrate a higher estimation accuracy for fixed traffic signal timings at low traffic demand levels, while the estimation accuracy is better when the adaptive phase split optimizer is activated for high traffic demand levels. The dissertation also investigates the sensitivity of the KF estimation approach to vehicle length,

demonstrating that the presence of longer vehicles (e.g. trucks) in the traffic link reduces the estimation accuracy. Data-driven approaches are also developed to estimate the traffic stream density, such as an artificial neural network (ANN), a k-nearest neighbor (k-NN), and a random forest (RF). The data-driven approaches also utilize solely CV data. Results demonstrate that the ANN approach outperforms the k-NN and RF approaches. Lastly, the dissertation compares the performance of the model-driven and the data-driven approaches, showing that the ANN approach produces the most accurate estimates. However, taking into consideration the computational time needed to train the ANN approach, the large amount of data needed, and the uncertainty in the performance when new traffic behaviors are observed (e.g., incidents), the use of the linear KF approach is highly recommended in the application of traffic density estimation due to its simplicity and applicability in the field.

Real-Time Estimation of Traffic Stream Density using Connected Vehicle Data

Mohammad Abdurraheem Aljamal

(GENERAL AUDIENCE ABSTRACT)

Estimating the number of vehicles (vehicle counts) on a road segment is crucial in advanced traffic management systems. However, measuring the number of vehicles on a road segment in the field is difficult because of the need for installing multiple detection sensors in that road segment. In this dissertation, several estimation approaches are developed to estimate the number of vehicles on signalized roadways using connected vehicle (CV) data. The CV is defined as the vehicle that can share its instantaneous location every time t . The dissertation develops model-driven approaches, such as a linear Kalman filter (KF), a linear adaptive KF (AKF), and a nonlinear Particle filter (PF), to estimate the number of vehicles using CV data only. The proposed model-driven approaches are evaluated using real and simulated data, the former of which were collected along a signalized roadway in downtown Blacksburg, VA. Results indicate that the number of vehicles produced by the linear KF approach is the most accurate. The results also show that the KF approach is the least sensitive approach to the initial conditions. Machine learning approaches are also developed to estimate the number of vehicles, such as an artificial neural network (ANN), a k-nearest neighbor (k-NN), and a random forest (RF). The machine learning approaches also use CV data only. Results demonstrate that the ANN approach outperforms the k-NN and RF approaches. Finally, the dissertation compares the performance of the model-driven and the machine learning approaches, showing that the ANN approach produces the most accurate estimates. However, taking into consideration the computational time needed to train the ANN approach, the huge amount of data needed, and the uncertainty in the performance when new traffic behaviors are observed (e.g., incidents), the use of the KF approach is highly recommended in the application of vehicle count estimation due to its simplicity and applicability in the field.

To my wonderful parents, Abdulraheem and Salwa

To my lovely wife, Lona

To my sweet daughter, Alma

To my future children

To my siblings

To my father- and mother-in-law

To my friends and colleagues

Acknowledgments

I would like to express my heartfelt gratitude to my advisor, Dr. Hesham Rakha, for giving me the opportunity to work with him. I will always remember his great advise, not only in the technical, but most importantly, his general advise, which has a great impact on my life. His continuous guidance and support make my doctoral research more valuable. I must admit that he has helped me to reach my childhood dream.

My thanks also go to my committee members: Dr. Kevin Heaslip, Dr. Susan Hotle, and Dr. Jianhe Du, for accepting to be in my doctoral committee and for their valuable feedback.

I would like also to thank my professors that taught me during my studies at Virginia Tech and Jordan University of Science and Technology. I would like also to acknowledge current and former CSM members especially Dr. Ihab El-Shawarby, Dr. Hossam Abdlghaffar, Dr. Huthaifa Ashqar, Dr. Ahmed Elbery, Dr. Mohammed Elhennawy, Dr. Mohammed Almanna, Maha Eloni, Dr. Abdallah Hassan, Asmaa Alazmi, and Dr. Karim Fadhloun.

Last but not least, I must thank the Urban Mobility and Equity Center (UMEC) and the MATS University Transportation Center for funding this research and allowing me to obtain my doctoral degree.

Contents

- List of Figures** **xiii**

- List of Tables** **xv**

- 1 Introduction** **1**
 - 1.1 Introduction 2
 - 1.2 Problem Statement 4
 - 1.3 Research Objectives 6
 - 1.3.1 Research Contributions 6
 - 1.3.2 Dissertation Layout 8

- 2 Literature Review** **11**
 - 2.1 Traffic State Estimation 12
 - 2.2 Vehicle Count Estimation 13
 - 2.2.1 Loop Detectors 14
 - 2.2.2 Video Detection System 15
 - 2.2.3 Fusion Data 16

| | | |
|----------|---|-----------|
| 2.3 | Traffic State Estimation via Machine Learning | 18 |
| 2.4 | Summary and Conclusions | 20 |
| 3 | Development of a Kalman Filter Approach on an Isolated Intersection | 21 |
| 3.1 | Introduction | 23 |
| 3.2 | Estimation Approach | 25 |
| 3.2.1 | Define the Estimation Interval Time | 25 |
| 3.2.2 | Estimation Approach Formulation | 26 |
| 3.2.3 | Define the LMP Rate (ρ) | 28 |
| 3.3 | Results and Discussion | 29 |
| 3.3.1 | Experimental Setup | 29 |
| 3.3.2 | Experimental Results | 31 |
| 3.3.2.1 | Variable vs. Fixed Estimation Time Interval | 32 |
| 3.3.2.2 | Fixed vs Optimized Green Traffic Signal Timing | 32 |
| 3.3.2.3 | Impact of Heavy Trucks | 34 |
| 3.4 | Summary and Conclusions | 36 |
| 4 | Development of an Adaptive Kalman and a Neural-Kalman Filtering Approaches | 38 |
| 4.1 | Introduction | 40 |
| 4.2 | Related Work | 41 |
| 4.3 | Development of Simulation Data | 45 |
| 4.4 | Estimation Approaches | 46 |

| | | |
|----------|---|-----------|
| 4.4.1 | Summary of the Developed KF Approach | 46 |
| 4.4.2 | Adaptive Kalman Filter (AKF) | 47 |
| 4.4.2.1 | Online Estimation of Noise Statistics | 49 |
| 4.4.3 | Artificial Neural Network | 50 |
| 4.4.3.1 | Characteristics of the ANN: Input and Output Variables | 51 |
| 4.5 | Results | 54 |
| 4.5.1 | Comparison of the KF and the AKF Approaches | 55 |
| 4.5.2 | Developed ANN Approach | 55 |
| 4.5.3 | Comparison of the AKF and the AKFNN Approaches | 59 |
| 4.5.4 | Impact of the Initial Conditions on the AKF Approach | 62 |
| 4.5.4.1 | Impact of Initial Estimate of the Vehicle Count (N_i) | 62 |
| 4.5.4.2 | Impact of Initial Mean Estimate of the State System (m_i) | 62 |
| 4.5.4.3 | Impact of Initial Prior Covariance Estimate of the State System (P_i) | 63 |
| 4.6 | Summary and Conclusions | 64 |
| 5 | Enhancement of the Kalman Filter Approach using a Bounded ρ in the State-Space Model | 67 |
| 5.1 | Introduction | 69 |
| 5.2 | Literature Review | 70 |
| 5.3 | Estimation Approach | 73 |
| 5.3.1 | Define the Estimation Interval Time | 73 |

| | | |
|----------|--|-----------|
| 5.3.2 | Formulation | 73 |
| 5.3.3 | Proposed Estimation Approaches | 79 |
| 5.3.3.1 | First Approach: CV Data Assuming Fixed LMP (ρ) | 79 |
| 5.3.3.2 | Second Approach: Fusion Data with Variable LMP (ρ) | 80 |
| 5.4 | Data Collection | 80 |
| 5.4.1 | Empirical Data | 81 |
| 5.4.2 | Simulation Data | 82 |
| 5.5 | Results and Discussion | 82 |
| 5.5.1 | Empirical Data | 83 |
| 5.5.1.1 | Sample Size Impact on KF Estimator Performance | 83 |
| 5.5.1.2 | Variable vs. Fixed Estimation Time Interval | 83 |
| 5.5.1.3 | Impact of Connected Vehicle LMPs | 86 |
| 5.5.1.4 | Impact of Fusing Connected Vehicle and Single Loop Detector Data | 88 |
| 5.5.2 | Simulation Data | 89 |
| 5.5.2.1 | Link Length and Traffic Demand Sensitivity Analysis | 89 |
| 5.5.2.2 | Connected Vehicle Impact on KF Estimator Performance using Fixed ρ Values | 91 |
| 5.5.2.3 | Fusion Data Impact on KF Performance using Variable ρ Values | 93 |
| 5.6 | Summary and Conclusions | 93 |
| 6 | Development of a Particle Filter Approach | 95 |

| | | |
|----------|---|------------|
| 6.1 | Introduction | 97 |
| 6.2 | Problem Formulation and Estimation Approaches | 101 |
| 6.2.1 | State-Space Model | 101 |
| 6.2.2 | Estimation Approaches | 103 |
| 6.2.2.1 | The PF Approach | 104 |
| 6.2.2.2 | The KF Approach | 105 |
| 6.2.2.3 | The AKF Approach | 106 |
| 6.3 | Results and Discussion | 108 |
| 6.3.1 | Performance of Estimation Approaches | 108 |
| 6.3.2 | Impact of Initial Conditions | 112 |
| 6.4 | Summary and Conclusions | 116 |
| 7 | Development of Data-Driven Approaches | 118 |
| 7.1 | Introduction | 120 |
| 7.1.1 | Model-Driven Estimation Approaches | 121 |
| 7.1.2 | Data-Driven Approaches | 122 |
| 7.2 | Development of Simulation Data | 123 |
| 7.2.1 | Generation of the Training Data Set | 124 |
| 7.3 | Methodology | 125 |
| 7.3.1 | First Approach: Model-Driven Approaches | 125 |
| 7.3.1.1 | The KF Approach | 126 |
| 7.3.1.2 | The AKF Approach | 127 |

| | | |
|----------|--|------------|
| 7.3.1.3 | The PF Approach | 128 |
| 7.3.2 | Second Approach: Integrating Data-Driven and Model-Driven Approaches | 129 |
| 7.3.2.1 | ANN Approach | 130 |
| 7.3.3 | Third Approach: Data-Driven Approaches | 132 |
| 7.3.3.1 | ANN Approach | 132 |
| 7.3.3.2 | k-NN Approach | 132 |
| 7.3.3.3 | RF Approach | 133 |
| 7.4 | Results and Discussion | 133 |
| 7.4.1 | First Research Approach | 133 |
| 7.4.2 | Second Research Approach | 134 |
| 7.4.3 | Third Research Approach | 136 |
| 7.5 | Summary and Conclusions | 137 |
| 8 | Summary and Conclusions | 140 |
| 8.1 | Summary and Conclusions | 141 |
| 8.2 | Recommendations for Future Work | 143 |
| | Bibliography | 145 |

List of Figures

| | | |
|-----|--|----|
| 3.1 | Actual LMP variations along the estimation steps. | 29 |
| 3.2 | Simulated intersection. | 30 |
| 3.3 | Four phasing scheme. | 31 |
| 4.1 | Tested link. | 51 |
| 4.2 | Flowchart for adaptive Kalman filter with a neural network (AKFNN) approach. | 54 |
| 4.3 | Error histogram for the training, validation, and testing data set. | 57 |
| 4.4 | Actual and estimated values of ρ_{out} for different level of market penetration (LMP) scenarios: (a) 10%, (b) 20%, (c) 30%, (d) 40%, (e) 50%, (f) 60%, (g) 70%, (h) 80%, and (i) 90% LMP. | 58 |
| 4.5 | Actual and estimated vehicle counts over estimation intervals for different LMP scenarios: (a) 10%, (b) 20%, (c) 30%, (d) 40%, (e) 50%, (f) 60%, (g) 70%, (h) 80%, and (i) 90% LMP. | 61 |
| 4.6 | Impact of the initial conditions on the AKF approach: (a) Initial estimate values N_i , (b) Initial mean estimate values m_i , and (c) Initial covariance estimate values P_i | 63 |
| 5.1 | Impact of applying a lower bound in the state equation estimates. | 77 |

| | | |
|-----|--|-----|
| 5.2 | Variation in actual LMP over all the estimation intervals. | 80 |
| 5.3 | Tested link in downtown Blacksburg, VA. (source: Google Maps) | 81 |
| 5.4 | Impact of sample size on the average time interval. | 86 |
| 5.5 | Actual and estimated vehicle counts using real data at different LMP scenarios: (a) 10%, (b) 20%, (c) 30%, (d) 40%, (e) 50%, (f) 60%, (g) 70%, (h) 80%, and (i) 90%. | 87 |
| 5.6 | Actual and estimated vehicle counts using simulated data at different LMP scenarios: (a) 10%, (b) 20%, (c) 30%, (d) 40%, (e) 50%, (f) 60%, (g) 70%, (h) 80%, and (i) 90%. | 92 |
| 6.1 | Tested link section includes connected vehicles (CVs) and non-CVs. | 102 |
| 6.2 | Actual and estimated vehicle counts at different LMP scenarios: (a) 10%, (b) 20%, (c) 30%, (d) 40%, (e) 50%, (f) 60%, (g) 70%, (h) 80% and (i) 90%. | 111 |
| 6.3 | RRMSE values using various initial vehicle count estimates at different LMP scenarios: (a) 10%, (b) 20%, (c) 30%, (d) 40%, (e) 50%, (f) 60%, (g) 70%, (h) 80% and (i) 90%. | 115 |
| 7.1 | Tested link section in downtown Blacksburg, VA. | 124 |
| 7.2 | Estimating the ρ_{in} and ρ_{out} variables. | 131 |
| 7.3 | Estimating the vehicle counts (N_T) on the tested link. | 132 |

List of Tables

| | | |
|-----|--|----|
| 2.1 | Summary of related studies for vehicle count estimation. | 18 |
| 3.1 | Origin destination demand matrix. | 30 |
| 3.2 | EB RRMSE of fixed and variable estimation time interval. | 33 |
| 3.3 | EB RRMSE and RMSE using fixed and phase split plans. | 34 |
| 3.4 | WB RRMSE and RMSE using fixed and phase split plans. | 34 |
| 3.5 | NB RRMSE and RMSE using fixed and phase split plans. | 35 |
| 3.6 | SB RRMSE and RMSE for fixed and phase split plans. | 35 |
| 3.7 | RRMSE in scenarios with no trucks, 5%, and 10% trucks. | 36 |
| 4.1 | Definition of the ANN approach inputs. | 53 |
| 4.2 | Root mean square error (RMSE) values using the Kalman filter (KF) and the adaptive Kalman filter (AKF) approaches. | 56 |
| 4.3 | Developed artificial neural network (ANN) model performance measures for the training, validation, and testing data set. | 56 |
| 4.4 | RMSE values using the AKF and the AKFNN approaches. | 60 |

| | | |
|------|--|-----|
| 4.5 | Impact of applying the trial-and-error technique for the initial value of covariance P_i | 64 |
| 4.6 | RMSE values for the KF, the AKF, the AKFNN, and the tuned AKFNN approaches. | 65 |
| 5.1 | Vehicle count estimation values of using Equations (5.9) and (5.15). | 78 |
| 5.2 | RRMSE values using different (ρ_{min}) values in Equation (5.15). | 78 |
| 5.3 | RRMSE values for 10 different sample sizes for different LMPs. | 84 |
| 5.4 | RRMSE values using variable and fixed estimation interval time periods. | 85 |
| 5.5 | Estimation time interval for different LMPs. | 85 |
| 5.6 | RRMSE and RMSE values for nine scenarios using various LMPs for real data. | 87 |
| 5.7 | RRMSE values using one-loop detector in different locations (entrance, middle, and exit). | 88 |
| 5.8 | RRMSE values under different link lengths. | 89 |
| 5.9 | RRMSE and RMSE values for different v/c ratios. | 90 |
| 5.10 | RRMSE and RMSE values for various LMPs. | 92 |
| 5.11 | RRMSE values using one-loop detector in different locations (entrance, middle, and exit). | 93 |
| 6.1 | Initial conditions for the KF, AKF, and PF approaches. | 109 |
| 6.2 | RRMSE of KF, AKF, and PF approaches for different LMPs. | 110 |
| 6.3 | RRMSE values for the KF, AKF, and PF approaches using different initial vehicle count estimates (i.e., 0, 5, and 10) for different LMPs. | 113 |

| | | |
|-----|--|-----|
| 6.4 | RRMSE values for the KF, AKF, and PF approaches using different initial vehicle count estimates (i.e., 15, 20, and 25) for different LMPs. | 114 |
| 6.5 | RRMSE values using different number of particles in the PF for different LMPs. | 116 |
| 7.1 | RRMSE and RMSE values of KF, AKF, and PF approaches for different LMPs. | 134 |
| 7.2 | RRMSE of ρ_{in} and ρ_{out} at different LMPs. | 135 |
| 7.3 | RRMSE of KF and KFNN approaches at different LMPs. | 136 |
| 7.4 | RRMSE of k-NN approach using different k values. | 137 |
| 7.5 | RRMSE and RMSE values using data-driven approaches. | 138 |
| 7.6 | RRMSE and RMSE values using model- and data-driven approaches. | 139 |

Preface

The co-authors of the chapters presented in this dissertation work at the Virginia Polytechnic Institute and State University, Blacksburg, VA. Hesham A. Rakha is the Samuel Reynolds Pritchard Professor of Engineering in the Chalres Via, Jr. Dept. of Civil & Environmental Engineering, a Courtesy Professor in the Bradley Dept. of Electrical and Computer Engineering at Virginia Tech, and the director of the Center for Sustainable Mobility (CSM) at the Virginia Tech Transportation Institute. He was involved in concept formation and contributed to paper edits as the primary advisor and committee chair. Dr. Rakha provided extensive guidance toward all the chapters of this dissertation and advice on the research.

Hossam Abdelghaffar is a postdoctoral researcher in CSM at the Virginia Tech Transportation Institute. He was listed as a co-author on the papers presented in chapters 3, 4, 5, and 6 as he provided feedback related to the control theory when developing the filtering techniques. I was responsible for all major work of concept formulation, coding, and data analysis, as well as paper composition.

Mohammed Farag is a research scholar in CSM at the Virginia Tech Transportation Institute. He was listed as a co-author on the paper presented in Chapter 7 because of his involvement on the data analytics effort and the coding of the algorithms.

Chapter 1

Introduction

The first chapter provides an introduction to the research described in the dissertation followed by defining the research problem statement. After that, the dissertation objectives and contributions are clearly presented. Lastly, the layout of the dissertation is provided.

1.1 Introduction

The number of on-road vehicles has increased rapidly over the past few decades. For example, in the U.S. alone, the number of motor vehicles registered from 1990 to 2016 increased by more than 75 million vehicles [1], leading to serious traffic congestion in many areas. Furthermore, the cost of traffic congestion has raised from 24 billion in 1982 to 115 billion in 2009, according to the 2015 Urban Mobility Report [2]. Traffic congestion is one of the most critical challenges compromising the efficiency of the transportation system. One potential approach of mitigating traffic congestion is expanding the current infrastructure by adding new lanes and roadways to accommodate growing traffic demands; however, this comes with significant associated costs and space challenges. A more efficient way of solving traffic congestion is improving traffic management strategies by using advanced technologies and algorithms. Among the more recent technologies utilized for traffic management are Intelligent Transportation Systems (ITSs). ITS applications are developed to enhance transportation system efficiency, mobility, and reduce environmental impacts [3]. In general, ITS aims at improving the infrastructure side of technology via sensors, communication, controllers, etc. Advance Traffic management Systems (ATMSs) constitute one ITS approach. ATMSs include advanced traffic signal timings in real-time [4, 5, 6, 7]. Adaptive traffic signal controllers require real-time traffic state estimation to improve intersection performance, as the real-time estimation plays a major role in capturing variations in traffic behavior (e.g., non-recurrent changes).

Traffic congestion is represented by traffic density. Traffic density is defined as the number of vehicles on a given roadway segment divided by the length of the segment [8]. Traffic density is also known as vehicle counts. Estimating the traffic density in freeways and arterial segments can improve the performance of adaptive traffic controllers by mitigating traffic congestion. For instance in the case of freeways, identifying bottleneck locations in early stages mitigates traffic congestion by informing drivers to find a new route. For signalized arterial segments, the traffic density measures are crucial for either traffic signal performance

[9, 10, 11], or signal optimization to develop traffic signal parameters such as cycle length, phase sequence, and phase split [12, 13, 14, 15, 16]. Hence, the traffic density measures must be precisely estimated to represent traffic demands at each intersection approach. Once accurate measurements are obtained, efficient adaptive traffic signal controllers can be developed. However, determining traffic density is not a trivial task and cannot be directly measured in the field since it is a spatial measurement. Consequently, traffic stream density is typically based on estimations. Hence, this dissertation introduces novel estimation approaches to estimate the traffic stream density along signalized links.

Signalized intersections are controlled by traffic signals to regulate traffic flow and mitigate traffic congestion. Traffic signal control systems can be categorized into fixed-timed control, actuated control (partially or fully), responsive control, or adaptive control [8]. Traffic signal controllers deploy optimization algorithms to reduce the intersection delay, queue lengths, and fuel consumption and emission levels. Optimization algorithms are utilized to determine traffic signal parameters, including the cycle length, phase sequence, phase split and offset [17]. Emerging technologies, such as connected vehicle (CV) technology, are introduced to make improvements in the roadway transportation system [18, 19]. These such improvements are resulted from exploiting the CV features of providing real-time information which can assist drivers in avoiding congestion and reducing vehicle stops. The CV is defined as the vehicle that can exchange information with other vehicles. This is generally referred to vehicle-to-vehicle, or V2V, communication. The CV can also exchange information with road infrastructure, which is referred to as vehicle-to-infrastructure, or V2I, communication. CVs can provide and share their real-time locations and speeds. Consequently, CV data can be provided to traffic signal controllers to enhance the intersection efficiency and mobility by developing adaptive traffic signal control systems that optimize traffic signal timings in real-time.

Real-time traffic state estimation has received increased attention with the introduction of CV technology. Adaptive traffic signal controllers require real-time traffic state estimation to improve intersection performance, as the real-time estimation plays a major role in capturing

variations in traffic behavior. Nowadays, conducting research with limited CV data is a challenge, especially when no additional data sources are provided. Past research has utilized CV data in conjunction with existing fixed detection techniques with the aim of achieving better accuracy than using only one source of data, given that fixed detection techniques (e.g., loop detectors) are subject to detection failures and thus always produce errors in their data [20, 21, 22]. Several benefits of using CV vehicle data have been recognized. For instance, the high quality of data compared with fixed detection techniques, and the data availability at any location inside the network, thus offering a clear picture about traffic behavior at any time. Therefore, transportation agencies are putting effort into facilitating the use of CV data.

1.2 Problem Statement

Vehicle count estimates along traffic roadways can be measured using video detection system, but this is difficult to obtain due to the high cost of the infrastructure, limited visibility, and image processing [23]. Time-occupancy measurements from loop detectors are used as an alternative data source to estimate the vehicle counts [24]. However, the time-occupancy measurements from loop detector represent a temporal estimate of the vehicle counts around the detection location. A recent study introduced a relationship between time-occupancy and space-occupancy to estimate the vehicle counts by dividing the roadway link into small segments and installing detectors on all of the small segments [25], but the installation cost is high. Papageorgiou et al. [26] derived a relationship between the time-occupancy and space-occupancy, considering the case of homogeneous traffic in uninterrupted traffic conditions. They claimed that the loop detector location influences the space-occupancy estimation, which can significantly affect the vehicle count estimation accuracy. A more common way of estimating the vehicle count is the use of the traffic flow continuity equation (input-output approach), which considers two traffic counting stations, one at the entrance and the other at the end of the roadway link [27]. Equation (1.1) presents the traffic flow continuity equation.

$$N(t) = N(t - \Delta t) + \Delta t [q_t^{in}(t) - q_t^{out}(t)] \quad (1.1)$$

Where $N(t)$ is the number of vehicles traversing the link at time (t) , $N(t - \Delta t)$ is the number of vehicles traversing the link in the previous interval, Δt is the duration of the updating time interval, q_t^{in} and q_t^{out} are the total flows entering and exiting the link between $(t - \Delta t)$ and (t) , respectively. These total flows can be measured using fixed sensors (i.g., loop detectors). However, Previous research has demonstrated that fixed sensors are subject to detection failures and thus they always produce errors in their data [23, 28, 29]. Consequently, the integral of the flow continuity equation results in an accumulation of error that requires fixing. Literature has been widely used a state-space model to tackle this accumulation of error. The state-space model is comprised of two systems: (a) a state and (b) a measurement system. The state system describes how the system behaves and provides a prior knowledge of the estimation. The measurement system is used to help correct and improve the prior estimation.

Different statistical approaches have been used to solve the state-space models such as the Kalman filter (KF) [30] and the Particle filter (PF) [31]. The KF is categorized as a linear approach, which assumes linear system transitions with a Gaussian distribution for the probability density function (PDF) of the system and measurement noise. In contrast, the PF is defined as a nonlinear approach, which deals with nonlinear system transitions without the assumption of the PDF noise distribution [31, 32].

Past research has used different data sources, such as stationary sensors (e.g., loop detectors) [23, 33, 34, 35, 36, 37, 38] or fusion data [20, 21, 39, 40, 41] (combining two different sources of data) to estimate the number of vehicles along traffic roadways using state-space models. Stationary sensors' data have been utilized to accurately estimate the vehicle counts. However, stationary sensors suffer from poor detection accuracy and have high installation and maintenance costs [28, 29, 42]. Recently, fusion data have been widely used to estimate the number of vehicles along certain roadway section, with the aim of achieving better es-

timation accuracy than using only one source of data. However, fusion data require more computational cost in both time and memory as the data include both trivial (data that are not needed) and nontrivial (data that are needed) information. The research described in this dissertation proposes several estimation approaches using CV data. Moreover, the dissertation presents the estimation approaches' performance considering two sources of data: (1) CVs, and (2) fusing single stationary sensor and CVs data.

1.3 Research Objectives

The proposed estimation approaches in this dissertation will provide key inputs to real-time traffic signal controllers, leading to improved intersection performance as a result of reduced traffic delays, vehicle emissions, and vehicle crashes. The specific research objectives are to:

1. Develop novel estimation approaches based on model-driven and data-driven techniques to provide real-time estimates of the traffic stream density along signalized links. The developed estimation approaches rely on CV data which can allow transportation agencies to save some installation and maintenance costs.
2. Develop a novel approach of estimating the level of market penetration (LMP) rate of CVs to reflect the total vehicle counts.
3. Test the sensitivity of the proposed estimation approaches to several factors, including the LMP of CVs, the level of traffic congestion, link length, vehicle length, and traffic signal control methods.

1.3.1 Research Contributions

This dissertation makes many significant contributions to the literature. These contributions include novel methods using statistical and machine learning techniques to provide real-time estimates of the traffic stream density along signalized links. Specifically, the contributions of this research effort can be summarized as follows:

1. Past research used a fixed estimation time interval (e.g., 20 s). However, using a fixed estimation period might lead to inaccurate estimation, especially at low LMPs. For example, if the link's LMP is 10%, the number of CVs will obviously be low. If we treat the problem using a fixed estimation interval, then the probability of observing zero CVs within an interval will be high for short estimation interval durations, making the estimation inefficient and inaccurate. Accordingly, low LMPs require long intervals (e.g., 300 s) to ensure that at least one CV is on the link. In contrast, links with high LMPs can use short estimation intervals (e.g., 20 s). One of the major contributions of this research is to address this issue to produce an efficient and convenient way of determining the duration of the estimation period. In this dissertation, the estimation time interval is defined as the point at which exactly a pre-defined sample size (n) of CVs traversed the tested link.
2. A linear KF approach is developed to estimate the vehicle counts. The proposed KF approach relies only on CV data. Different CV LMPs were also tested (ranging from 10% to 90% in increments of 10%). Furthermore, the KF estimation accuracy is also examined when adding a single loop detector, and a sensitivity analysis is made in terms of the optimum location of the stationary sensor.
3. The developed KF approach is utilized with predefined error values of the state and the measurement noise; these error values remain constant for the entire simulation. An adaptive KF (AKF) approach is developed to dynamically estimate the error values in the state and measurement estimates. The AKF approach also relies on CV data only.
4. An artificial neural network (ANN) approach is developed to provide real-time estimates of the LMP values for the CVs to reflect the total number of vehicles. In addition, a novel estimation approach; named AKFNN, is introduced to estimate the vehicle counts by integrating the AKF approach with the ANN approach.
5. A nonlinear PF approach is developed to estimate the vehicle counts. The proposed PF approach relies only on CV data. A comparison of the PF, KF, and AKF approaches

is made and some recommendations are proposed.

6. Data-driven approaches are developed to estimate the vehicle counts using solely CV data. In addition, a comparison of KF, AKF, PF, and the developed data-driven approaches is presented and some recommendations are made.
7. The dissertation investigates the sensitivity of the proposed estimation approaches to different factors including the length of the link approach, level of traffic congestion, LMP of CVs, vehicle length by introducing trucks into the traffic stream, traffic signal control methods (a fixed-time plan and an adaptive phase split optimizer), and initial conditions.

1.3.2 Dissertation Layout

After the introduction chapter, which describes the problem statement and dissertation objectives, an extensive review of the literature relevant to topics covered in the dissertation is presented in Chapter 2. Next, Chapter 3 discusses the development of the KF approach for an isolated signalized intersection. Chapter 4 illustrates the development of the AKF, ANN, and AKFNN approaches. Chapter 5 introduces a new strategy for enhancing the developed KF approach in Chapter 3. Thereafter, Chapter 6 presents the development of the nonlinear PF approach and compares the PF with the KF and AKF approaches. Chapter 7 develops data-driven approaches to estimate the vehicle counts and then compare the performance of the data-driven approaches with the model-driven approaches. Finally, Chapter 8 presents a summary of the dissertation conclusions and recommended future work.

The main contents of this dissertation have been published or are still under review in the listed journals and/or conferences as indicated below.

Journal Publications

1. **Mohammad A. Aljamal**, Hossam Abdelghaffar, and Hesham A. Rakha (2019), “Developing a Neural- Kalman Filtering Approach for Estimating Traffic Stream Density Using Probe Vehicle Data,” *Sensors*, volume 19, p.4325.
2. **Mohammad A. Aljamal**, Hossam Abdelghaffar, and Hesham A. Rakha (2020), “Real-Time Estimation of Vehicle Counts on Signalized Intersection Approaches Using Probe Vehicle Data,” *IEEE Transactions on Intelligent Transportation Systems*.
3. **Mohammad A. Aljamal**, Hossam Abdelghaffar, and Hesham A. Rakha (2020), “Estimation of Traffic Stream Density using Connected Vehicle Data: Linear and Nonlinear Filtering Approaches,” *Sensors*, volume 20, p.4066.
4. **Mohammad A. Aljamal**, Mohamed Farag, and Hesham A. Rakha (2020), “Developing Data-Driven Approaches for Traffic Density Estimation using Connected Vehicle Data,” in review, *IEEE Access*.

Conference Publications

1. **Mohammad A. Aljamal**, Hossam Abdelghaffar, and Hesham Rakha (2019), “Kalman Filter-based Vehicle Count Estimation Approach Using Probe Data: A Multi-lane Road Case Study,” in the *22nd International IEEE Conference on Intelligent Transportation Systems*, Auckland, New Zealand, pp. 4374-4379.
2. **Mohammad A. Aljamal**, Hossam Abdelghaffar, and Hesham Rakha (2020), “A Neural-Kalman Filtering Approach for Vehicle Count Estimates on Signalized Roadways Using Probe Vehicle Data,” in the *99th Annual Meeting Transportation Research Board*, Washington D.C.

3. **Mohammad A. Aljamal**, Hossam Abdelghaffar, and Hesham Rakha (2020), “Traffic Density Estimation via a Particle Filter using Connected Vehicle Data,” in review, *100th Annual Meeting Transportation Research Board*, Washington D.C.

Chapter 2

Literature Review

To further determine the significant of this dissertation and the proposed estimation approaches, this chapter is divided into three sections that cover the research objectives: 1) Traffic state estimation, 2) Vehicle count estimation, and 3) Traffic state estimation via machine learning.

2.1 Traffic State Estimation

Traffic state estimation refers to the process of inference of traffic state variables (i.e., density, speed, travel time, etc.) on traffic roadways, using a series of measurements that observed over a period of time. The estimates tend to be more accurate than the estimates from the observations by itself. It should be noted that traffic state estimation is crucial for traffic surveillance and control. Traffic measurements, that obtained from traffic stationary sensors, are not observed in every location and they always have errors. Hence, traffic estimation is introduced to provide traffic controllers with crucial traffic variables and thus improve the performance of traffic controllers. Furthermore, traffic estimation is performed to deal with noisy data.

Researchers have used different estimation techniques to estimate different traffic state variables on arterial roads and freeways, such as the Kalman filter (KF) [30], Bayesian statistics [43, 44], and Particle filter (PF) [23, 45, 46]. In some previous studies, the traffic state system has been treated as a linear system. Other studies have considered the system as nonlinear [46, 47, 48, 49]. For linear system models, a KF has been widely deployed to produce accurate estimates [20, 23, 42, 50] due to its simplicity and applicability in the field. The KF assumes linear system transitions with a Gaussian distribution for the probability density function (PDF) of the system and measurement noise. For nonlinear system models, an extended KF (EKF) has been utilized in estimation [47, 51, 52]. The EKF also assumes that the PDF distribution is Gaussian. The EKF is derived by linearizing the system using a Taylor series expansion by calculating the Jacobian expression. However, it was found that the use of the EKF approach is only valid if the system is near linearity during the updating time [53], and thus large errors may result from linearization. In addition, the task of deriving the Jacobian matrices may cause implementation difficulties [54]. A more robust nonlinear approach is a PF, which has been frequently employed in the literature to handle nonlinear dynamic problems [41, 48, 55]. The PF approach is a Monte Carlo sequential solution which deals with nonlinear system transitions without the assumption of the PDF

noise distribution [31, 32].

Several researchers have used the KF and PF techniques to enhance estimates in various transportation applications, such as speed [47, 56, 57, 58], travel time [46, 55, 59, 60, 61], and traffic flow [47, 48, 49, 62, 63]. An unscented KF deployed for speed estimation using single loop detectors with a nonlinear state-space equation to improve the speed estimates [56]. Another study employed a linear KF technique to estimate speed, relying on the relationship between the flow-occupancy ratio and vehicle speed [57], yielding acceptable speed estimates for congested traffic conditions. A cumulative travel-time responsive (CTR) real-time intersection control within a CV environment was also developed using the KF technique [60]. In that study, the authors recommended having at least 30% level of market penetration (LMP) rates in order to realize the CTR algorithm's benefits. Mihaylova et al. [48] proposed a robust PF approach to estimate the traffic flow and speed measurements. In another study, Mihaylova et al. [49] developed two nonlinear approaches, an unscented KF and a PF, to produce real-time traffic flow estimates in a freeway network using data from stationary sensors. Chen et al. [55] proposed a time series speed equation to estimate traffic speed. They claimed that the traffic system is nonlinear and thus presented two nonlinear approaches: (1) a PF, and (2) an ensemble KF. Another study developed a PF estimation approach for travel time predictions using real-time and historical data [46]. In addition, a comparison between the PF, KF, and k-nearest neighbor (k-NN) estimators found that the PF and the KF outperformed the k-NN. In summary, the existing literature showed the benefits of using the KF and the PF techniques to reduce errors and address different aspects of the traffic state estimation problem. Accordingly, the KF and the PF techniques were adopted in this dissertation.

2.2 Vehicle Count Estimation

Numerous studies have addressed the research problem using different traffic data sources to achieve the vehicle count estimation. Such sources have included loop detectors [23, 33, 34], camera systems [35, 64], or fusion data [20, 21, 39, 40, 65]. The following subsections present

and discuss the past works have done using different traffic data sources.

2.2.1 Loop Detectors

Loop detectors have been extensively used to collect traffic data. The loop detectors can be installed under/on the surface of traffic roadways to gather data for every vehicle. However, the loop detector system suffers from detection accuracy due to malfunctioning problems. In addition, it suffers from limited coverage since it can only provide data around the detector's location. Furthermore, they provide limited information as they cannot observe some important data such as vehicle type and vehicle length. Last not least, their capital and operation costs are expensive.

In the application of vehicle count estimation, Ghosh and Knoop [33] demonstrated that vehicle counts can be improved by dividing the roadway into small segments (half-mile) to produce an efficient estimation. They also demonstrated that the KF can be effectively applied for estimation of traffic variables, using a 5 s estimation interval time. Another study used traffic flow and occupancy data from two conventional loop detectors to estimate the number of vehicles traveling along a specific road segment using the flow continuity equation [34]. In that study, the KF was deployed to obtain accurate estimates every 5 s interval time. Vigos et al. [23] developed a robust algorithm that requires at least three loop detectors on a roadway segment in order to estimate the number of vehicles every 20 s interval time. In that study, two loop detectors, at the entrance and the exit, were deployed to derive the state equation using the flow continuity equation, while the third loop detector was installed in the middle of the link to derive the measurement equation from the relationship of the detector time-occupancy and space-occupancy. However, the cost of implementing such algorithms in the field is high. For example, imagine that the estimation is required for a city like New York, which has almost 12,460 signalized intersections. If each intersection has four approaches, it would be necessary to install 150,000 detectors in order to make a proper estimate, which is an unreasonable proposition. Another study employed the KF to

estimate the number of vehicles on multi-section freeways. The state equation was derived from the flow continuity equation, while the measurement equation was derived from the hydrodynamic relationship between traffic speed and density [66]. Two loop detectors were used in addition to speed sensors in the middle of the tested section. However, the proposed algorithm is hard to employ in the field due to the high cost of implementation.

2.2.2 Video Detection System

A video record, another fixed detection technique, has been widely used to collect traffic data, especially at traffic signals for detecting the presence of vehicles. This system is a cost-effective alternative for traditional loop detectors. However, the video system also suffers from detection failures due to different reasons such as a stability problem due to wind gusts, an occlusion problem, and a night vision problem.

The video detection system was used to estimate the number of vehicles for traffic roadways [64]. Bhourri et al. [35] proposed a scalar KF in order to estimate the number of vehicles on an on-ramp section, using both loop detectors and a recorded film to observe the real density measurements, utilizing the equation of conservation of cars as a state equation. Another study deployed video data, collected at the entrance and the exit of the roadway segment, to estimate the traffic density [67]. In that study, the authors used the space-mean speed rather than the traffic flow in the state equation due to high errors accompanied with sensor failures. Their argument takes into account that the space-mean speed is taken as an average quantity while the traffic flow is a cumulative quantity. They derived the KF state equation from the traffic flow continuity equation, they also demonstrated the importance of having knowledge about the system noise characteristics to improve the performance of the KF model. Padiath et al. [68] tested, different traffic density estimation techniques that used with homogeneous traffic conditions, to evaluate the heterogeneous traffic conditions using the Indian traffic scenario. They compared three different techniques: a historic technique, an artificial neural network (ANN) based technique, and a KF technique. Video data, at the

entrance and exit of the selected traffic link, were utilized to evaluate the three estimation techniques. Results showed that the ANN technique outperformed the KF and historic techniques; however, it should be noted that the ANN and historic techniques needed data from the previous four days in order to build the estimation models, which is not the case in the KF model. Another study proposed a new video analysis method for estimating the number of vehicles [38]. An adaptive background subtraction and KF were employed for road/vehicle detection and tracking, respectively. The KF is represented by two-state equations based on the constant-velocity motion model.

The aforementioned detection techniques (loop detectors and video system) suffer from poor detection accuracy and are not cost-effective due to high installation and maintenance costs. More accurate data, such as data collected using the advanced technologies, (i.e., CV data) are needed. In the next section, related works that used fusion data are presented.

2.2.3 Fusion Data

Fusion data are defined when two different source of data are used. Recently, data fusion has been widely used to estimate the number of vehicles along certain roadway sections, with the aim of achieving better accuracy than using only one source of data. In many of the works using data fusion, the KF technique was employed for estimating traffic density. One study achieved accurate estimated traffic density results using the traffic flow values measured from a video detection system and the travel time obtained from CVs [20]. The study proposed another way of estimating traffic density using the space-mean speed and flow measurements that obtained from fixed sensors only. They found that fusion data enhance the estimation accuracy. The developed KF approach in this dissertation is similar to that work in some aspects, but differs in two significant ways, namely: only CV data are used and furthermore the updating time interval is considered as a variable rather than a fixed value (the updating time interval was 1 minute in [20]). Another study used data fusion to estimate the number of vehicles along an on-ramp segment [39]. They used traffic flow data from loop detectors

and aggregated speeds from floating cars, the latter provided by Google, and set a 300 s fixed updating interval. In that study, the system state equation was derived from the traffic flow continuity equation, while the measurement equation was based on the hydrodynamic relationship between the macroscopic traffic stream parameters (flow, density, and space-mean speed). Anand et al. [21] used video and CV data to estimate the number of vehicles along a roadway segment. In that study, video captured the traffic flow at the segment's entrance and exit points, while CV data provided travel time measurements. Another study used loop detectors and CV data to estimate freeway traffic density [40], relying on IntelliDrive technology (vehicle infrastructure integration) at a predefined updating time interval.

A recent study utilized CVs and cameras to estimate traffic density in a 500 m highway segment. The model developments were based on the assumption that the average speed of CVs is approximately equal the average speed of traditional vehicles [69]. In that study, a KF model was developed under the consideration of having a linear parameter-varying system with known parameters. The state equation was based on the traffic flow continuity equation, while the measurement equation was based on the average speed of CVs. Di et al. [70] used two loop detectors in addition to CV data to estimate traffic density at signalized link. Their traffic model was treated as a nonlinear and thus the Extended KF was developed. A study addressed the research problem using mobile sensors and loop detectors data [71], showing that the estimation accuracy using fusion data outperformed the loop detectors data. Another study has utilized fused loop and CV measurements to estimate the traffic density in a freeway section [41]. In that study, the authors derived the estimation model using the PF estimation approach, considering two sources of measurements: (1) loop detectors, and (2) fusing loop detectors and CVs. They obtained a 30% reduction in the mean absolute percentage error from the fused measurements compared to the measurements from loop detectors, demonstrating that more data sources produce more-accurate outcomes. However, the use of different data sources requires more computational cost in both time and memory as the data include both trivial (data that are not needed) and nontrivial (data that are needed) information. Table 2.1 summarizes the related studies that deployed the

KF and PF as an estimation model.

Table 2.1: Summary of related studies for vehicle count estimation.

| Study Reference | Data | Estimation Interval Time | Tested Section |
|-----------------|--|--------------------------|-----------------|
| [33] | Four detectors (traffic flow and speed) | Fixed (5 s) | Tunnel |
| [34] | Two detectors (traffic flow and occupancy) | Fixed (5 s) | Freeway |
| [23] | Three detectors (traffic flow and occupancy) | Fixed (20 s) | Signalized link |
| [66] | Three detectors (traffic flow) and two speed sensors | Fixed | Freeway |
| [35] | Six detectors (traffic flow and occupancy) | Fixed (5 s) | Freeway |
| [67] | Two cameras (traffic flow and speed) | Fixed | Freeway |
| [68] | Two cameras (traffic flow and speed) | Fixed | Freeway |
| [38] | Multiple cameras | Fixed | Freeway |
| [20] | Video system (flow and speed) and CVs (TT) | Fixed (60 s) | N/A |
| [21] | Video system (flow) and CVs (TT) | Fixed (300 s) | N/A |
| [39] | Loop detector (flow) and CVs (speed) | Fixed (60 s) | Freeway |
| [40] | Loop detector (flow) and CVs (speed & position) | Fixed (20 s) | Freeway |
| [69] | Video system (flow) and CVs (speed) | Fixed | Freeway |
| [70] | Loop detector (flow) and CVs (speed) | Fixed | Signalized link |
| [71] | Loop detector (flow) and CVs (speed & position) | Fixed | Freeway |
| [41] | Loop detector (flow) and CVs (speed) | Fixed | Freeway |

2.3 Traffic State Estimation via Machine Learning

Machine learning has proven its ability to provide accurate estimates for different traffic state variables [72, 73, 74, 75, 76, 77, 78]. Traffic speed and density have been estimated using an artificial neural network (ANN) model [72]. Video and Bluetooth data were used to build the ANN model. The traffic flow data were manually extracted from the video records, while the speed data were constructed from the collected Bluetooth travel time data. It was found that the ANN model can address the research problem if a good quantity of training data is accessible. Another study conducted several machine learning techniques such as k-means clustering, k-nearest neighbor (k-NN) classification, and locally weighted regression to estimate traffic speed using archived data of speeds, counts, and densities [73]. They found that machine learning models can improve the accuracy of speed estimation. Khan

et al. [74] used artificial intelligence to classify the level of service in a freeway segment based on traffic density values. They used loop detectors and CV data to develop support vector machine and k-NN classification models. Results indicated higher accuracy from the support vector machine algorithm than the k-NN classification model. Estimating hourly traffic volumes between sensors was addressed using an ANN model in the Maryland highway network [77], deploying both CVs and automatic traffic recording station data to construct the ANN model. A comparison was also made between linear regression, k-NN, support vector machine (with linear kernel), random forest (RF), and ANN models, concluding that the ANN model performed the best. The proposed approach produced 24 more accurate estimates than current volume profiles. Another study developed two machine learning techniques: ANN and k-NN to estimate traffic density using the traffic flow and speed from automated sensors as models' inputs [78]. The study demonstrated that the ANN and k-NN are promising for traffic state estimation problems.

Previous research has used different features to build machine learning models [72, 73, 74, 75]. Fusing video and Bluetooth data were used to estimate traffic density and speed. The traffic flow data were manually extracted from the video records, while the speed data were constructed from the collected Bluetooth travel time data [72]. Another study relied on archived data of traffic speeds, counts, and density to estimate traffic speed [73]. Distance headway, number of stops, and speed data were identified as useful features to achieve accurate density estimates [74]. They employed loop detectors and CV data. In a recent study, Sekula et al. [77] used CV and automatic traffic recording station data to extract the features of the ANN model. The selected features were the (1) speed of CVs, (2) weather data such as temperature, visibility, precipitation, and weather status, (3) infrastructure data (speed limits, number of lanes, class of the road, and type of the road), (4) temporal data such as the day of the week, and (5) volume profiles based on historical data. From the literature, it can be noted that the traffic speed is always used as a model feature, especially when CV data are used. In contrast, the traffic flow is always used when stationary sensors are used.

2.4 Summary and Conclusions

Reviewing the literature, the model-driven models (e.g., the KF) have proven its ability to reduce errors and address different aspects of the traffic state estimation problem. In addition, the literature showed the benefits of using the machine learning models in different transportation applications. One commonality of the aforementioned studies is that they all estimated the number of vehicles using one source of data from fixed sensors (e.g., loop detectors) or using fused source data (e.g., video with CV data) utilizing a predefined updating interval. A few studies experienced lack of information about the CVs in some estimation steps when using a predefined time interval [70, 71]. In that case, they assumed that the posterior is equal to the prior estimate. In this dissertation, several estimation approaches are developed to estimate real-time vehicle counts along signalized links using CV data. Specifically, This dissertation develops a linear KF, a linear adaptive KF (AKF), a nonlinear PF, an ANN, a k-NN, and a RF approaches. Moreover, the research described in this dissertation introduces a novel way of defining the estimation time interval as a variable rather than a fixed, allowing for higher estimation precision, as the updating time interval always contains a fixed number of CVs.

Chapter 3

Development of a Kalman Filter Approach on an Isolated Intersection

This chapter is an edited version of: Mohammad A. Aljamal, Hossam Abdelghaffar, and Hesham A. Rakha (2019), "Kalman Filter-based Vehicle Count Estimation Approach Using Probe Data: A Multi-lane Road Case Study," presented in the *IEEE Intelligent Transportation Systems Conference (ITSC)* [79].

The chapter presents a novel approach for estimating the number of vehicles on multi-lane signalized links using only CV data. A model-based estimation technique is developed using the Kalman Filtering technique. The model-based state equation employs the traffic flow continuity equation, while the measurement equation uses the hydrodynamic equation. This chapter also proposes a novel variable estimation interval, leading to estimation improvements. The chapter evaluates the proposed estimation method on multi-lane traffic signal links using simulated data. Results show that vehicle count estimates are robust. The estimation approach is evaluated considering two traffic signal control methods: a fixed-time plan and an adaptive phase split optimizer. The results demonstrate a higher estimation accuracy for fixed traffic signal timings at low traffic demand levels, while the estimation ac-

curacy is better when the adaptive phase split optimizer is activated for high traffic demand levels. Finally, the chapter investigates the sensitivity of the estimation approach to vehicle length, demonstrating that the presence of longer vehicles (e.g. trucks) in the traffic stream reduces the estimation accuracy.

3.1 Introduction

Real-time traffic estimation has been given increased attention following the introduction of advanced technologies, such as GPS units, in vehicles. For instance, researchers have developed models to estimate the state of on-road traditional vehicles from known smart vehicle data. Smart vehicles are defined as vehicles that can exchange information, such as instantaneous speed, position, and acceleration, with other vehicles. This is generally referred to as vehicle-to-vehicle, or V2V, communication. These smart vehicles can also exchange information with road infrastructure, which is referred to as vehicle-to-infrastructure, or V2I, communication. However, there are currently a limited number of smart vehicles on the road and thus estimation becomes a crucial tool for obtaining a full picture of the traffic state.

This chapter employs real-time CV data to estimate one of the most important variables of signalized links: traffic density. Traffic density is defined as the number of vehicles per unit length along a given roadway segment [8]. Knowing the number of vehicles on a specific roadway segment is crucial in traffic management applications. To accomplish this, this chapter attempts to estimate the number of vehicles along signalized roadway links using only CV data. These estimation outcomes are considered as an input to traffic signal controllers, leading to improved intersection performance as a result of reduced traffic delays, vehicle crashes, and vehicle emissions.

Previous studies have addressed this research problem using different traffic data sources to achieve the vehicle count estimation. Such sources have included traditional loop detectors [23, 33, 34, 35], camera systems [80] or fusion data [20, 21, 39, 40, 81]. Fusion data combines two different sources of data, such as loop detectors with camera system, camera with GPS data, etc. The aforementioned detection techniques suffer from poor detection accuracy and are not cost-effective due to high installation fees and maintenance costs. More accurate data, such as data collected using the most recent technologies, (i.e., CV data) are needed.

A loop detector can capture the traffic state changes only around its location (stationary de-

tection) and thus cannot address the research problem of estimating traffic density. Instead, two loop detectors, located at the entrance and exit of the traffic link, have generally been used to achieve the research goal after applying the traffic flow continuity equation. However, the noise in the extracted loop detector data leads to some errors in the estimation, an issue which is noted in the literature [21, 23]. To address the noise, the literature suggests using an additional source of data. Vigos et al. [23] used an additional loop detector in the middle of the tested link to reduce noise. However, the cost of implementing this model in the field is high, as it requires at least three loop detectors. The Kalman Filtering (KF) technique can be employed as a lower cost method [30] to estimate the number of vehicles. In a study by Anand et al., KF was combined with a video detection system and GPS data to estimate the traffic density [21]; the vehicle GPS data supplied the model with GPS-equipped vehicles' travel times. This approach is similar to the approach presented in this chapter, but differs in two significant ways: 1) we only use CV data, and 2) we treat the estimation interval time as a variable rather than keeping it constant (the estimation interval time was 60 s in [21]). Van et al. [39] used data fusion to estimate the number of vehicles along an on-ramp link. They employed traffic count data from loop detectors and aggregated speeds from floating cars, the latter provided by Google, and set a 300 s fixed updating interval.

Several studies have utilized KF to improve the estimation of various traffic variables, such as speed [82, 83], travel time [84, 85], and traffic flow [51]. An unscented KF deployed for speed estimation using single loop detectors [82] with a nonlinear state-space equation was able to improve speed estimates. Another study employed a linear KF technique to estimate speed, relying on the relationship between the flow-occupancy ratio and vehicle speed [83], yielding acceptable speed estimates for congested traffic conditions. A cumulative travel-time responsive real-time intersection control within a connected vehicle environment was also developed using the KF technique [84]. In that study, the authors recommended having levels of market penetration (LMP) of at least 30% in order to realize the algorithm's benefits. In summary, KF proves its ability to provide accurate estimates.

The proposed KF approach extends the-state-of-the-art in vehicle count estimates by making

four major contributions:

1. The estimation approach relies solely on CV data. The approach was evaluated considering different CV LMPs ranging from 10% to 90% at increments of 10%.
2. The approach, unlike past applications, uses a variable estimation interval. Using a fixed estimation interval leads to inaccurate estimates, especially at low LMPs. Treating the estimation interval as a variable leads to an improved estimation technique. In this work, we defined the estimation interval once exactly n CVs exit the link.
3. The chapter evaluates the impact of the signal control method (a fixed-time plan and an adaptive phase split optimizer) on the estimation accuracy.
4. The chapter investigates the sensitivity of the proposed estimation approach to vehicle length by introducing trucks into the traffic stream.

3.2 Estimation Approach

3.2.1 Define the Estimation Interval Time

This new approach improves the estimation accuracy, especially for low LMPs, as shown later in the Results section. The new proposed approach defines the estimation interval time as the time when an exact number of CVs (n) exit the link. This ensures that sample of CVs remains the same in each estimation interval. For instance, if the LMP is low (e.g., 10%) and the estimation interval time is fixed and short (e.g., 20 s), there is no guarantee that CVs will be present on the link during the predefined short fixed-time interval, thus making the estimation inefficient and inaccurate. Accordingly, low LMPs require long intervals (e.g., 300 s). In contrast, links with high LMPs can use short fixed intervals (e.g., 20 s). However, the LMP is not a predefined factor and thus we cannot change the estimation interval time accordingly. A flexible approach is needed to overcome this issue and make the estimation

more accurate and effective. The approach proposed in this work is a major contribution to traffic estimation, as it introduces the use of variable estimation periods to produce an efficient and convenient way of determining estimation interval periods. For the purpose of this chapter, the sample size is set to equal five CVs ($n = 5$) after testing different values (i.e., 1, 2, 3, 4, 5, 6, 7, 8, 9, and 10).

3.2.2 Estimation Approach Formulation

This section formulates the approach that estimates the total number of vehicles along signalized intersection links. The proposed estimation approach employs KF, using the state and measurement equations. The state equation utilizes the traffic flow continuity equation as defined in Equation (3.1), while the measurement equation is derived based on the hydrodynamic relation of traffic flow as in Equation (3.3). Equation (3.1) defines the number of vehicles by continuously adding the difference in the number of vehicles entering and exiting the link to the previously computed cumulative number of vehicles. This integral results in an accumulation of error that requires fixing, and thus requires the measurement equation.

$$N(t) = N(t - \Delta t) + \frac{\Delta t}{\rho} [q^{in}(t) - q^{out}(t)] \quad (3.1)$$

where $N(t)$ is the number of vehicles traversing the link at time t , $N(t - \Delta t)$ is the number of vehicles traversing the link in the previous time interval, q^{in} and q^{out} are the CV flows entering and exiting the link between $(t - \Delta t)$ and t , respectively. ρ is the LMP of CVs, defined as the ratio of the number of CVs (N_{CV}) to the total number of vehicles (N_{total}), shown in Equation (3.2). For instance, if ρ is 0.1 and the number of CVs is 2, then the expected total number of vehicles is 20.

$$\rho = N_{CV}/N_{total} \quad (3.2)$$

Equation (3.3) describes the hydrodynamic relationship between the macroscopic traffic stream parameters (flow, density, and space-mean speed).

$$q = ku \quad (3.3)$$

where q is the traffic flow (vehicles per unit time), k is the traffic stream density (vehicles per unit distance), and u is the space-mean speed (distance per unit time) shown in Equation (3.4).

$$u = D/TT \quad (3.4)$$

where D is the link length and TT is the average vehicle travel time. Since CVs can share their instantaneous locations every Δt , the travel time of each CV can be computed for any road section. Thus, the CV travel time is used in the measurement equation, using Equations (3.3) and (3.4). The measurement equation can be written as shown in Equation (3.7):

$$TT(t) = D \times \frac{k(t)}{\bar{q}(t)} \quad (3.5)$$

$$TT(t) = \frac{1}{\bar{q}} [k(t) \times D] = \frac{1}{\bar{q}(t)} N(t) \quad (3.6)$$

$$TT(t) = H(t) \times N(t) \quad (3.7)$$

where \bar{q} is the average traffic flow entering and exiting the link, and $H(t)$ is a transition vector that converts the vehicle counts to travel times, and is the inverse of the average flow (i.e. the first term of Equation (3.6)), as shown in Equation (3.8).

$$H(t) = \frac{1}{\bar{q}(t)} = \frac{2 \times \rho}{q^{in}(t) + q^{out}(t)} \quad (3.8)$$

Note that the value of ρ in Equations (3.1) and (3.8) plays a major role in delivering accurate estimation outcomes. The proposed estimation approach (KF) equations are shown below:

$$\hat{N}^-(t) = \hat{N}^+(t - \Delta t) + \frac{\Delta t}{\rho} [q^{in}(t) - q^{out}(t)] \quad (3.9)$$

$$\hat{TT}(t) = H(t) \times \hat{N}^-(t) \quad (3.10)$$

$$\hat{P}^-(t) = \hat{P}^+(t - 1) \quad (3.11)$$

$$G(t) = \hat{P}^-(t)H(t)^T [H(t)\hat{P}^-(t) H(t)^T + R]^{-1} \quad (3.12)$$

$$\hat{N}^+(t) = \hat{N}^-(t) + G(t) [TT(t) - \hat{TT}(t)] \quad (3.13)$$

$$\hat{P}^+(t) = \hat{P}^-(t) \times [1 - H(t) G(t)] \quad (3.14)$$

Where \hat{N}^- is the a priori estimate of the vehicle counts calculated using the measurement prior to instant t , and \hat{P}^- is the a priori estimate of the covariance error at instant t . The Kalman gain (G) is computed using Equation (3.12). The R variable is the covariance error of the measurements. The posterior state estimate (\hat{N}^+) and the posterior error covariance estimate (\hat{P}^+) are updated as shown in Equations (3.13) and (3.14), considering the CVs travel time measurements.

3.2.3 Define the LMP Rate (ρ)

This work tests the estimation approach using a predefined fixed ρ value over all the estimation intervals. For instance, the ρ value would be 10% for the entire evaluation if the scenario of 10% LMP is tested. The ρ values here are defined based on historic data. The ρ value is an important variable in the proposed estimation approach, as it scales up the CV observations to compute the total number of vehicles. The predefined ρ value is computed as the arithmetic mean of all ρ value observations. For instance, Figure 3.1 shows the actual ρ values (blue lines) versus the predefined ρ value (red line $\rho = 20\%$), which represent an error in the approach estimating the ρ values. However, the KF can handle this error, as will be demonstrated later in the Results section.

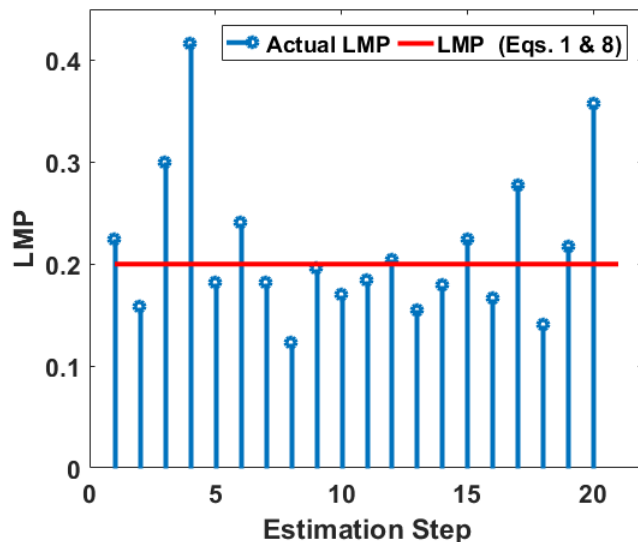


Figure 3.1: Actual LMP variations along the estimation steps.

3.3 Results and Discussion

This section presents the experimental setup (section 3.3.1) and the experimental results (section 3.3.2) of applying the proposed approach on an isolated intersection.

3.3.1 Experimental Setup

The proposed approach was tested on an intersection with four approaches comprised of three lanes each located in the heart of downtown Toronto [86], as shown in Figure 3.2. The traffic origin-destination (O-D) demand matrix provided in Table 3.1, represents the highest total demand approaching the intersection during the afternoon rush hour (PM Peak) for the year 2005.

The simulations were conducted using the following parameter values: speed-at-capacity = 60 (km/h), free-flow speed = 80 (km/h), jam density = 160 (veh/km/lane), saturation flow rate = 1900 (veh/h/lane). The four-legged intersection's phasing scheme is shown in Figure 3.3. In this chapter, two signal operational approaches were conducted in order to

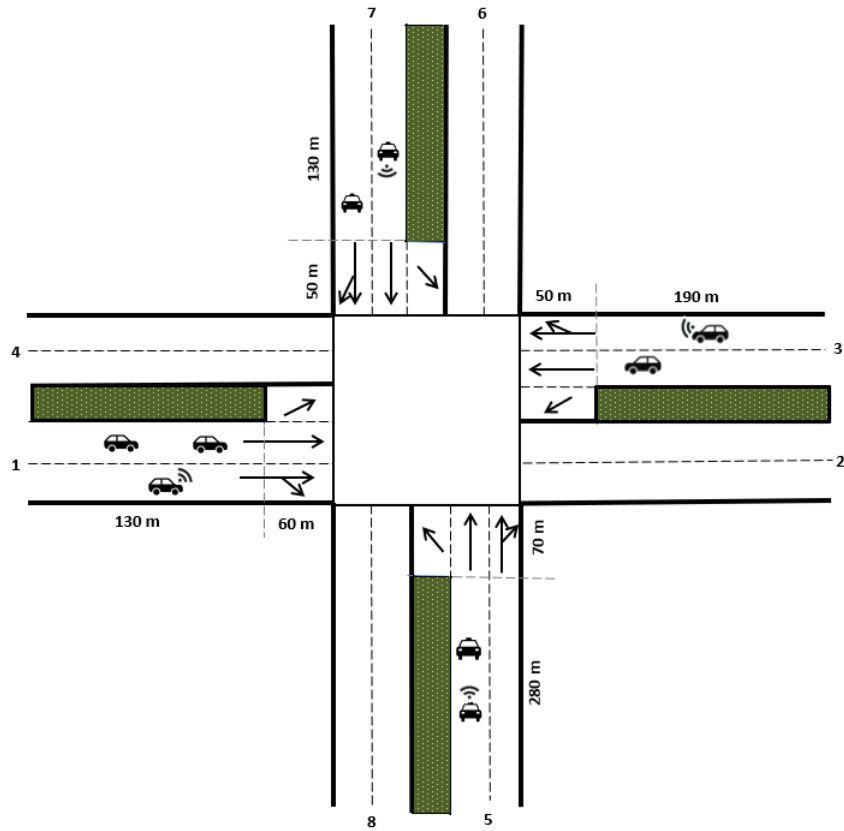


Figure 3.2: Simulated intersection.

Table 3.1: Origin destination demand matrix.

| Zone # | 2 | 4 | 6 | 8 | Total |
|--------|------|------|-----|------|-------|
| 1 | 1223 | - | 134 | 121 | 1478 |
| 3 | - | 844 | 86 | 278 | 1208 |
| 5 | 88 | 71 | 721 | - | 880 |
| 7 | 188 | 100 | - | 806 | 1094 |
| Total | 1499 | 1015 | 941 | 1205 | 4660 |

achieve a more comprehensive analysis: a fixed-time traffic signal plan and an adaptive phase split optimizer (phase split). The fixed plan was computed using the Webster method [87], with yellow and all-red times set at 3 s. The optimized effective green times for the four phases were 17 s, 13 s, 8 s, and 9 s. The phase split was optimized every 120 s. The optimization here allocates green time on the basis of the link's volume/saturation flow ratios

according to the Canadian capacity guide and the highway capacity manual [88].

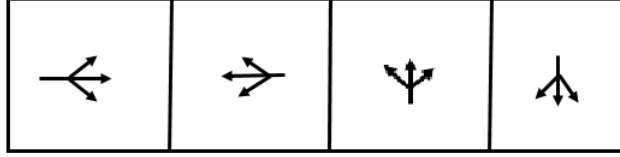


Figure 3.3: Four phasing scheme.

The accuracy of the proposed KF estimator was tested using the INTEGRATION microscopic traffic assignment and simulation software [89] on an isolated intersection. The proposed estimation approach accuracy was evaluated based on the root mean square error (RMSE) and the relative root mean square error (RRMSE), as shown in Equations (3.15) and (3.16), respectively.

$$RMSE(veh) = \sqrt{\sum_{s=1}^S [\hat{N}^+(s) - N(s)]^2 / S} \quad (3.15)$$

$$RRMSE(\%) = 100 \sqrt{S \sum_{s=1}^S [\hat{N}^+(s) - N(s)]^2 / \sum_{s=1}^S N(S)} \quad (3.16)$$

Where $N(s)$ represents the actual vehicle count, $\hat{N}^+(s)$ represents the estimated vehicle count values, and S is the total number of estimations. The simulation starts with an initial estimate of ($\hat{N}^+(0) = 5$ veh) as in [23], an initial posterior estimate error of ($\hat{P}^+(0) = 5$), and measurement error covariance of ($R = 5$).

3.3.2 Experimental Results

This section compares the performance of the proposed estimation approach using two estimation interval times: a fixed estimation interval (i.e., 60 and 120 s) and the proposed variable estimation interval approach. Recall that the variable estimation interval time is defined when a certain number of CVs (e.g. 5veh) reach the end of the link (i.e., the traffic

signal stop bar; section 3.3.2.1). Section 3.3.2.2 describes the effect of the signal timing plan on the estimation results. Section 3.3.2.3 describes the impact of heavy trucks on the estimation accuracy.

3.3.2.1 Variable vs. Fixed Estimation Time Interval

Previous research has considered fixed estimation intervals (e.g., 30 s). This is an appropriate approach if data from all vehicles are available and can be used (LMP of 100%). However, this condition is impossible to obtain when CV data is used. Consequently, the use of variable interval time steps is crucial for obtaining high estimation accuracy and avoiding the absence of CV data in any estimation interval.

This section illustrates the benefits of using variable time steps as opposed to a constant value. Table 3.2 presents the estimation efficiency using fixed and variable time steps in the eastbound (EB) approach. The fixed intervals are considered to be the same as traffic cycle lengths (i.e., 60 and 120 s). Moreover, different LMPs were considered to provide a comprehensive comparison. It is clear that the proposed strategy of using variable time steps significantly improves the estimation accuracy results and always ensures that the same amount of information is present for every time step (five CVs). It is clear that the estimation approach with fixed intervals is not applicable, as the scenario for 10% LMP shows; this is due to the absence of observed CVs in most time intervals. In conclusion, longer estimation intervals are required when LMPs are low (e.g., 200 s) to ensure that some CVs are on the link, and thus available information is employed in the KF. In contrast, shorter estimation intervals are utilized when LMPs are high (e.g., 30 s). The strategy proposed herein ensures flexibility of the estimation interval times.

3.3.2.2 Fixed vs Optimized Green Traffic Signal Timing

This section studies the impact of allocated green signal timing on the estimation accuracy using a fixed plan (green times for all traffic signal phases are predefined and remain fixed)

Table 3.2: EB RRMSE of fixed and variable estimation time interval.

| LMPs % | RRMSE (%) | | |
|--------|----------------------------|-----------------------------|-------------------|
| | Fixed ($\Delta t = 60$ s) | Fixed ($\Delta t = 120$ s) | Proposed Approach |
| 10 | Nan | 48 | 41 |
| 20 | 45 | 42 | 39 |
| 30 | 44 | 39 | 35 |
| 40 | 41 | 36 | 31 |
| 50 | 39 | 35 | 27 |
| 60 | 37 | 36 | 25 |
| 70 | 36 | 34 | 23 |
| 80 | 34 | 34 | 21 |
| 90 | 34 | 33 | 20 |

and an adaptive phase split optimizer. The total number of vehicles along the tested links were estimated considering different LMPs (10 – 90%). A Monte Carlo simulation was conducted to create 100 random CV samples from the entire data set for each scenario. This section presents the estimation results of the intersection links: EB (Table 3.3), westbound (WB, Table 3.4), northbound (NB, Table 3.5), and southbound (SB, Table 3.6).

The results show that the algorithm produces more accurate estimations for the fixed-time plan for the minor approaches (NB, SB). In contrast, the estimation accuracy improves with optimization for high demand approaches (EB and WB). The phase split optimizer positively impacts approaches with high traffic demand levels, as more green times are allocated, and thus the estimation polling interval is shorter (more vehicles are expected to traverse the intersection). In addition, the results show that the estimation accuracy increases as the LMP increases, as the CVs supply more data. For example, if the entire data set contains 1,000 vehicles (CVs and traditional), and the LMP on the link is equal to 10%, then the number of CVs is 100. On the other hand, if the LMP is equal to 90%, the number of CVs is 900. In conclusion, having more information will significantly improve estimation accuracy.

The proposed approach addresses the research goal appropriately, producing reasonable error values. Vigos et al. considered their model a robust model with up to a 27.5% RRMSE using

Table 3.3: EB RRMSE and RMSE using fixed and phase split plans.

| LMPs % | Fixed Plan | | Phase Split | |
|--------|------------|------------|-------------|------------|
| | RRMSE (%) | RMSE (veh) | RRMSE (%) | RMSE (veh) |
| 10 | 41 | 4.4 | 39 | 4.5 |
| 20 | 39 | 4.1 | 37 | 4.2 |
| 30 | 35 | 3.8 | 33 | 3.9 |
| 40 | 31 | 3.3 | 31 | 3.5 |
| 50 | 27 | 3.0 | 27 | 3.1 |
| 60 | 25 | 2.7 | 24 | 2.8 |
| 70 | 23 | 2.4 | 21 | 2.4 |
| 80 | 21 | 2.2 | 18 | 2.1 |
| 90 | 20 | 2.2 | 15 | 1.7 |

Table 3.4: WB RRMSE and RMSE using fixed and phase split plans.

| LMPs % | Fixed Plan | | Phase Split | |
|--------|------------|------------|-------------|------------|
| | RRMSE (%) | RMSE (veh) | RRMSE (%) | RMSE (veh) |
| 10 | 48 | 4.5 | 39 | 4.6 |
| 20 | 44 | 4.1 | 36 | 4.2 |
| 30 | 40 | 3.7 | 33 | 4.0 |
| 40 | 38 | 3.5 | 31 | 3.7 |
| 50 | 38 | 3.5 | 28 | 3.4 |
| 60 | 37 | 3.3 | 26 | 3.1 |
| 70 | 37 | 3.3 | 24 | 2.8 |
| 80 | 33 | 3.0 | 22 | 2.6 |
| 90 | 27 | 2.5 | 21 | 2.6 |

three loop detector measurements [23]. Our approach used no loop detectors and low LMPs, and still produced RRMSE values close to Vigos et al.'s model, which used an LMP of 100% and the three aforementioned loop detectors.

3.3.2.3 Impact of Heavy Trucks

This section investigates the sensitivity of the proposed estimation approach to vehicle length. Trucks with 4 times the normal vehicle length were introduced to the EB base scenario on

Table 3.5: NB RRMSE and RMSE using fixed and phase split plans.

| LMPs % | Fixed Plan | | Phase Split | |
|--------|------------|------------|-------------|------------|
| | RRMSE (%) | RMSE (veh) | RRMSE (%) | RMSE (veh) |
| 10 | 25 | 4.4 | 36 | 5.2 |
| 20 | 25 | 4.4 | 33 | 4.6 |
| 30 | 23 | 4.1 | 29 | 4.2 |
| 40 | 23 | 3.9 | 29 | 4.1 |
| 50 | 22 | 3.7 | 28 | 3.9 |
| 60 | 20 | 3.5 | 26 | 3.7 |
| 70 | 19 | 3.3 | 25 | 3.5 |
| 80 | 19 | 3.3 | 23 | 3.3 |
| 90 | 17 | 3.0 | 23 | 3.3 |

Table 3.6: SB RRMSE and RMSE for fixed and phase split plans.

| LMPs % | Fixed Plan | | Phase Split | |
|--------|------------|------------|-------------|------------|
| | RRMSE (%) | RMSE (veh) | RRMSE (%) | RMSE (veh) |
| 10 | 29 | 3.8 | 45 | 4.6 |
| 20 | 29 | 3.7 | 43 | 4.4 |
| 30 | 26 | 3.3 | 36 | 3.8 |
| 40 | 25 | 3.2 | 32 | 3.3 |
| 50 | 22 | 2.8 | 29 | 3.0 |
| 60 | 20 | 2.6 | 26 | 2.9 |
| 70 | 19 | 2.5 | 24 | 2.5 |
| 80 | 19 | 2.4 | 22 | 2.2 |
| 90 | 18 | 2.3 | 22 | 2.2 |

all movements. Two different percentages were used to define the number of trucks on the tested links: 5% and 10% of the entire data set. Table 3.7 illustrates the impact of trucks on estimation accuracy. In the presence of trucks, the maximum link accommodation was less compared to the base scenario. As these results show, trucks reduce estimation accuracy by increasing bias in our approach. This finding is in line with Vigos et al.'s conclusion [23].

Table 3.7: RRMSE in scenarios with no trucks, 5%, and 10% trucks.

| LMPs % | Base Scenario | 5% Trucks | 10% Trucks |
|--------|---------------|-----------|------------|
| 10 | 41 | 43 | 49 |
| 20 | 39 | 42 | 46 |
| 30 | 35 | 39 | 41 |
| 40 | 31 | 34 | 36 |
| 50 | 27 | 29 | 31 |
| 60 | 25 | 26 | 27 |
| 70 | 23 | 24 | 24 |
| 80 | 21 | 25 | 22 |
| 90 | 20 | 25 | 21 |

3.4 Summary and Conclusions

This chapter proposes a novel approach for estimating the number of vehicles approaching a traffic signal using CV data only. The approach uses a novel variable estimation interval rather than the traditional approach using a fixed interval. Specifically, the duration of the interval is dynamically computed when a pre-defined sample size (n) exits the link. This improves the estimation accuracy, especially for low LMPs, and makes the proposed estimation approach flexible. The estimation approach uses the known KF technique to achieve the research goal. The proposed KF estimator was employed to test the model's accuracy on signalized multi-lane roads. The results showed that the proposed KF addressed the research goal by producing reasonable errors, even at low LMPs. The results indicated, as would be expected, that estimation errors decrease as the LMP increases.

In addition, the approach was evaluated considering two traffic signal timing scenarios, namely: a fixed-time plan and an adaptive phase split optimizer. The results demonstrated that the approach works better for the fixed plan at lower traffic demand levels. Alternatively, the approach works better for the adaptive traffic signal controller for high approach traffic demand levels. This was a result of extending the green times for the higher traffic demand approaches, which produced shorter estimation intervals, as n CVs traversed the

link in shorter time periods. Finally, the chapter investigates the sensitivity of the KF's accuracy when adding some trucks to the traffic flow. Specifically, the chapter tested for 5% and 10% trucks for the original demand. The estimation accuracy was found to decrease as the percentage of trucks increased.

Chapter 4

Development of an Adaptive Kalman and a Neural-Kalman Filtering Approaches

This chapter is an edited version of: Mohammad A. Aljamal, Hossam Abdelghaffar, and Hesham A. Rakha (2019), "Developing a Neural–Kalman Filtering Approach for Estimating Traffic Stream Density Using Probe Vehicle Data," published in *Sensors Journal* [50].

This chapter presents a novel approach for estimating the number of vehicles along signalized links. The proposed estimation approach utilizes the adaptive Kalman filter (AKF) to produce reliable traffic vehicle count estimates, considering real-time estimates of the system noise characteristics. The AKF utilizes only real-time connected vehicle data. The AKF is demonstrated to outperform the traditional Kalman filter, reducing the estimation error by up to 29%. In addition, the chapter introduces a novel approach that combines the AKF with an artificial neural network (AKFNN) to enhance the vehicle count estimates, where the artificial neural network is employed to estimate the connected vehicles' market penetration rate. Results indicate that the accuracy of vehicle count estimates is significantly

improved using the AKFNN approach (by up to 26%) over the AKF. Moreover, the chapter investigates the sensitivity of the proposed AKF approach to the initial conditions, such as the initial estimate of vehicle counts, initial mean estimate of the state system, and the initial covariance of the state estimate. The results demonstrate that the AKF is sensitive to the initial conditions. More accurate estimates could be achieved if the initial conditions are appropriately selected. In conclusion, the proposed AKF is more accurate than the traditional Kalman filter. Finally, the AKFNN approach is more accurate than the AKF and the traditional Kalman filter since the AKFNN uses more accurate values of the connected vehicle market penetration rate.

4.1 Introduction

Real-time traffic state estimates have been increasingly recognized following the introduction of recent advanced technologies such as connected vehicle (CV) technologies. CVs aim to improve road safety by potentially reducing human errors, mitigating traffic congestion levels by offering alternative routes, and reducing on-road emissions and fuel consumption [19]. Nowadays, conducting research with limited probe vehicle data (e.g., CVs) is a challenge, especially when no additional data sources are provided. Hence, past research has utilized CV data in conjunction with existing detection systems to enhance proposed traffic models, despite the limitation that fixed detection techniques (e.g., loop detectors) always have some noise in their data [20, 21, 22].

A CV is defined as a vehicle that provides real-time information, such as its instantaneous position and speed. Several benefits of using CV data have been recognized; for example, the high quality of data compared with existing data sources (e.g., cameras and loop detectors), and data can be collected at any location inside the network, thus offering a clear picture about traffic behavior at any time. Therefore, transportation agencies are putting effort into facilitating the use of CV data.

Limited studies have used only information from CV data to estimate the state of on-road traditional vehicles [79], such as traffic travel time, traffic density, traffic speed, and traffic volume. The real-time estimation of traffic density is important to achieving better traffic operations management in urban areas. This chapter aims to estimate the total number of vehicles on signalized links using only CV data. The estimate outcomes can be provided to traffic signal controllers to optimally determine the allocation of green time for each traffic signal phase [6, 90], leading to better intersection performance measures such as intersection delays and vehicle crashes [4, 5]. One concern with using CVs is measuring their level of market penetration (LMP). The LMP is defined as the ratio of the total number of CVs to the total number of vehicles. Providing accurate LMP estimates improves the estimation accuracy of the vehicle counts [79]. Therefore, in this chapter, a machine-learning technique

is developed to provide reliable LMP estimates.

4.2 Related Work

Different statistical tools have been used to estimate the total number of vehicles on arterial roads and freeways, such as the Kalman filter (KF) [30], Bayesian statistics [91], and Particle filter [45] approaches. The literature shows the benefits of using the KF technique in addressing different aspects of the traffic estimation problem. The KF has been used to estimate the traffic travel time [61, 92], traffic speed [56, 57], and traffic density [23, 79]. Different detection techniques have been employed to estimate the number of vehicles, such as loop detectors, camera systems, and probe data. Two loop detectors, one at the entrance and the other at the exit of the link, are utilized to measure the total number of arrivals and departures, then the number of vehicles are simply obtained by applying the flow continuity equation [8]. A robust KF model with at least three loop detectors on the tested link was employed to estimate the number of vehicles on the link in [23]. The study derived the KF state equation from the flow continuity equation, while the measurement equation was derived from the relationship of the detector time-occupancy and space-occupancy; however, the cost of implementing such an algorithm in the field is high given the number of sensors needed. Another study employed the KF to estimate the number of vehicles on multi-section freeways. The state equation was derived from the flow continuity equation, while the measurement equation was derived from the hydrodynamic relationship between traffic speed and density [66]. Loop detectors were used in addition to speed sensors in the middle of the tested section. However, the proposed algorithm is hard to employ in the field due to the high cost of implementation. A video record, another detection technique, was used to estimate the traffic density for signalized links [67]. In that study, the authors used the space-mean speed rather than the traffic flow in the state equation due to high errors accompanied with sensor failures. Their argument takes into account that the space-mean speed is taken as an average quantity while the traffic flow is a cumulative quantity. They also demonstrated the importance of having knowledge about the system noise characteristics to improve the

performance of the KF model. Consequently, an adaptive Kalman filter (AKF) is developed to enable real-time estimates of statistical parameters of the system noise rather than using predefined values for the entire simulation (as assumed in the traditional KF approach).

As illustrated in the literature, stationary sensors, such as loop detectors and camera systems, suffer from poor detection accuracy and have high installation and maintenance costs. Advanced detection techniques such as CV data have proven to be more accurate without the need to install additional hardware. Consequently, recent studies have developed several traffic estimation models using fusion data (combination of two different data sources) to estimate the number of vehicles with the aim of achieving better accuracy than using only one source of data. In many of the works using fusion data, the KF technique was employed for estimating traffic density. One study achieved accurate estimated traffic density results using the traffic flow values measured from a video detection system and the travel time obtained from vehicles equipped with GPS devices [20]. The proposed estimation approach in this study differs in two significant ways from the proposed AKF approach, namely only CV data are used with a variable time interval rather than a fixed value (the updating time interval was 1 minute in [20]), and the proposed estimation approach uses the AKF to allow for real-time estimates of statistical parameters of the state and measurement noise.

Reviewing the literature, the KF model has proven its ability to address estimation research problems for different traffic applications. However, it is hard to implement in real-world applications due to hard estimates of statistical characteristics of the system noise (mean and variance). Consequently, researchers have developed the AKF to solve this issue and make field implementation possible. Chu et al. proposed an AKF approach to estimate freeway travel time using both loop detectors and CVs data [59]. They presented the estimation method for noise statistic parameters that was proposed in [93]. This estimation method of statistical parameters is known for its simplicity in handling errors and its fast processing time. Hence, in this chapter, the estimation of the statistical parameters uses the same estimation procedure as in Chu et al.'s study. It should be noted that the main difference between the proposed estimation approach and Chu et al.'s approach is that our approach

uses only CV data.

In a recent study, the KF approach was proposed to estimate the number of vehicles on signalized links using only CV data [79]. The KF state equation was based on the traffic flow continuity equation and thus one value of CV LMP (ρ), for the entire link, is used to scale up the CV measurements to reflect the total flow in the second term of the flow continuity equation as presented in Equation (4.1). It was found that using two LMP values (at the entrance and the exit of the link) produce more accurate vehicle count estimates, especially when dealing with low LMPs, as described later in Section 4.4.3. In Equation (4.1), $N(t)$ is the number of vehicles traversing the link at time (t), Δt is the variable duration of the updating time interval, $N(t - \Delta t)$ is the number of vehicles traversing the link in the previous interval, q^{in} and q^{out} are the CV flows entering and exiting the link between ($t - \Delta t$) and (t), respectively, and ρ is the LMP of CVs.

$$N(t) = N(t - \Delta t) + \frac{\Delta t}{\rho} [q^{in}(t) - q^{out}(t)] \quad (4.1)$$

Machine learning has proven its ability to provide accurate estimates for different traffic characteristics [72, 73, 74, 75, 76, 77]. Traffic speed and density have been estimated using an artificial neural network (ANN) model [72]. Video and Bluetooth data were used to build the ANN model. The traffic flow data were manually extracted from the video records, while the speed data were constructed from the collected Bluetooth travel time data. The ANN model is able to address the research problem if a good quantity of training data is accessible. Another study conducted several machine learning techniques such as k-means clustering, k-nearest neighbor classification, and locally weighted regression to estimate traffic speed [73] using archived data of speeds, counts, and densities. They found that machine learning models can improve the accuracy of speed estimation. Khan et al. [74] used artificial intelligence to classify the level of service in a freeway segment based on traffic density values. They used loop detectors and CV data to develop support vector machine and k-nearest neighbor classification. Results indicated higher accuracy from the support vector machine algorithm than the k-nearest neighbor classification algorithm. Estimating hourly traffic volumes between sensors was addressed using an ANN model in the Maryland highway

network [77], deploying both CVs and automatic traffic recording station data to construct the ANN model. A comparison was also made between linear regression, k-nearest neighbor, support vector machine with linear kernel, random forest, and ANN models, concluding that the ANN model performed the best. The proposed approach produced 24% more accurate estimates than current volume profiles.

In this chapter, an AKF approach was applied to estimate real-time vehicle counts along signalized links using only CV data. The study then considers the recommendation of Aljamal et al's study [42] by using two LMP values at the entrance and the exit of the tested link. To achieve this task, an ANN approach was developed to provide real-time estimates of the LMP values to improve the accuracy of the proposed AKF approach. After that, the chapter develops the new AKFNN approach after combining the AKF with the developed ANN approach. This chapter extends the state-of-the-art in vehicle count estimates by making four major contributions:

1. This chapter tests the proposed AKF approach using only CV data. The approach was evaluated considering different CV LMPs ranging from 10% to 90% at increments of 10%.
2. The chapter develops an ANN approach to estimate the LMP of CVs at the exit of the link to reflect the total vehicle departures.
3. The chapter tests the developed AKFNN approach by using a fusion of CV and single-loop detector data. A comparison between the traditional KF, AKF, and AKFNN approaches is presented.
4. The chapter examines the impact of the initial conditions on the AKF estimation approach. Three initial condition parameters are tested: the initial vehicle count estimate, the initial mean estimate of the state noise errors, and the a priori initial covariance of the state system.

This chapter is organized as follows. Section 4.3 describes the development of the simulation data. Section 4.4 describes the development of the KF, AKF, and AKFNN estimation approaches. Section 4.5 discusses the results of the estimation approaches. Section 4.6 provides the conclusions of the chapter.

4.3 Development of Simulation Data

This chapter relies on the INTEGRATION traffic simulation model [89] to validate and test the accuracy of the proposed approaches. The INTEGRATION software has been extensively validated and demonstrated to replicate empirical observations [94, 95, 96, 97, 98, 99]. Specifically, INTEGRATION was used to create synthetic data for conditions not observed in the field to quantify the sensitivity of the proposed method to the link length and traffic demand level. The selected tested link is located in downtown Blacksburg, Virginia, with an approximate length of 102 m based on ArcGis software, and connects two signalized intersections. The link characteristics were calibrated to local conditions using typical values, which included a free-flow speed of 40 (km/h), a speed-at-capacity of 32 (km/h), a jam density of 160 (veh/km/lane), and a base saturation flow rate of 2100 (veh/h/lane), which resulted in a roadway capacity of 700 (veh/h) given the cycle length and green times of the traffic signal. The traffic signal cycle length is 75 s and it has four phases with the following displayed green times: 5, 25, 5, and 28 s. The tested link here is assigned with a displayed green time of 25 s. These values were consistent with what was coded in the field.

The INTEGRATION simulation model was used to ease the generation of CV data as real CV data are not easy to access. For each LMP, a total of 50 scenarios were generated with different random seeds as conducted in [74]. Forty-nine scenarios were used to train and validate the proposed ANN approach, and scenario number 50 was considered the testing data set. The INTEGRATION model generates a "time-space" file which provides some information about the CVs during their trips for every second. The time-space file records the instantaneous position, speed, and spacing for each CV. In addition to that, a loop detector is installed at the entrance of the tested link to create a detector output file which provides

some data about the simulation behavior such as speed, traffic volume, and occupancy at the detection location.

4.4 Estimation Approaches

This section first summarizes some crucial points regarding estimating the vehicle count as discussed in Chapter 3. In addition, this section describes the proposed AKF estimation approach for estimating the vehicle count along signalized link approaches, and demonstrates the difference of the state-of-the-art KF approach in [79] and the new proposed AKF approach. Finally, an ANN approach is developed to provide estimates of the CV LMPs to be used in the proposed AKF approach equations to attain higher accuracy. Two vehicle count estimation approaches are described in this section: (1) the AKF, which uses only CV data; and (2) the AKFNN, which fuses CV and single-loop detector data. The single-loop detector data were mainly used to develop the ANN approach.

4.4.1 Summary of the Developed KF Approach

In a previous study [79], the authors developed a KF approach to produce reliable vehicle count estimates using only CV data. In that study, the authors introduced a novel variable estimation time interval as opposed to the traditional fixed time interval. The estimation time interval was defined as the time when exactly n CVs traversed the tested link. It was proven that the variable time interval, compared to a fixed time interval (e.g., 20 s), led to improved estimation accuracy. An illustrative example to show the benefits of using the variable time interval. if the approach's LMP is 10%, the number of CVs will obviously be low. If we treat the problem using a fixed estimation interval, then the probability of observing zero CVs within an interval will be high for short estimation time intervals, making the estimation inefficient and inaccurate. Accordingly, low LMPs require long intervals (e.g., 300 s) to ensure that at least one CV is on the approach. In contrast, approaches with high LMPs can use short estimation intervals (e.g., 20 s). Consequently, treating the estimation

time interval as a variable produces an efficient and convenient way of determining the duration of the estimation period.

One concern about the KF approach is the use of predefined fixed values of the statistical parameters, mean and variance, of the KF state and measurement errors. Applying the KF in real-world problems is limited since the statistical parameters are assumed to be known [59]. The mean and variance entities are known as variable rather than fixed values. To produce a flexible model, this chapter employs the AKF to provide real-time estimates of the statistical parameters of the KF state and measurement errors as described in the following section.

4.4.2 Adaptive Kalman Filter (AKF)

The traditional KF is utilized with predefined error values of the state and measurement noise; these error values remain constant for the entire simulation. However, these values are hard to obtain in the field and they are always changing with time. Hence, an AKF is developed to overcome this issue and to dynamically estimate the error values in the state and measurement estimates. The AKF is comprised of two equations: (a) state equation and (b) measurement equation. The state equation is derived from the traffic flow continuity equation as defined in Equation (4.2). The state equation computes the number of vehicles by continuously adding the difference in the number of vehicles entering and exiting the section to the previously computed cumulative number of vehicles traveling along the section. This integral results in an accumulation error which requires fixing, and thus the measurement equation is needed. In Equation (4.2), the ρ value can be observed from historical data.

$$N(t) = N(t - \Delta t) + \frac{\Delta t}{\rho} [q^{in}(t) - q^{out}(t)] \quad (4.2)$$

The state equation produces accurate results if the scaled traffic flows (q^{in}/ρ_{in} and q^{out}/ρ_{out}) are accurate [79], as shown in Section 4.4.3. The total counts can be extracted from traditional loop detectors or video detection systems. We should note here that the ρ value in Equation (4.2) plays a major role in delivering accurate outcomes. ρ is defined as the ratio of the number of CVs (N_{CV}) to the total number of vehicles (N_{total}), as shown in Equation

(4.3). For instance, if ρ is equal 0.1, and the number of CVs is 5, then the expected total number of vehicles is 50.

$$\rho = N_{CV}/N_{total} \quad (4.3)$$

Equation (4.4) describes the hydrodynamic relationship between the macroscopic traffic stream parameters (flow, density, and space-mean speed),

$$q = k u_s \quad (4.4)$$

where q is the traffic flow (vehicles per unit time), k is the traffic stream density (vehicles per unit distance), and u_s is the space-mean speed (distance per unit time). The u_s can be represented as shown in Equation (4.5),

$$u_s = D/TT \quad (4.5)$$

where D is the link length and TT is the average vehicle travel time. Since CVs can share their instantaneous locations every Δt , the travel time of each CV can be computed for any road section. Thus, the CV travel time is used in the measurement equation, using Equations (4.4) and (4.5). The measurement equation can be written as shown in Equation (4.8):

$$TT(t) = D \times \frac{k(t)}{\bar{q}(t)} \quad (4.6)$$

$$TT(t) = \frac{1}{\bar{q}} [k(t) \times D] = \frac{1}{\bar{q}(t)} N(t) \quad (4.7)$$

$$TT(t) = H(t) \times N(t) \quad (4.8)$$

where \bar{q} is the average traffic flow entering and exiting the link, and $H(t)$ is a transition vector that converts the vehicle counts to travel times, and is the inverse of the average flow (i.e., the first term of Equation (4.7)), as shown in Equation (4.9).

$$H(t) = \frac{1}{\bar{q}(t)} = \frac{2 \times \rho}{q^{in}(t) + q^{out}(t)} \quad (4.9)$$

The system state and measurement equations can be written as in Equations (4.10) and (4.11), considering the errors (noise). The term $u(t)$ is the given inputs for the system. The vector $H(t)$ is used to convert the vehicle counts to travel times. The vector $w(t - \Delta t)$ is the state noise and is assumed to be Gaussian noise with the mean of $m(t)$ and variance of $M(t)$. The measurement noise $v(t)$ is assumed to be Gaussian noise with the mean of $r(t)$

and variance of $R(t)$.

$$\text{State Equation : } N(t) = N(t - \Delta t) + u(t) + w(t - \Delta t) \quad (4.10)$$

$$u(t) = \frac{\Delta t}{\rho} [q^{in}(t) - q^{out}(t)]$$

$$\text{Measurement Equation : } TT(t) = H(t) \times N(t) + v(t) \quad (4.11)$$

$$H(t) = \frac{1}{\bar{q}(t)} = \frac{2 \times \rho}{q^{in}(t) + q^{out}(t)}$$

The proposed AKF estimation approach can be solved using the following equations:

$$\hat{N}^-(t) = \hat{N}^+(t - \Delta t) + u(t) + m(t - \Delta t) \quad (4.12)$$

$$\hat{P}^-(t) = \hat{P}^+(t - \Delta t) + M(t - \Delta t) \quad (4.13)$$

$$G(t) = \hat{P}^-(t)H(t)^T [H(t)\hat{P}^-(t)H(t)^T + R(t)]^{-1} \quad (4.14)$$

$$\hat{N}^+(t) = \hat{N}^-(t) + G(t) [TT(t) - H(t)\hat{N}^-(t) - r(t)] \quad (4.15)$$

$$\hat{P}^+(t) = \hat{P}^-(t) \times [1 - H(t)G(t)] \quad (4.16)$$

where \hat{N}^- is the a priori estimate of the vehicle counts calculated using the measurement prior to instant t , and \hat{P}^- is the a priori estimate of the covariance error at instant t . The Kalman gain (G) is demonstrated in Equation (4.14). The posterior state estimate (\hat{N}^+) and the posterior error covariance estimate (\hat{P}^+) are updated as shown in Equations (4.15) and (4.16), considering the CV travel time measurements. In the next section, the estimation steps of the noise statistical parameters (m, M, r, R) are described.

4.4.2.1 Online Estimation of Noise Statistics

An online estimate is conducted to optimally find the errors in the state and the measurement variables, to make the KF more efficient and applicable in real-world applications. As pointed out in the literature, the traditional KF assumes predefined errors in the system, which is not the case in real applications. A set of unknown noise statistical parameters, (m, M, r, R), needs to be estimated at every estimation step. The online estimate procedure follows the

same procedure presented in [59].

The mean (m) and variance (M) of the state noise are shown in Equations (4.17) and (4.18), respectively.

$$m = \frac{1}{n} \sum_{t=1}^n m(t), \quad \text{where } m(t) = \hat{N}^+(t) - \hat{N}^+(t - \Delta t) - u(t) \quad (4.17)$$

$$M = \frac{1}{n-1} \sum_{t=1}^n [(m(t) - m).(m(t) - m)^T - (\frac{n-1}{n})\hat{P}^+(t - \Delta t) - \hat{P}^+(t)] \quad (4.18)$$

where $m(t)$ is the state noise at time t , the first term of Equation (4.18) is the covariance of w at time t , n is the number of state noise samples.

The mean (r) and variance (R) of the measurement noise are shown in Equations (4.19) and (4.20), respectively.

$$r = \frac{1}{n} \sum_{t=1}^n r(t), \quad \text{where } r(t) = TT(t) - H(t) \hat{N}^-(t) \quad (4.19)$$

$$R = \frac{1}{n-1} \sum_{t=1}^n [(r(t) - r).(r(t) - r)^T - (\frac{n-1}{n})H(t)\hat{P}^-(t)H^T(t)] \quad (4.20)$$

where $R(t)$ is the observation noise at time t . The first term of Equation (4.20) is the covariance of v at time t , and n is the number of measurement noise samples. As a summary, the KF and AKF approaches use the same equations except for the fact that the AKF estimates the statistical parameters of the noise for every estimation step using Equations (4.17) to (4.20).

As found in Chapter 3, providing the system equations real-time estimates of ρ_{in} and ρ_{out} should improve the estimation accuracy. In this chapter, a single-loop detector was installed at the entrance of the tested link to produce real-time estimates of ρ_{in} . In contrast, in the next section, an ANN is developed to obtain real-time estimates for the ρ_{out} values.

4.4.3 Artificial Neural Network

ANN is a machine learning technique that aims to recognize relationships between vast amounts of data by employing a certain number of neurons in every single hidden layer to

achieve better accuracy [100]. The network consists of three main layers: the input layer, the hidden layer, and the output layer. This section takes into account the recommendation of using two market penetration rates (at the entrance and exit of the link) rather than one market penetration rate along the tested link in the KF equations [79]. Accordingly, the state equation and the H vector in the measurement equation are revised as presented in Equations (4.21) and (4.22). ρ_{in} and ρ_{out} are the CV LMP at the entrance and the exit of the link, respectively.

$$N(t) = N(t - \Delta t) + \Delta t \left[\frac{q^{in}(t)}{\rho_{in}(t)} - \frac{q^{out}(t)}{\rho_{out}(t)} \right] \quad (4.21)$$

$$H(t) = \frac{1}{\bar{q}(t)} = \frac{2}{\frac{q^{in}(t)}{\rho_{in}(t)} + \frac{q^{out}(t)}{\rho_{out}(t)}} \quad (4.22)$$

A single-loop detector was installed at the entrance of the link to measure ρ_{in} and also to use as an input to the ANN approach. Accordingly, this chapter develops an ANN approach to estimate ρ_{out} . The tested link is shown in Figure 4.1. The next section describes the selected inputs (features) and the output variables of the ANN approach.

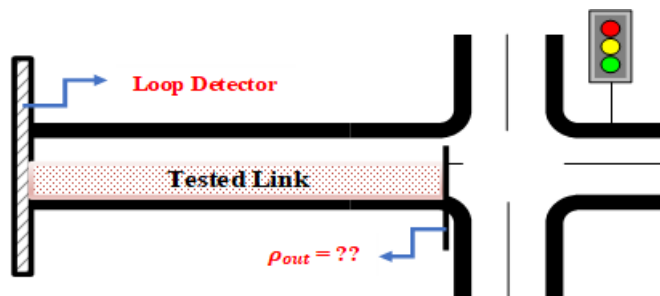


Figure 4.1: Tested link.

4.4.3.1 Characteristics of the ANN: Input and Output Variables

Previous research has used different features to build machine learning models [72, 73, 74, 75]. Fusing video and Bluetooth data was used to estimate traffic density and speed. The traffic

flow was manually extracted from the video records, while the speed data were constructed from the collected Bluetooth travel time data [72]. Another study relied on archived data of traffic speeds, counts, and density to estimate traffic speed [73]. Distance headway, number of stops, and speed data were identified as useful features to achieve accurate density estimates [74]. They employed loop detectors and CV data. In a recent study, Sekula et al. [77] used probe and automatic traffic recording station data to extract the features of the ANN model. The selected features were the (1) speed of CVs, (2) weather data such as temperature, visibility, precipitation, and weather status, (3) infrastructure data (speed limits, number of lanes, class of the road, and type of the road), (4) temporal data such as the day of the week, and (5) volume profiles based on historical data. The literature showed that the traffic speed is always used as a model feature, especially when CV data are used. In contrast, the traffic flow is always used when stationary sensors (e.g., loop detector) are used.

In this research, a fusion of CV and single-loop detector data is utilized to produce the ANN features. The single-loop detector was installed at the entrance of the link and thus ρ_{in} can be computed directly using Equation (4.3). The ρ_{out} variable is calculated from the ANN (the ANN output). Seven possible inputs (features) were considered in the ANN, as defined in Table 4.1. Conducting a feature selection technique to validate the importance of each feature for the ANN approach, the number of the model features was dropped to five features. It should be noted that the selected inputs can be easily extracted when CVs are on the link. ρ_{out} can be expressed as a function of the selected inputs, as presented in Equation (4.23).

$$\rho_{out} = f(A_t, A_p, u_s, S_1, S_2) \quad (4.23)$$

The ρ_{out} values vary between 0 and 1, the 0 value means that no CVs were observed at the exit of the link, while the value of 1 means that the D_{CV} value is the same as the D_t . The selected inputs must be relevant to the model output ρ_{out} to allow the ANN model to

Table 4.1: Definition of the ANN approach inputs.

| Input Symbol | Definition | Unit |
|----------------|---|-------|
| A_t | Total number of arrivals obtained from the single-loop detector | veh |
| A_{CV} | Total number of CV arrivals | veh |
| \bar{D}_{CV} | Total number of CV departures | veh |
| S_1 | Average speed for CVs at link entrance | km/hr |
| S_2 | Average speed for CVs at link exit | km/hr |
| u_s | Space-mean speed for CVs | km/hr |
| u_t | Time-mean speed for CVs | km/hr |

build a strong relationship between the model inputs and outputs, and therefore produce high estimation accuracy. For instance, in our case, the ρ_{out} value decreases as A_t and A_{CV} increase. For instance, a high value of A_t means that the link is more congested and thus the number of departures (D_t) is expected to be high. The ρ_{out} value also decreases with increasing speed (S_1 , S_2 , and u_s). The speed is an indicator of the congestion level of the link; for instance, if the speed is low, then more vehicles are expected to be on the link, leading to higher values of D_t .

A single hidden layer with one neuron, with a transfer function of hyperbolic tangent sigmoid, was used to build the ANN model as shown in Figure 4.2. The Levenberg–Marquardt (LM) optimization has been proven in the literature to outperform the gradient decent and conjugate gradient methods for medium-sized problems [101]. Furthermore, the LM is considered the fastest back-propagation algorithm and thus was implemented in the proposed approach. The weights and biases of the developed ANN approach are described below. w_1 depicts the weights between the input layer and the hidden layer, while w_2 represents the weight between the hidden layer and the output layer. b_1 and b_2 represent the biases at the hidden and output layers, respectively. Figure 4.2 describes the proposed AKFNN approach, combining the AKF approach with the ANN approach.

$$w_1 = [0.43 \quad 0.19 \quad -47.28 \quad 0.36 \quad -0.43], \quad w_2 = [1.70], \quad b_1 = [-46.62], \quad b_2 = [0.95]$$

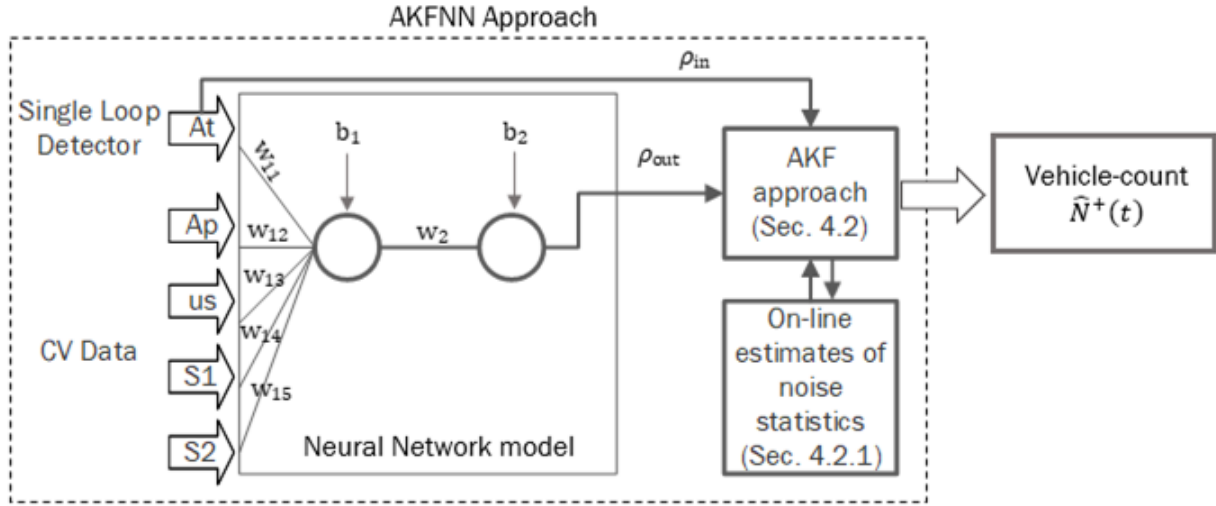


Figure 4.2: Flowchart for adaptive Kalman filter with a neural network (AKFNN) approach.

4.5 Results

This section evaluates the performance of the proposed estimation approaches. The first subsection evaluates the performance of the AKF approach and then compares the AKF with the KF (Section 4.5.1). The second subsection presents the performance of the ANN approach used for estimating the LMP of CVs at the exit of the link (ρ_{out}) (Section 4.5.2). The third subsection compares the performance of AKF with the AKFNN approach (Section 4.5.3). The fourth subsection investigates the sensitivity of the AKF estimation approach to the initial conditions (Section 4.5.4). The accuracy of the proposed approaches was evaluated based on the root mean square error (RMSE) as shown in Equation (4.24). The RMSE has been frequently used in the literature to measure the difference between the approach estimates and the actual values.

$$RMSE (veh) = \sqrt{\sum_{t=1}^n [\hat{N}^+(t) - N(t)]^2 / n} \quad (4.24)$$

where $\hat{N}^+(t)$ represents the estimated vehicle count values, $N(t)$ represents the actual vehicle count values, and n is the total number of estimations. All simulation scenarios start with the following initial conditions: an initial vehicle count estimate of zero ($\hat{N}^+(0) = 0$ veh), which is the same value of the actual vehicle count, and initial mean and the prior covariance

estimates of the state system ($m(0) = 2$ veh and $\hat{P}^-(0) = 75$ veh²) if the LMP scenario is less than or equal 60%, and ($m(0) = 9$ veh $\hat{P}^-(0) = 120$ veh²) if the LMP scenario is greater than 60%. The proposed approaches were evaluated using different CV LMPs, including 10%, 20%, 30%, 40%, 50%, 60%, 70%, 80%, and 90%. For each scenario, a Monte Carlo simulation was conducted to create 300 random samples of CVs from the full data set.

4.5.1 Comparison of the KF and the AKF Approaches

This section evaluates the proposed AKF approach with real-time estimates of the error statistical parameters for the state and the measurement. This section also compares the proposed AKF with the developed KF approach in [79], as shown in Table 4.2. Results show that the AKF outperforms the KF approach in most scenarios except for the scenarios with high LMPs (i.e., LMP of 80% and 90%). Results demonstrate the need to provide real-time estimates for the mean and variance error values in the state and measurement when dealing with low/medium LMPs. This happened due to high error in the fixed ρ value that was used, which then produced high error in the vehicle count estimate. The AKF improved the traditional KF vehicle count estimation accuracy by up to 29%. In contrast, for high LMPs, the user may proceed with predefined statistical values for the state and measurement (mean and variance error values), due to low errors in the vehicle count estimates (low error in the ρ value). In conclusion, a simple KF can be used with high LMPs without the need to change statistical noise parameters at every estimation step.

4.5.2 Developed ANN Approach

The ANN model was employed to estimate the (ρ_{out}) value, which is used to reflect the total number of vehicle departures from the given number of CV departures. The data set was divided into 70% for training, 15% for validation, and 15% for testing. The validation data set is used to measure network generalization and to avoid any over fitting problems [102].

Table 4.2: Root mean square error (RMSE) values using the Kalman filter (KF) and the adaptive Kalman filter (AKF) approaches.

| LMPs % | RMSE (veh) | | |
|--------|------------|-----|-----------------|
| | KF | AKF | Improvement (%) |
| 10 | 6.0 | 4.3 | 29 |
| 20 | 5.6 | 4.0 | 28 |
| 30 | 5.0 | 3.8 | 23 |
| 40 | 4.6 | 3.6 | 22 |
| 50 | 4.1 | 3.6 | 11 |
| 60 | 3.6 | 3.2 | 11 |
| 70 | 3.0 | 3.0 | 0 |
| 80 | 2.3 | 2.6 | -13 |
| 90 | 1.6 | 2.0 | -25 |

The developed ANN performance is shown in Table 4.3. The mean square error (MSE) is 0.01 and the R value is close to 1.0. The R value measures the correlation between model outputs and desired outputs. A value close to 1.0 means that the model outputs are very close to desired outputs. Figure 4.3 shows the error histogram for the training, validation, and testing data and their deviations from the zero error bar. Most of the errors lie around the zero error bar, which means that the developed ANN model appropriately addressed the research goal (i.e., estimating ρ_{out}). Figure 4.4 presents the estimated and actual values for the ρ_{out} at different LMPs.

Table 4.3: Developed artificial neural network (ANN) model performance measures for the training, validation, and testing data set.

| Data Set | Samples | MSE | R |
|------------|---------|--------|-------|
| Training | 346881 | 0.0171 | 0.872 |
| Validation | 74331 | 0.0170 | 0.872 |
| Testing | 74331 | 0.0173 | 0.871 |

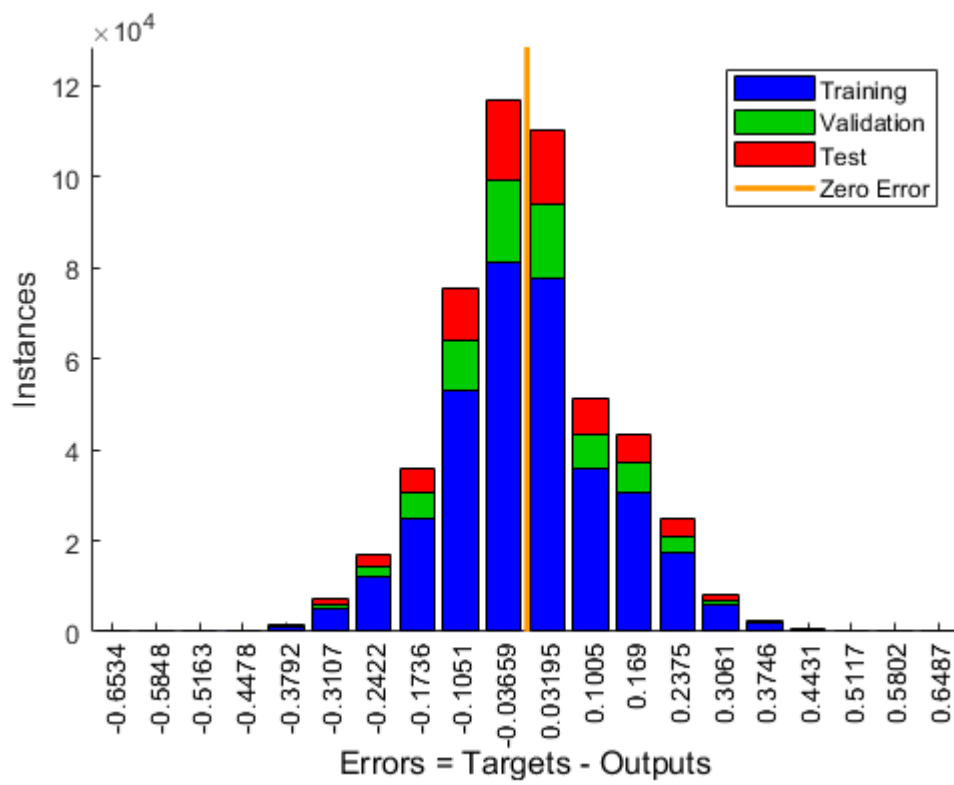


Figure 4.3: Error histogram for the training, validation, and testing data set.

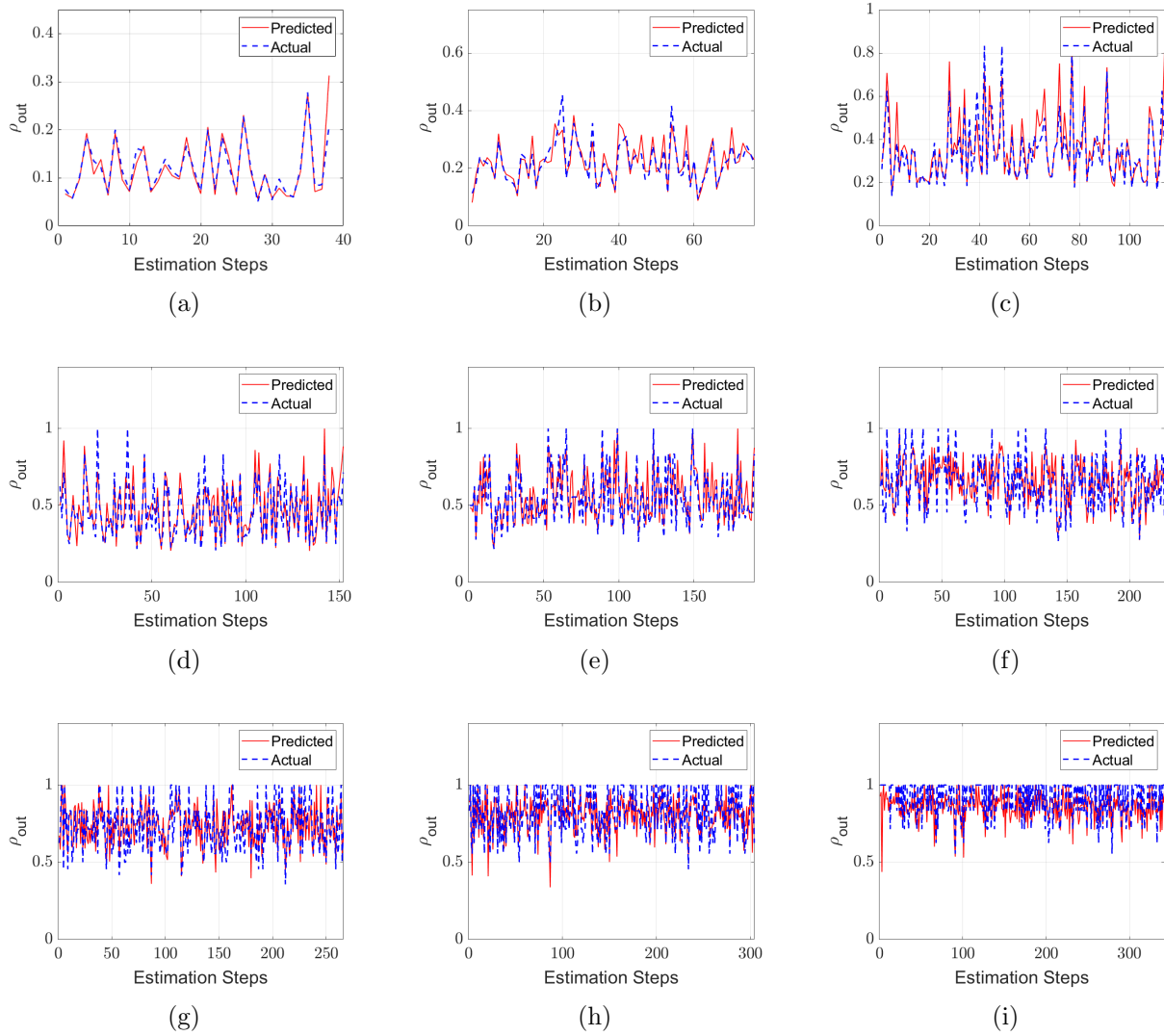


Figure 4.4: Actual and estimated values of ρ_{out} for different level of market penetration (LMP) scenarios: (a) 10%, (b) 20%, (c) 30%, (d) 40%, (e) 50%, (f) 60%, (g) 70%, (h) 80%, and (i) 90% LMP.

4.5.3 Comparison of the AKF and the AKFNN Approaches

This section demonstrates the impact of using two ρ values rather than using one predefined ρ value. The average predefined ρ value is defined as the value for the entire tested link. The average ρ value remains constant for the entire simulation for each LMP scenario. For instance, if the scenario of 10% LMP is tested, the ρ value in both the state and measurement is treated as a value of 0.1. In this chapter, we proposed the use of two ρ values; one at the entrance and one at the exit of the link to reflect the total number of arrivals and departures from the given total number of CV arrivals and departures, respectively.

ρ_{in} is measured directly using the installed loop detector at the entrance of the link. The developed ANN approach is used to estimate the ρ_{out} values (Section 4.5.2). Then, the ρ_{in} and ρ_{out} values are utilized in the AKF equations. Recall that the AKF approach relies only on CV data, while the AKFNN approach uses a fusion of CV and single-loop detector data.

In Table 4.4, the RMSE values using the AKF and the AKFNN approaches are presented. The results demonstrate the benefits of using the AKFNN approach rather than the AKF approach, where the estimation accuracy is improved by up to 26%. This finding proves what was recommended by Aljamal et al.'s previous study [42] to consider two ρ values rather than one value. As a result, the proposed AKFNN approach is robust and produces reasonable errors even with low LMPs. For instance, the estimated vehicle count values are off by 3.7 veh when the LMP is equal to 10%. Figure 4.5 presents the vehicle count estimation for different LMPs using the proposed AKFNN Approach.

Table 4.4: RMSE values using the AKF and the AKFNN approaches.

| LMPs % | RMSE (veh) | | |
|--------|------------|-------|-----------------|
| | AKF | AKFNN | Improvement (%) |
| 10 | 4.3 | 3.7 | 13 |
| 20 | 4.0 | 3.6 | 11 |
| 30 | 3.8 | 3.5 | 9 |
| 40 | 3.6 | 3.3 | 8 |
| 50 | 3.6 | 2.7 | 26 |
| 60 | 3.2 | 2.4 | 25 |
| 70 | 3.0 | 2.4 | 20 |
| 80 | 2.6 | 2.3 | 12 |
| 90 | 2.0 | 1.8 | 10 |

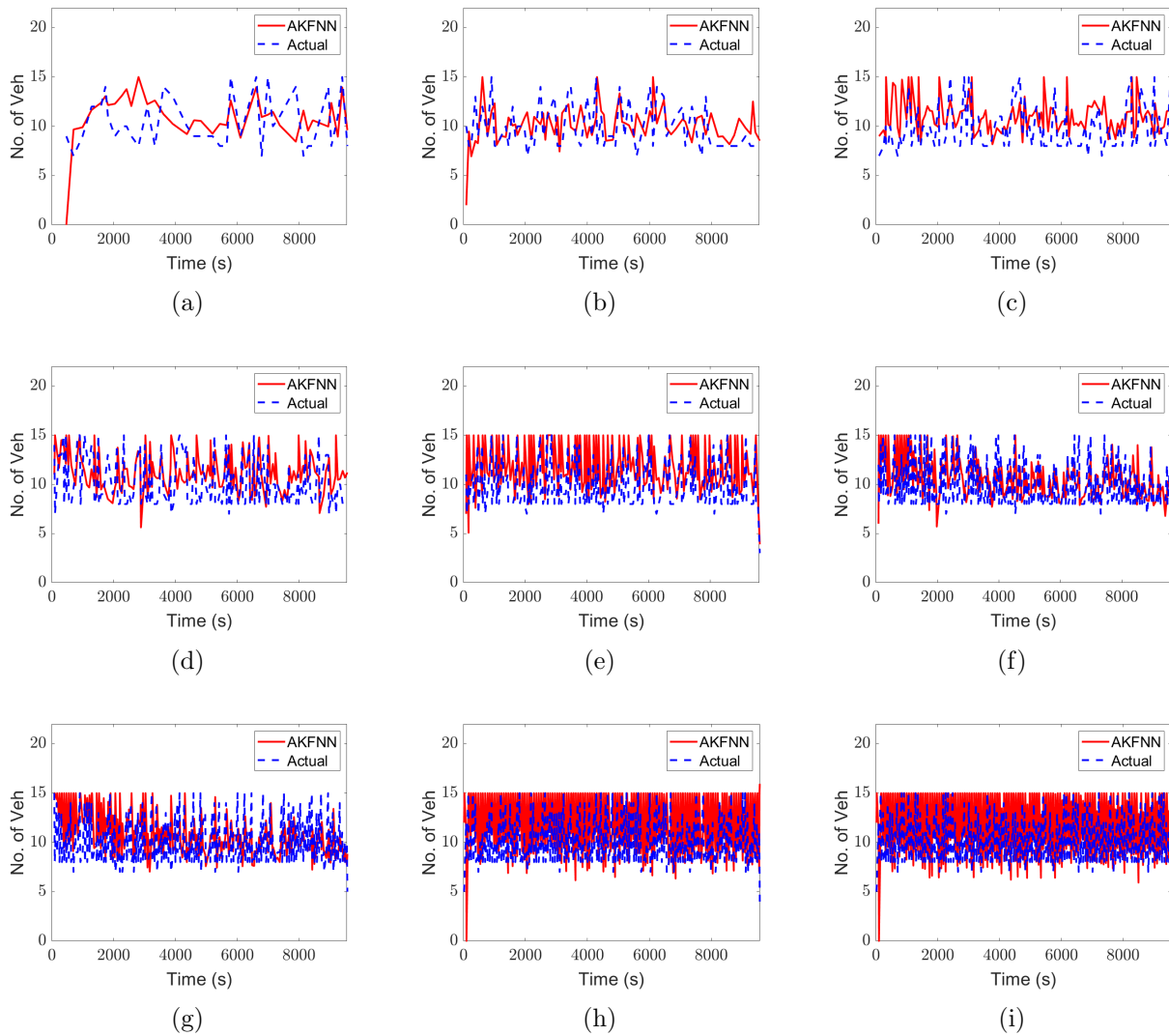


Figure 4.5: Actual and estimated vehicle counts over estimation intervals for different LMP scenarios: (a) 10%, (b) 20%, (c) 30%, (d) 40%, (e) 50%, (f) 60%, (g) 70%, (h) 80%, and (i) 90% LMP.

4.5.4 Impact of the Initial Conditions on the AKF Approach

The KF, traditional and adaptive, is sensitive to the initial condition parameters, such as the posterior state estimate ($N_i = \hat{N}^+(0)$), the mean of state noise ($m_i = m(0)$), and the prior error covariance estimate ($P_i = \hat{P}^-(0)$). These parameters are tuned by a trial-and-error technique to find the best initial condition values for seeking better KF estimation outcomes. However, in real applications, trial-and-error is not realistic and not easy to achieve. Hence, this section investigates the impact of initial conditions on the accuracy of the vehicle count estimation.

4.5.4.1 Impact of Initial Estimate of the Vehicle Count (N_i)

For the initial estimate value of the vehicle count (N_i), different values were evaluated (ranges from 0 to 10 at increments of 1). In this chapter, remember that all simulation scenarios start with an initial estimate of zero ($N_i = 0$ veh), which is the same value as the actual vehicle count. Figure 4.6(a) presents the RMSE values for different N_i values for the scenario of 10% LMP. As shown in the figure, the values of 8 and 10 produce the lowest RMSE. The RMSE value is equal to 4.3 veh when N_i is equal to 0. In contrast, the RMSE value is equal to 3.9 veh when N_i is equal to 8. As a result, starting the AKF approach with the best initial estimate (e.g., $N_i = 8$ veh) would reduce the errors and therefore improve the estimation accuracy.

4.5.4.2 Impact of Initial Mean Estimate of the State System (m_i)

Another critical initial parameter in the AKF approach is m_i . This parameter represents the mean value of the noise in the state equation. This chapter tests 16 different m_i values (i.e., 0, 1, 2, 3, 4, 5, 6, 7, 8, 9, 10, 11, 12, 13, 14, and 15). Figure 4.6(b) presents the vehicle count estimation RMSE values for different m_i values. The RMSE value is equal to 4.7 veh when the simulation starts with a 0 value of m_i . In contrast, the RMSE value is 3.9 veh when the

value of m_i is equal to 11.

4.5.4.3 Impact of Initial Prior Covariance Estimate of the State System (P_i)

The last parameter tested in this chapter is the initial prior estimate of error covariance P_i . The error covariance parameter describes the accuracy of the state system. For instance, if the covariance value is low, then the state outcome is accurate and close to the actual value. As stated in the literature, the initial parameters should always be tuned to achieve accurate estimation accuracy. Thirteen different P_i values were tested (i.e., 5, 10, 15, 20, 25, 50, 75, 100, 120, 150, 200, and 250). Figure 4.6(c) presents the RMSE values using different P_i values. The P_i value of 150 veh² produces the lowest RMSE values.

The research presented in this chapter evaluates the proposed approaches as they should be in real-world applications. Therefore, the trial-and-error technique was avoided since it is not a valid solution in the field. However, it was noticed that previous research always tunes the initial parameters to determine the best initial conditions when testing their estimation approaches [20, 21, 23]. If that is the case, let us assume that the proposed AKFNN approach always starts with the best initial value of P_i , which would produce less errors. Table 4.5 presents the RMSE when considering the trial-and-error technique (Tuned AKFNN). The AKFNN and the Tuned AKFNN approaches used the same values of N_i and m_i , but they

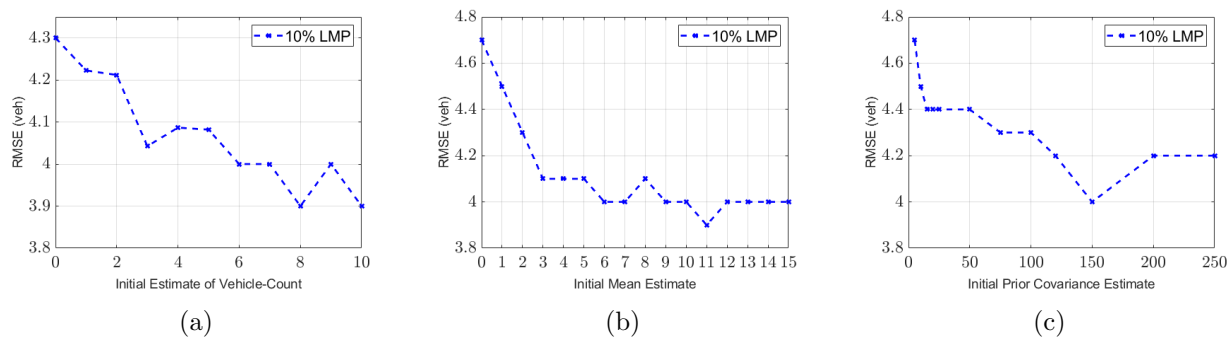


Figure 4.6: Impact of the initial conditions on the AKF approach: (a) Initial estimate values N_i , (b) Initial mean estimate values m_i , and (c) Initial covariance estimate values P_i .

used different P_i values. N_i is assumed to be zero, while m_i has two values based on the tested scenario: a value of 2 veh when low LMP scenarios are tested (LMP $\leq 60\%$), and a value of 9 veh with high LMP scenarios (LMP $> 60\%$). From the table, tuning the P_i value significantly improves the estimation accuracy for all scenarios (by up to 27%). For instance, at 10% LMP, the estimation error dropped from 3.7 to 3.3 vehicles. On the other hand, the estimated vehicle count values are off by 2.8 vehicles instead of 3.6 vehicles for the scenario of 20% LMP.

In conclusion, the AKF approach was proven to be very sensitive to the initial conditions (N_i, m_i, P_i). Hence, starting the simulation with good assumptions of the initial conditions can significantly improve the estimation accuracy, as shown in Table 4.5. Finally, Table 4.6 presents the performance of the approaches discussed in the chapter.

Table 4.5: Impact of applying the trial-and-error technique for the initial value of covariance P_i .

| LMPs % | RMSE (veh) | | |
|--------|------------|-------------|-----------------|
| | AKFNN | Tuned AKFNN | Improvement (%) |
| 10 | 3.7 | 3.3 | 11 |
| 20 | 3.6 | 2.8 | 22 |
| 30 | 3.5 | 2.7 | 23 |
| 40 | 3.3 | 2.4 | 27 |
| 50 | 2.7 | 2.1 | 22 |
| 60 | 2.4 | 2.1 | 13 |
| 70 | 2.4 | 2.1 | 13 |
| 80 | 2.3 | 1.8 | 22 |
| 90 | 1.8 | 1.5 | 17 |

4.6 Summary and Conclusions

The chapter proposed a novel AKF approach for estimating the number of vehicles on signalized approaches using only CV data. An AKF approach was developed to provide real-time estimates of the statistical properties (mean and variance) for the state and measurement errors. The state equation is derived from the traffic flow continuity equation, while the measurement equation is constructed using the traffic hydrodynamic equation. Results show

Table 4.6: RMSE values for the KF, the AKF, the AKFNN, and the tuned AKFNN approaches.

| LMPs % | RMSE (veh) | | | |
|--------|------------|-----|-------|-------------|
| | KF | AKF | AKFNN | Tuned AKFNN |
| 10 | 6.0 | 4.3 | 3.7 | 3.3 |
| 20 | 5.6 | 4.0 | 3.6 | 2.8 |
| 30 | 5.0 | 3.8 | 3.5 | 2.7 |
| 40 | 4.6 | 3.6 | 3.3 | 2.4 |
| 50 | 4.1 | 3.6 | 2.7 | 2.1 |
| 60 | 3.6 | 3.2 | 2.4 | 2.1 |
| 70 | 3.0 | 3.0 | 2.4 | 2.1 |
| 80 | 2.3 | 2.6 | 2.3 | 1.8 |
| 90 | 1.6 | 2.0 | 1.8 | 1.5 |

that the proposed AKF approach outperforms the traditional KF (improves the estimation accuracy by up to 29%), demonstrating the need to use real-time values of the statistical noise parameters in the KF approach.

Two estimation approach were presented, namely (a) the AKF and (b) the AKFNN. The AKF approach uses only CV data assuming a fixed LMP value that is obtained from historical data, while the AKFNN uses a fusion of CV and single-loop detector data with real-time estimates of the LMP values (ρ_{in} and ρ_{out}). In this chapter, a robust ANN approach was developed to provide accurate real-time estimates of the ρ_{out} values. The selected features of the ANN approach are A_t (observed from the single-loop detector), A_{CV} , u_s , S_1 , and S_2 (observed from CVs).

The AKF and the ANN were combined to develop the novel AKFNN approach. Results demonstrate that the AKFNN approach significantly improves the vehicle count estimation accuracy since the ρ_{in} and ρ_{out} values are estimated better. Subsequently, the chapter compared the AKF with the AKFNN approaches, showing that the AKFNN approach outperforms the AKF, enhancing the estimation accuracy by up to 26%.

Finally, the chapter investigated the impact of the initial conditions (N_i , m_i , and P_i) on the AKF performance. Results show that the AKF approach is very sensitive to the initial

conditions. For instance, starting the simulation with an N_i value of 8 instead of 0 improves the estimation accuracy by 10%. In addition, starting the simulation with an m_i value of 11 instead of 2 enhances the estimation accuracy by up to 10%. For the P_i parameter, an improvement of 7% could occur if the simulation starts with an initial value of 150 instead of 75 veh^2 . The chapter also tested the accuracy of the AKFNN estimation by allowing the P_i parameter to be tuned (Tuned AKFNN approach), showing that more improvement could be achieved. Specifically, the Tuned AKFNN improves the accuracy by up to 27%.

In conclusion, both approaches (AKF and AKFNN) produce high estimation accuracy when compared with the state-of-the-art KF approach.

Chapter 5

Enhancement of the Kalman Filter Approach using a Bounded ρ in the State-Space Model

This chapter is an edited version of: Mohammad A. Aljamal, Hossam Abdelghaffar, and Hesham A. Rakha (2020), “Real-Time Estimation of Vehicle Counts on Signalized Intersection Approaches Using Probe Vehicle Data,” published in the *IEEE Transactions on Intelligent Transportation Systems* [42].

This chapter presents a novel approach for estimating the number of vehicles traveling along signalized links using connected vehicle data only. The proposed approach uses the Kalman Filtering technique to produce reliable vehicle count estimates using real-time connected vehicle estimates of the expected travel times. The proposed approach introduces a novel variable estimation interval that allows for higher estimation precision, as the updating time interval always contains a fixed number of connected vehicles. The proposed approach is evaluated using empirical and simulated data, the former of which were collected along a signalized roadway in downtown Blacksburg, VA. Results indicate that vehicle count esti-

mates produced by the proposed approach are accurate. The chapter also examines the model's accuracy when installing a single stationary sensor (e.g., loop detector), producing slight improvements especially when the connected vehicle market penetration rate is low. Finally, the chapter investigates the sensitivity of the estimation approach to traffic demand levels, showing that the model works better at higher demand levels given that more connected vehicles exist for the same market penetration rate.

5.1 Introduction

The number of on-road vehicles has increased rapidly over the past few decades. For example, in the U.S., the number of motor vehicles registered from 1990 to 2016 increased by more than 75 million vehicles [1], leading to serious traffic congestion in many areas. One potential approach of mitigating traffic congestion is expanding the current infrastructure by adding new lanes and roadways to accommodate growing traffic demands; however, this comes with significant associated costs. A more efficient way of solving traffic congestion is improving traffic management strategies by using advanced technologies and algorithms. Among the more recent technologies utilized for traffic management are Intelligent Transportation Systems (ITSs). ITS applications are developed to enhance transportation system efficiency, mobility, and reduce environmental impacts. In general, ITS aims at improving the infrastructure side of technology via sensors, communication, controllers, etc. Advanced Traffic Management Systems (ATMSs) constitute one ITS approach. ATMSs include advanced traffic signal control systems that optimize traffic signal timings in real-time [4, 7, 103, 104].

Traffic density is defined as the number of vehicles on a given roadway segment divided by the length of the segment [8]. Knowing the number of vehicles on a specific roadway segment is crucial in developing efficient adaptive traffic signal controllers; however, it is difficult to measure traffic density directly in the field. Moreover, traffic occupancy measurements from loop detectors represent a temporal estimate of the traffic stream density around the measurement location. The research described herein attempts to estimate the number of vehicles, both queued and moving, along signalized roadway links (e.g., urban roadways) using only connected vehicle (CV) data. To the authors' knowledge, this work is the first attempt to estimate vehicle counts based solely on CV data. This estimation approach will provide key input to real-time traffic signal controllers, leading to a reduction in intersection delays, vehicle emissions, and vehicle crashes.

5.2 Literature Review

Past research has used different technologies/techniques, such as loop detectors [23, 33, 34, 35], video detection systems [36], or data fusion techniques [20, 21, 39, 40] (combining two different sources of data) to estimate the number of vehicles on signalized links. However, these techniques suffer from poor detection accuracy and have high installation costs. Emerging technologies, such as connected vehicle (CV) technology, can provide and share vehicle real-time location and speed data. These sample data can be exploited and used to estimate the traffic density without the need to install additional hardware.

Numerous studies have attempted to estimate vehicle counts. For example, Ghosh and Knoop [33] demonstrated that vehicle counts can be improved by dividing the roadway into small segments (half-mile) to produce an efficient estimation. Another study used traffic flow and occupancy data from two conventional loop detectors to estimate the number of vehicles traveling along a specific road segment using the flow continuity equation [34]. Vigos et al. proposed a robust algorithm that requires at least three loop detectors on a roadway segment in order to estimate the number of vehicles [23]; however, the cost of implementing such algorithms in the field is high. For example, imagine that the estimation is required for a city like New York, which has almost 12,460 signalized intersections [105]. If each intersection has four approaches, it would be necessary to install 150,000 detectors in order to make a proper estimate, which is an unreasonable proposition. Bhourri et al. proposed a scalar KF in order to estimate the number of vehicles on an on-ramp section, using a recorded film to observe the density measurements [35], utilizing the equation of conservation of cars as a state equation. Another study measured vehicle counts by matching vehicle signatures recorded by a network of wireless magnetic sensors [106]. An algorithm of video image processing was deployed by Beucher et al., in which images were first collected from different scenes along a 150 m section, and then filters were used to detect the vehicle markers; however, this approach is difficult to utilize in the field.

Recently, data fusion has been widely used to estimate the number of vehicles along certain

roadway sections, with the aim of achieving better accuracy than using only one source of data. In many of the works using data fusion, the Kalman Filtering (KF) technique [30] was employed for estimating traffic density. One study achieved accurate estimated traffic density results using the traffic flow values measured from a video detection system and the travel time obtained from vehicle GPSs [20]. The approach in this chapter is similar to that work in some aspects, but differs in two significant ways, namely: only CV data are used and furthermore the updating time interval is considered as a variable rather than a fixed value (the updating time interval was 1 minute in [20]). Van Erp et al. used data fusion to estimate the number of vehicles along an on-ramp segment [39]. They used traffic flow data from loop detectors and aggregated speeds from floating cars, the latter provided by Google, and set a 300 s fixed updating interval. Another study used loop detectors and CV data to estimate freeway traffic density [40], relying on IntelliDrive technology (vehicle infrastructure integration) at a predefined updating time interval. Anand et al. used video and GPS data to estimate the number of vehicles along a roadway segment [21]. In that study, video captured the traffic flow at the segment's entrance and exit points, while GPS data provided travel time measurements.

Several researchers have used the KF technique to enhance estimates in various transportation applications, such as speed [57, 82], travel time [59, 84], and traffic flow [47]. An unscented KF deployed for speed estimation using single loop detectors [82] with a nonlinear state-space equation, was able to improve the speed estimates. Another study employed a linear KF technique to estimate speed, relying on the relationship between the flow-occupancy ratio and vehicle speed [57], yielding acceptable speed estimates for congested traffic conditions. A cumulative travel-time responsive (CTR) real-time intersection control within a CV environment was also developed using the KF technique [84]. In that study, the authors recommended having at least 30% levels of market penetration (LMPs) in order to realize the CTR algorithm's benefits.

In summary, the existing literature showed the benefits of using the KF technique to reduce errors and address different aspects of the traffic state estimation problem. Accordingly,

the KF technique was adopted in this chapter. One commonality of the aforementioned studies is that they all estimated the number of vehicles using one source of data from fixed sensors (e.g., loop detectors) or using fused source data (e.g., video with GPS data) utilizing a predefined updating interval.

In this chapter, a scalar KF approach was applied to estimate real-time vehicle counts along signalized links using both real and simulated traffic data. This estimation technique was applied to a signalized link in downtown Blacksburg, VA. The proposed approach extends the-state-of-the-art in vehicle count estimates by making four major contributions:

1. This chapter defines the estimation interval as a variable rather than a fixed value. The estimation time interval is defined as the point at which exactly n CVs traversed the tested link.
2. This chapter relies only on CV data. Different CV LMPs were also tested, and recommendations for future research are presented.
3. This chapter examines the estimation accuracy when adding a single loop detector, and a sensitivity analysis is made in terms of the optimum location of the stationary sensor.
4. This chapter investigates the sensitivity of the proposed estimation model to different factors including the length of the link and the level of traffic congestion.

This chapter is organized as follows: Section 5.3 describes the estimation method and the problem formulation. Section 5.4 describes the data collected from downtown Blacksburg, VA. Section 5.5 shows the results of the new proposed model. Section 5.6 presents the conclusions of the chapter.

5.3 Estimation Approach

5.3.1 Define the Estimation Interval Time

Unlike other studies, this work defined the estimation time interval as a variable rather than a fixed value. This new approach enhances the estimation at low LMPs, as shown later in the Results section. For example, if the link's LMP is 10%, the number of CVs will obviously be low. If we treat the problem using a fixed estimation interval, then the probability of observing zero CVs within an interval will be high for short estimation interval durations, making the estimation inefficient and inaccurate. Accordingly, low LMPs require long intervals (e.g., 300 s) to ensure that at least one CV is on the link. In contrast, links with high LMPs can use short estimation intervals (e.g., 20 s). One of the major contributions of this chapter was to address this issue to produce an efficient and convenient way of determining the duration of the estimation period.

For this work, the updating time interval was defined as the time when an exact number of CVs traversed the link (i.e. reached the traffic signal stop bar) reflecting a pre-defined sample size (n). This new approach ensures that the same number of CVs are used for each updating time interval. Thus, using this approach, the population confidence interval will be a fixed scaling of the sample confidence interval. This approach also ensures that there will be sufficient information about the CVs. Consequently, the average travel time (TT) value in Equation (5.13) will always be observed.

5.3.2 Formulation

This section defines the proposed formulation to estimate the total number of vehicles along a signalized link. The proposed approach utilizes the KF technique, which is comprised of two equations: (a) a state equation and (b) a measurement equation. The state equation is based on the traffic flow continuity equation as defined in Equation (5.1), while the measure-

ment equation is based on the hydrodynamic relation of traffic flow given in Equation (5.3). The KF is a recursive estimation model that continuously repeats the state estimations and corrections. Equation (5.1) computes the number of vehicles by continuously adding the difference in the number of vehicles entering and exiting the section to the previously computed cumulative number of vehicles traveling along the section. This integral results in an accumulation of error that requires fixing, and thus the need for the measurement equation.

$$N(t) = N(t - \Delta t) + \frac{\Delta t}{\rho} [q^{in}(t) - q^{out}(t)] \quad (5.1)$$

Here $N(t)$ is the number of vehicles traversing the link at time (t) , Δt is the duration of the variable updating time interval, $N(t - \Delta t)$ is the number of vehicles traversing the link in the previous interval, q^{in} and q^{out} are the CV flows entering and exiting the link between $(t - \Delta t)$ and (t) , respectively, and ρ is the LMP of CVs. The equation above produces accurate results if the scaled traffic flows (q^{in}/ρ^{in} and q^{out}/ρ^{out}) are accurate [107]. The total counts can be extracted from traditional loop detectors or video detection systems. We should note here that the ρ value in Equation (5.1) plays a major role in delivering accurate outcomes. The ρ is defined as the ratio of the number of CVs (N_{CV}) to the total number of vehicles (N_{total}), as shown in Equation (5.2). For instance, if ρ is 0.5, and the number of CVs is 5, then the expected total number of vehicles is 10.

$$\rho = N_{CV}/N_{total} \quad (5.2)$$

Equation (5.3) describes the hydrodynamic relationship between the macroscopic traffic stream parameters (flow, density, and space-mean speed).

$$q = ku \quad (5.3)$$

Where q is the traffic flow (vehicles per unit time), k is the traffic stream density (vehicles per unit distance), and u is the space-mean speed (distance per unit time). The space-mean speed can be replaced using Equation (5.4).

$$u = D/TT \quad (5.4)$$

where D is the link length, and TT is the average vehicle travel time. Since CVs can share their instantaneous locations every Δt , the travel time of each CV can be computed for any

road section. Thus, the CV travel time is used in the measurement equation, as shown in Equations (5.5), (5.6), and (5.7).

$$TT(t) = D \times \frac{k(t)}{\bar{q}(t)} \quad (5.5)$$

$$TT(t) = \frac{1}{\bar{q}(t)} [k(t) \times D] = \frac{1}{\bar{q}(t)} N(t) \quad (5.6)$$

$$TT(t) = H(t) \times N(t) \quad (5.7)$$

Where \bar{q} is the average traffic flow entering and exiting the link, and $H(t)$ is a transition vector that converts the vehicle counts to the average travel time. $H(t)$ is the inverse of the average flow (i.e. the first term of Equation (5.6)), as shown in Equation (5.8).

$$H(t) = \frac{1}{\bar{q}(t)} = \frac{2 \times \rho}{q^{in}(t) + q^{out}(t)} \quad (5.8)$$

The proposed estimation approach can be solved using the KF equations, as follows:

$$\hat{N}^-(t) = \hat{N}^+(t - \Delta t) + \frac{\Delta t}{\rho} [q^{in}(t) - q^{out}(t)] \quad (5.9)$$

$$\hat{TT}(t) = H(t) \times \hat{N}^-(t) \quad (5.10)$$

$$\hat{P}^-(t) = \hat{P}^+(t - \Delta t) \quad (5.11)$$

$$G(t) = \hat{P}^-(t)H(t)^T [H(t)\hat{P}^-(t)H(t)^T + R]^{-1} \quad (5.12)$$

$$\hat{N}^+(t) = \hat{N}^-(t) + G(t) [TT(t) - \hat{TT}(t)] \quad (5.13)$$

$$\hat{P}^+(t) = \hat{P}^-(t) \times [1 - H(t)G(t)] \quad (5.14)$$

Where \hat{N}^- is the a priori estimate of the vehicle counts calculated using the measurement prior to instant t , and \hat{P}^- is the a priori estimate of the covariance error at instant t . The Kalman gain (G) is computed using Equation (5.12). The R variable is the covariance error of the measurements. The posterior state estimate \hat{N}^+ and the posterior error covariance estimate \hat{P}^+ are updated using Equations (5.13) and (5.14), after considering the CV travel time measurements.

It should be noted here that the ρ value in Equation (5.9) impacts the estimation accuracy significantly especially for low LMPs (e.g., LMP < 30%) given that it scales the estimated values. For instance, for a ρ value of 0.1, the second term of Equation (5.9) is scaled by a factor of 10, which results in large errors in the vehicle counts. A real illustrative example using empirical data is described in Table 5.1. This example shows the impact of low LMPs in the state equation (i.e., $\rho = 0.1$). For the first estimation step, the total number of arrivals (A_T) and departures (D_T) within the polling interval are 65 and 60 as displayed in Table 5.1, whereas the number of CV arrivals (A_{CV}) and departures (D_{CV}) for the same polling interval are 6 and 5, respectively. The first estimation starts with an erroneous initial vehicle count estimate $\hat{N}^+(0) = 5$ vehicles while the real number is zero as is done in [23], the actual total number of vehicles on the link would then be 5 vehicles ($0 + (65 - 60)$). Applying Equation (5.9) would produce an estimated total of 15 ($5 + (6 - 5)/0.1 = 15$). Note that if the ρ value in Equation (5.9) is constrained by a lower bound it can prevent the state equation from producing such large errors. For the same example, if the ρ lower bound in Equation (5.9) is set to be equal 0.5, the total number of vehicles is estimated to be 7 ($5 + (6 - 5)/0.5$). As can be seen from this example, the absolute error using a lower bound of 0.5 is 2 vehicles, whereas the absolute error using the estimated total counts is 10 vehicles. Consequently, it is much easier for the KF to correct a small error rather than a large error after applying the measurement equation. Figure 5.1 compares the vehicle counts using the state equation; Equation (5.9) with and without a lower bound on ρ , along the estimation steps for the 10% LMP scenario. It is clear that having a lower bound on ρ in the state equation improves its accuracy by reducing the distance from the actual vehicle count line (the green line in Figure 5.1). The reason behind not allowing the market penetration to be very small is that: (1) we use a single ρ value estimate to approximate the two ρ values (upstream and downstream of the link); and (2) if the ρ value is very small, the approximation error is inflated, producing a larger error in the estimated total number of vehicles. Consequently, Equation (5.9) can be re-written as presented in Equation (5.15). The ρ factor in the state equation becomes the maximum of the historic ρ value and a lower bound (ρ_{min}), taken to be

0.5 in the analysis after examining different ρ_{min} values; from 0.1 to 0.9 as presented in Table 5.2. Note that further work in the future is needed to develop procedures to provide more accurate estimates of the two market penetration rates; namely, the one at the entrance of the link and the one at the exit of the link.

$$\hat{N}^-(t) = \hat{N}^+(t - \Delta t) + \Delta t \frac{[q^{in}(t) - q^{out}(t)]}{\max(\rho, \rho_{min})} \quad (5.15)$$

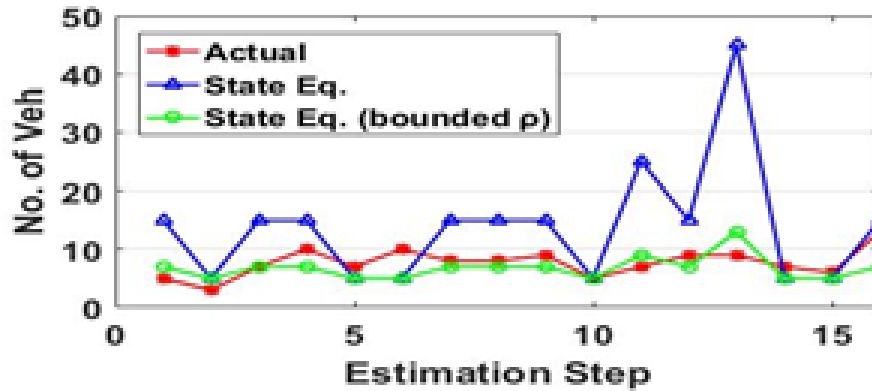


Figure 5.1: Impact of applying a lower bound in the state equation estimates.

5.3.3 Proposed Estimation Approaches

This section describes two estimation approaches. The first approach uses only CV data with a fixed ρ along the estimation intervals (e.g., $\rho = 20\%$), while the second approach utilizes fused data (CV and single loop detector data), where the single loop detector provides the estimation model with actual ρ values.

5.3.3.1 First Approach: CV Data Assuming Fixed LMP (ρ)

The ρ value is an important variable in the proposed estimation approach since it scales the CV measurements to reflect the total flow. The first estimation approach uses a fixed ρ value in the estimation steps, observed from historical data. It should be noted that producing accurate estimates of the actual ρ values will produce perfect estimation outcomes as long as there are no errors in the data; the ρ values can be observed every time interval with the addition of a fixed sensor (e.g., a traditional loop detector or video detection system) to measure the total flow. The predefined ρ value in Equations (5.8) and (5.9) is computed as the arithmetic mean of all ρ observations. For instance, Figure 5.2 shows the actual ρ values versus the predefined ρ value as the red line ($\rho = 20\%$). This figure clearly shows errors in the ρ value estimate. However, the KF reduces the errors produced from the fixed ρ assumption, as shown later in the Results section. The varying ρ values that appear in the figure is evidence that the proposed approach works well with noisy data.

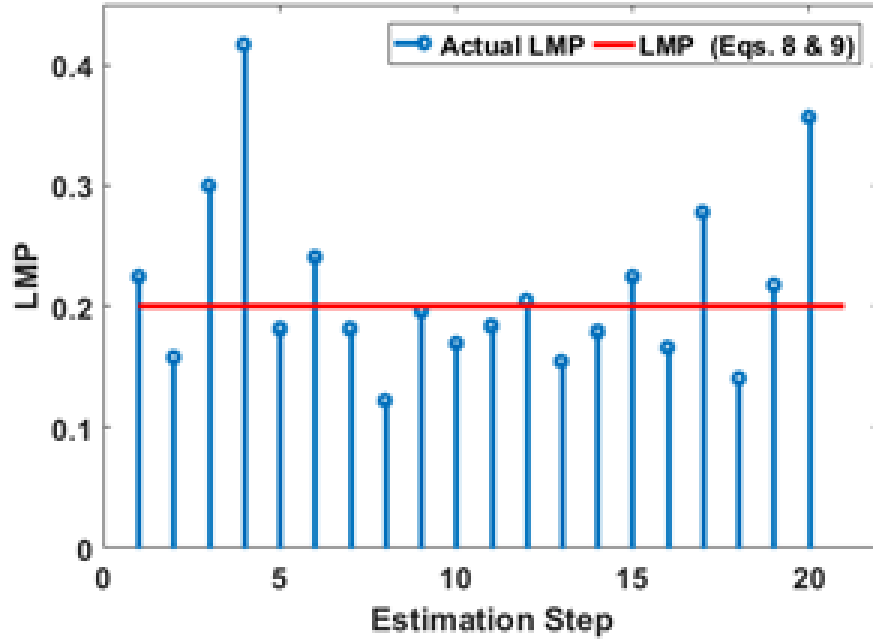


Figure 5.2: Variation in actual LMP over all the estimation intervals.

5.3.3.2 Second Approach: Fusion Data with Variable LMP (ρ)

This section employs a single loop detector in addition to CV vehicle data to estimate the LMP. The loop detector is used to observe the actual total flow and then compute the ρ values in the measurement equation for all the estimation times (t). The loop detector produces the total traffic flow, which can then be used to compute (N_{total}) in Equation (5.2). The new proposed estimation approach uses the same equations in the formulation section except that the measurement equation considers the actual ρ values in the H vector, as shown in Equation (5.16).

$$H(t) = \frac{2 \times \rho(t)}{q^{in}(t) + q^{out}(t)} \quad (5.16)$$

5.4 Data Collection

This chapter evaluates the proposed estimation approaches using both empirical and simulated data. This section will describe both the data and the link characteristics. The

simulated data were used to provide additional data to test the KF estimator for varying conditions (e.g., traffic demand levels and link lengths).

5.4.1 Empirical Data

Figure 5.3 shows the tested link in downtown Blacksburg, VA. The link falls between two traffic signals. The two observer locations define the link length, as shown in Figure 5.3. The link length is approximately 74 meters based on Google Maps, and the speed limit is 25 mi/h (40 km/h). The two observers recorded the time stamp that each vehicle passed them. Using the data, it was possible to conduct a Monte Carlo simulation to extract a random sample of CVs to compute (q^{in} and q^{out}) and use them in Equation (5.15).

The team went to the field to collect actual field data for 75 minutes on March 29, 2018, between 4:00 and 5:15 p.m., observing a total of 813 vehicles. The full data served as the ground truth values, and thus our estimation approach outputs were compared to these actual values. The collected data also included the observed travel time between Observer 1 and Observer 2 (from the beginning to the end of the link). The tested link had no roadway entrances or exits between the two observers and thus the flow continuity was maintained.

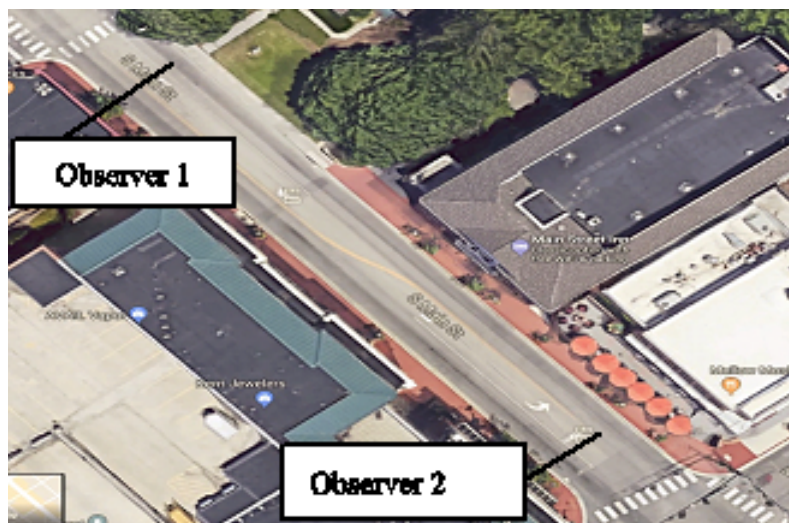


Figure 5.3: Tested link in downtown Blacksburg, VA. (source: Google Maps)

5.4.2 Simulation Data

INTEGRATION [108, 109, 110], a microscopic traffic simulation software, was used to validate and test the accuracy of the proposed approach. The INTEGRATION software has been extensively validated and demonstrated to replicate empirical observations [94, 95, 96, 97, 98, 99]. Specifically, INTEGRATION was used to create synthetic data for conditions not observed in the field to quantify the sensitivity of the proposed approach to the link length and traffic demand level. Specifically, a range of link lengths were tested (i.e., 74, 150, 200, 300, and 400 m), as shown later in the Results section. The link characteristics were calibrated to local conditions using typical values, which included a free-flow speed of 40 km/h, a speed-at-capacity of 32 km/h, a jam density of 160 veh/km/lane, and a base saturation flow rate of 1800 veh/h/lane, which resulted in a roadway capacity of 855 veh/h given the cycle length and green times of the traffic signal. The traffic signal operated at a cycle length of 120 s and a 50:50 phase split. The amber and all-red interval was 3 s. These values were consistent with what was coded in the field.

5.5 Results and Discussion

The accuracy of the proposed KF approach was tested using real and simulated data. The evaluation of all scenarios was based on the Relative Root Mean Square Error (RRMSE) and the Root Mean Square Error (RMSE), shown in Equations (5.17) and (5.18), respectively. The two measures are frequently used in the literature to compute the difference between the approach estimates and the actual values.

$$RRMSE(\%) = 100 \sqrt{S \sum_{s=1}^S [\hat{N}^+(s) - N(s)]^2 / \sum_{s=1}^S N(s)} \quad (5.17)$$

$$RMSE(veh) = \sqrt{\sum_{s=1}^S [\hat{N}^+(s) - N(s)]^2 / S} \quad (5.18)$$

Where $N(s)$ represents the actual values, $\hat{N}^+(s)$ represents the estimated vehicle count values, and S is the total number of estimations. The simulation starts with an erroneous initial estimation $\hat{N}^+(0) = 5$ veh while the real number is zero as in [23], initial posterior estimate error $\hat{P}^+(0) = 5$, and measurement error covariance (R) is assumed to be 5. The proposed approach was evaluated using different CV LMPs, including 10, 20, 30, 40, 50, 60, 70, 80, and 90%.

5.5.1 Empirical Data

5.5.1.1 Sample Size Impact on KF Estimator Performance

In this study, the estimation time interval was defined as the time when a prescribed number of CVs traversed the link (vehicles passed the traffic signal stop bar) representing the desired sample size (n). This new approach ensures that the same number of CVs are used every updating estimation time interval. First, an optimal sample size (n) is needed in the estimation equations. Different sample size values were tested (i.e., 1, 2, 3, 4, 5, 6, 7, 8, 9, and 10). In the proposed approach, the sample size (n) was used to identify the estimation time step; producing a variable estimation time step. Table 5.3 presents the RRMSE values for the tested sample sizes, RRMSE values for some sample sizes are close, especially in the values between five and eight. Consequently, the sample size (n) can be different depending on the data. In this section, the optimal sample size was defined to be five, once the fifth vehicle passed the second observer, the TT variable (the arithmetic mean travel time for the five vehicles) was updated in Equation (5.13).

5.5.1.2 Variable vs. Fixed Estimation Time Interval

Previous research always considers a constant estimation time step (e.g., 20 s). This is an appropriate approach if the entire data set is available (LMP of 100%) and/or the traffic demand is high. However, it is impossible to access the entire data set when dealing with

Table 5.3: RRMSE values for 10 different sample sizes for different LMPs.

| Sample Size | LMP = 10% | LMP = 50% | LMP = 80% |
|-------------|-----------|-----------|-----------|
| 1 | 43 | 34 | 19 |
| 2 | 41 | 32 | 19 |
| 3 | 40 | 33 | 20 |
| 4 | 40 | 33 | 25 |
| 5 | 38 | 32 | 20 |
| 6 | 40 | 32 | 20 |
| 7 | 40 | 32 | 20 |
| 8 | 40 | 33 | 20 |
| 9 | 40 | 37 | 22 |
| 10 | 39 | 38 | 24 |

CVs. Consequently, a variable estimation time step is used rather than a fixed one.

This section demonstrates the benefits of using variable time steps as opposed to constant values, as is done in the literature. Table 5.4 presents the RRMSE values using variable and fixed estimation time steps. The proposed variable time step method was compared to the traditional fixed interval method (i.e., 15, 20, 30, 40, 50, 60, 120, and 240 s), with the results in Table 5.4 showing that low LMPs produce infinite values from the H vector in Equation (5.8) in most fixed intervals. Consequently, the system produces NaN (Not a Number) values in Equation (5.17) due to lack of TT data.

Table 5.5 shows the average and maximum time interval for different LMPs. The results demonstrate that low LMPs require long intervals (e.g., 300 s) to ensure that some CVs are on the approach. In contrast, links with high LMPs use short estimation intervals (e.g., 30 s). The proposed strategy ensures flexibility of the estimation intervals. Figure 5.4 shows the relationship between the sample size (n) and the average time interval for different LMPs. It should be noted here that as the sample size (n) increases, the time interval increases. This approach ensures that a sufficient number of observations are available to estimate the traffic stream density within a desired margin of error. However, a smaller sample size can be used when faster computations are needed. The user can make the trade-off between the time

Table 5.4: RRMSE values using variable and fixed estimation interval time periods.

| Time Interval (s) | RRMSE (%) | | |
|--|-----------|-----------|-----------|
| | LMP = 20% | LMP = 50% | LMP = 80% |
| 15 | NaN | NaN | NaN |
| 20 | NaN | NaN | NaN |
| 30 | NaN | NaN | 91 |
| 40 | NaN | NaN | 96 |
| 50 | NaN | NaN | 43 |
| 60 | NaN | 57 | 40 |
| 120 | 63 | 49 | 36 |
| 240 | 59 | 60 | 39 |
| Proposed Algorithm (variable time interval) | 36 | 32 | 20 |

interval and associated error they are willing to accept. In conclusion, the proposed algorithm enhances the estimation by reducing the estimation errors and allowing the algorithm to respond more quickly for high LMPs and ensuring that sufficient observations are available to achieve the estimations for low LMPs.

Table 5.5: Estimation time interval for different LMPs.

| LMPs % | Avg Time Interval (s) | Max Time Interval (s) |
|--------|-----------------------|-----------------------|
| 10 | 254 | 450 |
| 20 | 131 | 234 |
| 30 | 86 | 177 |
| 40 | 66 | 123 |
| 50 | 53 | 111 |
| 60 | 43 | 99 |
| 70 | 37 | 101 |
| 80 | 33 | 97 |
| 90 | 29 | 78 |

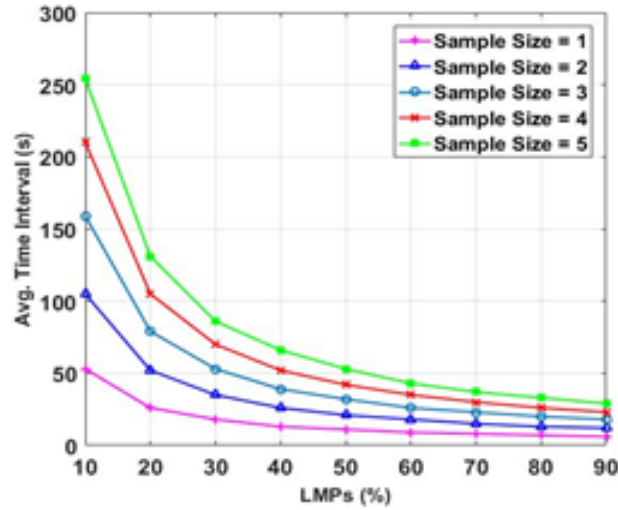


Figure 5.4: Impact of sample size on the average time interval.

5.5.1.3 Impact of Connected Vehicle LMPs

The number of vehicles along the link was estimated considering different LMPs (i.e., 10, 20, 30, 40, 50, 60, 70, 80, and 90%). A Monte Carlo simulation was conducted to create 100 random samples from the collected data for each scenario, creating a random sample of CVs. The proposed approach used the optimal sample size obtained in the previous section ($n = 5$ veh). The more vehicle information available (i.e., the higher the LMP), the shorter the estimation interval and the more estimation steps are possible. Figure 5.5 presents the estimation along different LMPs for the empirical data. The RRMSE values produced reasonable values even with low LMPs, as shown in Table 5.6. For instance, the estimated vehicle count values are off by 2.8 vehicles when the LMP is equal to 10%. On the other hand, the estimated vehicle count values are off by 1.0 vehicle when the LMP is equal to 90%. From Table 5.6, it is clear that the error increases as the LMP decreases. It should be noted that the total field-collected data was not enough to test the KF approach accuracy at low LMPs. Thus, the model’s accuracy was further tested using simulated data.

Table 5.6: RRMSE and RMSE values for nine scenarios using various LMPs for real data.

| LMPs % | RRMSE (%) | RMSE (veh) |
|--------|-----------|------------|
| 10 | 38 | 2.8 |
| 20 | 36 | 2.6 |
| 30 | 35 | 2.5 |
| 40 | 34 | 2.4 |
| 50 | 32 | 2.3 |
| 60 | 28 | 2.0 |
| 70 | 25 | 1.8 |
| 80 | 20 | 1.4 |
| 90 | 14 | 1.0 |

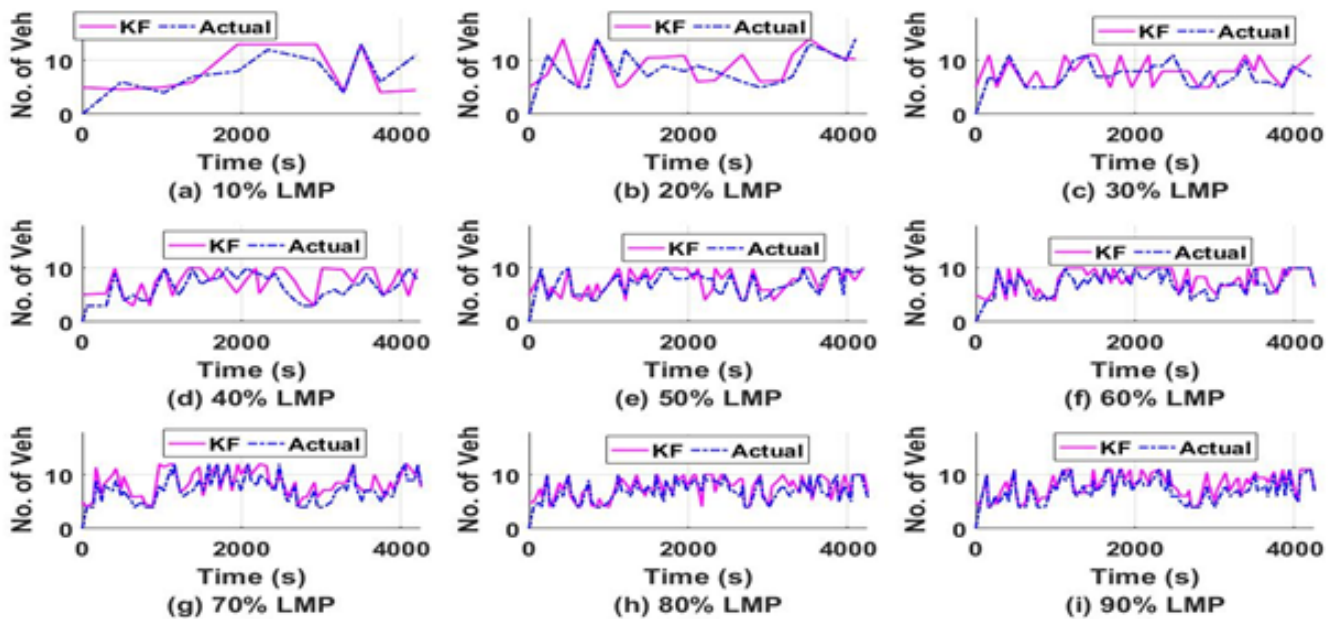


Figure 5.5: Actual and estimated vehicle counts using real data at different LMP scenarios: (a) 10%, (b) 20%, (c) 30%, (d) 40%, (e) 50%, (f) 60%, (g) 70%, (h) 80%, and (i) 90%.

5.5.1.4 Impact of Fusing Connected Vehicle and Single Loop Detector Data

This section computes the actual ρ in the measurement equation (Equation (5.16)) using a stationary sensor in addition to the CV data. The ρ value is defined as the ratio of the number of CVs to the total number of vehicles, as in Equation (5.2). The RRMSE values using the developed two estimation approaches, namely: (1) CV data approach assuming fixed ρ values (named CV approach), and (2) CV and single loop detector data using variable ρ values (named fusion approach) are shown in Table 5.7. Different loop detector locations were tested for the fusion approach (entrance, middle, and exit) to measure the actual ρ values. Based on the RRMSE values, in some cases, installing a loop detector in the middle of the tested link would slightly improve the model’s accuracy at low LMPs by up to 4% however, installing a loop detector may not be cost effective. In conclusion, we recommend using data from existing detection sensors (e.g., loop detectors or video surveillance) if they already exist on the roads, otherwise, we recommend using a fixed ρ value that can be estimated from historic data rather than the actual ρ .

Table 5.7: RRMSE values using one-loop detector in different locations (entrance, middle, and exit).

| LMPs % | RRMSE (%) | | | |
|--------|-----------------------------|------------------------------------|--------|------|
| | CV Approach (Fixed ρ) | Fusion Approach (Variable ρ) | | |
| | | Entrance | Middle | Exit |
| 10 | 38 | 37 | 34 | 38 |
| 20 | 36 | 35 | 33 | 36 |
| 30 | 35 | 34 | 32 | 36 |
| 40 | 34 | 34 | 33 | 34 |
| 50 | 32 | 31 | 31 | 32 |
| 60 | 28 | 28 | 28 | 28 |
| 70 | 25 | 25 | 24 | 25 |
| 80 | 20 | 19 | 19 | 20 |
| 90 | 14 | 14 | 12 | 14 |

5.5.2 Simulation Data

The simulation software used the same link characteristics that were observed during the data collection in downtown Blacksburg. This section first investigates the sensitivity of the vehicle count estimation approach to the link length and to the traffic demand level. Then, the simulated data were used to examine the effect of the choice of the ρ value on the estimation accuracy. First, the KF estimation approach is tested considering a constant predefined ρ in the model equations (CV approach). Second, the approach accuracy is examined using the actual ρ obtained from the installation of a single loop detector (fusion approach). In this section, the optimal sample size for simulated data was eight.

5.5.2.1 Link Length and Traffic Demand Sensitivity Analysis

First, the simulated data were used to study the sensitivity of the estimation approach to the link length. Different link lengths were investigated in addition to the original link length (i.e., 150, 200, 300, and 400 m). Table 5.8 presents the RRMSE values for different link lengths for different LMPs. The results demonstrate that the estimation accuracy increases with an increase in the link length, which is in line with Vigos et al.'s conclusion [23]. For the rest of this study, we used a 400m link length to ensure that the link accommodates more vehicles.

Table 5.8: RRMSE values under different link lengths.

| link Length | LMP = 20% | LMP = 50% | LMP = 80% |
|-------------|-----------|-----------|-----------|
| 74 | 39 | 37 | 29 |
| 150 | 36 | 30 | 19 |
| 200 | 33 | 26 | 16 |
| 300 | 29 | 22 | 13 |
| 400 | 25 | 21 | 13 |

Second, the impacts of traffic demand level on the estimation approach were then examined, considering both under- and over-saturated conditions. Different v/c (flow/capacity) ratios

were tested (from 0.1 to 1.1 at 0.1 increments) as shown in TABLE 5.9. The original v/c ratio was 0.79 ($650/855 = 0.79$) based on the collected data. In general, the RMSE and the RRMSE decrease with the increase of LMPs for the same traffic demand level. However, the RMSE is expected to increase with increasing traffic demand levels for the same LMP, the reason behind that is the increment in the total number of vehicles on the tested link. For instance, at 10% LMP, for the 0.2 v/c , the RRMSE is 59%, and the RMSE is 2.0, so we are off by 2.0 out of the actual 3.4 vehicles, while for a 1.0 v/c ratio, the RRMSE is 24%, and the RMSE is 6.5, so we are off by 6.5 vehicles out of the actual 27 vehicles. In conclusion, the RMSE value can be higher but represents better results (in our case the total number of vehicles). The results from the table demonstrate that the estimation approach works better as the level of congestion increases (e.g., v/c of 0.9, 1.0, and 1.1). The proposed approach therefore demonstrates the KF's efficiency with over-saturation scenarios (e.g., $v/c = 1.1$), especially for low LMPs, indicating its usefulness within a real-time traffic signal controller. Accordingly, 1.1 v/c ratio is used in the next section given that real-time traffic signal control is mostly needed during congested periods.

Table 5.9: RRMSE and RMSE values for different v/c ratios.

| LMPs % | RRMSE (%), RMSE (veh) | | | | | | | | | | |
|--------|-----------------------|-----------|-----------|-----------|-----------|-----------|-----------|-----------|-----------|-----------|-----------|
| | $v/c=0.1$ | $v/c=0.2$ | $v/c=0.3$ | $v/c=0.4$ | $v/c=0.5$ | $v/c=0.6$ | $v/c=0.7$ | $v/c=0.8$ | $v/c=0.9$ | $v/c=1.0$ | $v/c=1.1$ |
| 10 | 75, 0.8 | 59, 2.0 | 48, 2.7 | 43, 3.2 | 36, 3.4 | 33, 3.9 | 34, 4.7 | 29, 5.3 | 25, 6.3 | 24, 6.5 | 16, 5.1 |
| 20 | 73, 1.2 | 58, 1.9 | 45, 2.5 | 40, 3.1 | 34, 3.2 | 32, 3.7 | 29, 4.3 | 27, 5.0 | 23, 5.9 | 23, 6.3 | 14, 4.7 |
| 30 | 73, 1.2 | 55, 1.8 | 44, 2.4 | 40, 3.0 | 33, 3.1 | 29, 3.5 | 27, 4.0 | 26, 4.7 | 23, 5.7 | 22, 5.8 | 13, 4.4 |
| 40 | 73, 1.2 | 55, 1.8 | 41, 2.2 | 36, 2.7 | 30, 2.9 | 28, 3.3 | 26, 3.8 | 24, 4.3 | 21, 5.3 | 20, 5.4 | 13, 4.4 |
| 50 | 69, 1.2 | 46, 1.5 | 40, 2.2 | 33, 2.5 | 28, 2.7 | 26, 3.1 | 24, 3.5 | 22, 4.0 | 19, 4.8 | 18, 4.7 | 13, 4.4 |
| 60 | 59, 1.0 | 43, 1.4 | 35, 1.9 | 30, 2.3 | 25, 2.4 | 23, 2.7 | 20, 3.0 | 18, 3.4 | 15, 3.9 | 15, 4.1 | 12, 3.9 |
| 70 | 52, 0.9 | 42, 1.3 | 32, 1.8 | 27, 2.0 | 22, 2.1 | 20, 2.3 | 16, 2.4 | 15, 2.8 | 13, 3.3 | 13, 3.5 | 10, 3.4 |
| 80 | 48, 0.8 | 35, 1.2 | 29, 1.6 | 24, 1.8 | 19, 1.8 | 16, 1.9 | 13, 2.0 | 14, 2.5 | 11, 2.8 | 11, 3.0 | 9, 2.9 |
| 90 | 45, 0.8 | 28, 1.0 | 24, 1.3 | 22, 1.6 | 16, 1.5 | 14, 1.6 | 11, 1.5 | 11, 2.0 | 9, 2.2 | 9, 2.4 | 9, 2.9 |

In the next results sections, the simulated data were employed to examine the effect of the choice of ρ on the estimation accuracy, namely: using a constant ρ versus using the actual ρ

that could be obtained if a single loop detector was installed.

5.5.2.2 Connected Vehicle Impact on KF Estimator Performance using Fixed ρ Values

The proposed KF approach was evaluated using simulation data. Again a Monte Carlo simulation was run to create 100 samples from the full data set for each scenario. In this approach, we assume the ratio between the number of CVs and the number of total vehicles is constant. The estimation equations use a predefined fixed ρ value (e.g., an average value from historical data). Table 5.10 presents the RRMSE and RMSE values using the simulation data. The RRMSE values produced reasonable values even with low LMPs, as shown in Table 5.10. For instance, the vehicle count estimates were off by 16% when the LMP equaled 10%. On the other hand, our vehicle count estimates values were off by 9% for LMPs of 90%. Furthermore, the vehicle count approach produced RMSE values of up to 5.1 vehicles. Knowing that the tested link can accommodate up to 64 vehicles based on the jam density value, these RMSE values are low. Figure 5.6 presents the estimation at different LMPs. As a result, the proposed approach addresses the research goal appropriately, producing reasonable error values. Vigos et al. considered their model a robust model with up to a 27.5% RRMSE using at least three loop detector measurements [23]. It is obvious that using the predefined ρ values results in errors. However, the KF is able to reduce these errors.

Table 5.10: RRMSE and RMSE values for various LMPs.

| LMPs % | RRMSE (%) | RMSE (veh) |
|--------|-----------|------------|
| 10 | 16 | 5.1 |
| 20 | 14 | 4.7 |
| 30 | 13 | 4.4 |
| 40 | 13 | 4.4 |
| 50 | 13 | 4.4 |
| 60 | 12 | 3.9 |
| 70 | 10 | 3.4 |
| 80 | 9 | 2.9 |
| 90 | 9 | 2.9 |

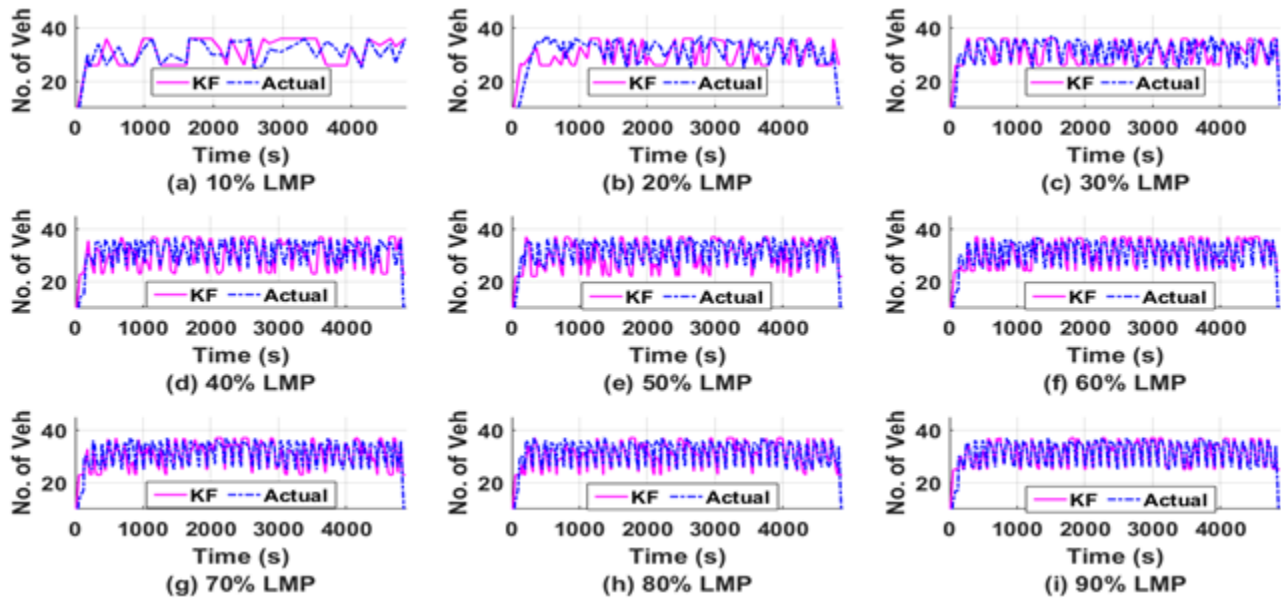


Figure 5.6: Actual and estimated vehicle counts using simulated data at different LMP scenarios: (a) 10%, (b) 20%, (c) 30%, (d) 40%, (e) 50%, (f) 60%, (g) 70%, (h) 80%, and (i) 90%.

5.5.2.3 Fusion Data Impact on KF Performance using Variable ρ Values

This section compares the two estimation approaches: The CV approach and the fusion approach. Again, different loop detector locations were tested for the fusion approach (entrance, middle, and exit) to measure the actual ρ values. The variation of the RRMSE considering a stationary sensor (e.g., loop detector) are shown in Table 5.11 for different traffic demand levels (v/c ratio of 0.2, 0.5, and 1.1). Based on the RRMSE values, in some scenarios, installing a loop detector in the middle of the tested link would slightly improve the model's accuracy by up to 8%; however, installing a loop detector may not be cost effective. In conclusion, we recommend using a fixed ρ value that can be estimated from historic data rather than the actual ρ .

Table 5.11: RRMSE values using one-loop detector in different locations (entrance, middle, and exit).

| LMPs % | V/C = 0.2 | | | | V/C = 0.5 | | | | V/C = 1.1 | | | |
|-----------|----------------|-----------------|--------|------|----------------|-----------------|--------|------|----------------|-----------------|--------|------|
| | CV Approach | Fusion Approach | | | CV Approach | Fusion Approach | | | CV Approach | Fusion Approach | | |
| | | Entrance | Middle | Exit | | Entrance | Middle | Exit | | Entrance | Middle | Exit |
| 10 | 59 | 55 | 51 | 53 | 36 | 35 | 34 | 37 | 16 | 15 | 14 | 15 |
| 20 | 58 | 54 | 51 | 53 | 34 | 33 | 33 | 34 | 14 | 15 | 15 | 15 |
| 30 | 55 | 53 | 51 | 53 | 33 | 32 | 32 | 33 | 13 | 14 | 14 | 14 |
| 40 | 55 | 49 | 50 | 51 | 30 | 30 | 30 | 30 | 13 | 15 | 15 | 16 |
| 50 | 46 | 47 | 46 | 48 | 28 | 27 | 27 | 28 | 13 | 14 | 13 | 14 |
| 60 | 43 | 43 | 43 | 43 | 25 | 25 | 25 | 25 | 12 | 12 | 12 | 12 |
| 70 | 42 | 39 | 39 | 40 | 22 | 21 | 21 | 22 | 10 | 10 | 10 | 11 |
| 80 | 35 | 34 | 34 | 36 | 19 | 19 | 20 | 19 | 9 | 8 | 8 | 9 |
| 90 | 28 | 27 | 27 | 28 | 16 | 16 | 16 | 16 | 9 | 9 | 9 | 9 |

5.6 Summary and Conclusions

This research proposed a novel approach for estimating the number of vehicles on a signalized link using connected vehicle (CV) data only. The proposed estimation approach uses a variable estimation interval that ensures a predefined number of CVs are observed in each estimation interval. The estimation equations use the linear KF technique. The state-space equation is based on the conservation equation while the travel time measurements together

with the hydrodynamic equation are used to construct the measurement equation. Two estimation approaches were presented, namely: (a) using only the CV data to estimate the vehicle counts; this approach uses a predefined LMP value (obtained from historical data) (b) using a single loop detector located somewhere near the middle of the section to estimate the actual LMP values. The KF estimation accuracy was evaluated using both empirical data (collected in downtown Blacksburg, VA) and simulated data.

The work done for this chapter demonstrates the importance of having a variable estimation interval, and its benefits on the estimation accuracy, especially when dealing with low LMPs. In computing the estimation interval, the algorithm first needs a certain sample size (n) to be defined.

The study also investigated the sensitivity of the KF to the link length and traffic demand level, showing that the KF's relative accuracy increases as the link length increases given that the number of vehicles increases. The study also examined different demand levels (v/c ratios) in order to evaluate the KF's efficiency, with results showing that dealing with a high traffic demand levels improved the estimation approach.

In both estimation approaches, the results show that the estimation error increases as the LMP decreases. In some scenarios, the second approach (real-time estimated LMP) produces smaller errors since the actual LMP values can be observed. However, use of the second approach is not recommended, as it adds only slight improvements to the estimation outcomes with the additional cost associated with installing a loop detector, which may be cost prohibitive especially in large urban areas.

Chapter 6

Development of a Particle Filter Approach

This chapter is an edited version of: Mohammad A. Aljamal, Hossam Abdelghaffar, and Hesham A. Rakha (2020), "Estimation of Traffic Stream Density using Connected Vehicle Data: Linear and Nonlinear Filtering Approaches," published in *Sensors Journal* [111].

The chapter presents a nonlinear filtering approach to estimate the traffic stream density on signalized links based solely on connected vehicle (CV) data. Specifically, a particle filter (PF) is developed to produce reliable traffic density estimates using CV travel-time measurements. Traffic flow continuity is used to derive the state equation, whereas the measurement equation is derived from the hydrodynamic traffic flow relationship. Subsequently, the PF filtering approach is compared to linear estimation approaches; namely, a Kalman filter (KF) and an adaptive KF (AKF). Simulated data are used to evaluate the performance of the three estimation techniques on a signalized approach experiencing oversaturated conditions. Results demonstrate that the three techniques produce accurate estimates—with the KF, surprisingly, being the most accurate of the three techniques. A sensitivity of the estimation techniques to various factors including the CV level of market penetration, the

initial conditions, and the number of particles in the PF is also presented. As expected, the chapter demonstrates that the accuracy of the PF estimation increases as the number of particles increases. Furthermore, the accuracy of the density estimate increases as the level of CV market penetration increases. The results indicate that the KF is least sensitive to the initial vehicle count estimate, while the PF is most sensitive to the initial condition. In conclusion, the chapter demonstrates that a simple linear estimation approach is best suited for the proposed application.

6.1 Introduction

Real-time traffic estimation has received increased attention with the introduction of advanced applications and technologies such as intelligent transportation systems (ITSs). Adaptive traffic signal controllers require real-time traffic state estimation to improve intersection performance, as real-time estimation plays a major role in capturing variations in traffic behavior (e.g., nonrecurrent changes). As inputs to traffic signal controllers, traffic state variables (e.g., travel time and traffic density) assist with green time allocation and help to enhance intersection performance by reducing traffic delays, vehicle emissions, and fuel consumption [103, 112]. Several estimation techniques have been developed to estimate traffic state variables [23, 42, 46, 113, 114]. In some previous studies, the traffic state system has been treated as a linear system [23, 42, 50, 79, 85]. Other studies have considered the system as nonlinear [46, 47, 48, 49]. For linear system models, a Kalman filter (KF) has been widely deployed to produce accurate estimates [20, 23, 42, 50] due to its simplicity and applicability in the field. The KF assumes linear system transitions with a Gaussian distribution for the probability density function (PDF) of the system and measurement noise. For nonlinear system models, an extended KF (EKF) has been utilized in estimation [47, 52, 115]. The EKF also assumes that the PDF distribution is Gaussian. The EKF is derived by linearizing the system using a Taylor series expansion by calculating the Jacobian expression. However, it was found that use of the EKF approach is only valid if the system is near linearity during the updating time [53], and thus, large errors may result from linearization. In addition, the task of deriving the Jacobian matrices may cause implementation difficulties [54]. A more robust nonlinear approach is a particle filter (PF), which has been frequently employed in the literature to handle nonlinear dynamic problems [41, 48, 55]. The PF approach is a Monte Carlo sequential solution that deals with nonlinear system transitions without the assumption of the PDF noise distribution [31, 32]. In this chapter, a PF approach is developed to estimate the traffic stream density along signalized intersection approaches using only connected vehicle (CV) data. Moreover, the chapter compares the performance of the

PF to the KF and adaptive KF (AKF) approaches.

Traffic density is defined as the number of vehicles per unit length on a specific roadway segment [8]. Estimating the traffic stream density is critical in the development of effective traffic controllers [116]. For instance in the case of freeways, identifying bottleneck locations in the early stages is critical in developing congestion mitigation strategies that include ramp metering, variable speed limits, and traffic routing. For signalized segments, the traffic density measures are crucial for either traffic signal performance [10, 11, 117] or traffic signal optimization [13, 90, 118]. Hence, traffic density measures must be precisely estimated to represent traffic demands at each signalized intersection approach. Once accurate measurements are obtained, efficient adaptive traffic signal controllers can be developed. However, determining traffic density is not a trivial task and cannot be directly measured in the field since it is a spatial measurement. Consequently, traffic stream density is typically based on estimations.

Previous research has utilized different data sources, such as stationary sensors (e.g., loop detectors), fused data (combining two distinct data sources), and CV data to estimate traffic stream density. Traffic density estimates can be measured using video detection systems, but this is difficult due to the high cost of the infrastructure and the limited visibility of roadway segments [23]. Time-occupancy measurements from loop detectors are used as an alternative data source to estimate the traffic density [24]. However, time-occupancy measurements only represent the temporal density estimates around the location of the detector. A recent study introduced a relationship between time-occupancy and space-occupancy to estimate traffic density by dividing the link into small segments and installing detectors on all of the small segments [25], but the installation cost is high. A more common way of estimating the traffic density is the use of the traffic flow continuity equation (input–output approach), which considers two traffic counting stations, one at the entrance and the other at the end of the link [27]. Vigos et al. [23] proposed a robust linear KF approach with at least three loop detectors to estimate the traffic density along signalized approaches. However, the implementation cost is high. Another study [34] employed two conventional loop detectors

to estimate the traffic density using the flow continuity equation. The two loop detectors provide the estimation model with traffic flow and occupancy data. Bhourri et al. [35] proposed a KF approach to estimate the traffic stream density along a freeway segment using both loop detectors and a recorded film [35]. One commonality about the use of fixed sensors is that they are subject to detection failures and thus always produce errors in their data [28, 29].

Recent research has fused different data sources to estimate the traffic stream density along certain roadway sections, increasing the accuracy of the estimate over using just one data source [20, 42]. Many works have employed the KF approach [20, 21, 39]. For instance, traffic flow data at the entrance and the exit of the roadway section observed from stationary sensors together with CV data were used to estimate the traffic density [21]. The CV data provided travel-time measurements to correct the prior estimate from the state equation. Another study has utilized fused loop and CV measurements to estimate the traffic density in a freeway section [41]. In that study, the authors derived the estimation model using the PF estimation approach, considering two sources of measurements: (1) loop detectors, and (2) fusing loop detectors and CVs. They obtained a 30% reduction in the mean absolute percentage error from the fused measurements compared to the measurements from loop detectors, demonstrating that more data sources produce more-accurate outcomes. However, the use of different data sources requires more computational cost in both time and memory as the data include both trivial (data that are not needed) and nontrivial (data that are needed) information.

Limited studies have used CV data as the only source of inputs to estimate the traffic stream density [42, 50, 79]. These studies developed the linear KF estimator approach. The CV data used were the number of CVs at the entry and at the exit of the tested roadway section, in addition to the travel time experienced for the CVs to traverse the tested section. Moreover, Aljamal et al. [42] demonstrated that treating the estimation interval time as a variable instead of a fixed value is mandatory when dealing with only CV data, as the variable approach always ensures that sufficient information is gathered from the CVs in

every estimation interval. This approach enhances the accuracy of the estimation, especially for the scenarios with low CV level of market penetration (LMP) rate. The estimation time interval for this chapter is therefore defined as the time when an exact number of CVs (i.e., 5 vehicles) reach the end of the tested link.

Several researchers have employed the PF approach to improve traffic stream estimates for different transportation applications, including traffic flow [48, 49], travel time [46, 55], and traffic speed [58]. In one study, magnetic loop detectors were placed at the boundaries of the tested freeway section to estimate the traffic flow, and a PF estimation approach was developed using traffic flow and speed measurements [48]. In another study, Mihaylova et al. [49] developed two nonlinear approaches, an unscented KF and a PF, to produce real-time traffic flow estimates in a freeway network using data from stationary sensors. They found that the PF approach outperformed the unscented KF. Chen et al. [55] proposed a time series speed equation to estimate traffic speed. They claimed that the traffic system is nonlinear and thus presented two nonlinear approaches, a PF and an ensemble KF, using available speed measurements from loop detectors. They found that the PF approach is more accurate than the ensemble KF. Another study developed a PF estimation approach for travel-time predictions using real-time and historical data [46]. They used the historical data to generate particles as opposed to using a state-transition model. In addition, a comparison between the PF, KF, and k-nearest neighbor estimators found that the PF is the most accurate approach. CV data were employed to estimate the traffic speed and flow using the PF approach [58]. In that study, each link in the network was assumed to have base stations to retrieve and transfer the data. Results found that other data sources (e.g., loop detectors) should be incorporated with CVs to enhance the estimation performance. However, our recent study developed a KF approach, showing that the use of CV data alone is sufficient to obtain accurate results [42].

In summary, the existing literature shows that the PF has been widely used to address nonlinear systems and has been proven to outperform other nonlinear estimation techniques; however, to our best of knowledge in the application of traffic stream density estimation, only

a few studies have applied the PF approach using data from stationary sensors and fusing data from different sources. In addition, no comparison between the PF and the linear KF has been reported. Therefore, the PF was adopted in this chapter. The primary objective of this chapter is to develop a nonlinear PF estimation approach to estimate the traffic stream density based solely on CV data on signalized approaches. Subsequently, we compare the PF approach to linear estimation approaches—namely, KF and AKF—to identify the best approach for the application of the traffic density estimation, given that no comparison has been reported in the literature between these filtering techniques. Consequently, this research will recommend a specific approach to estimate the traffic stream density. The proposed three approaches are employed to estimate the vehicle counts based solely on CV data. In addition, this chapter also investigates the sensitivity of the proposed estimation approaches to several factors, such as the LMP rate of the CVs, the initial conditions, and the number of PF particles.

The chapter is organized as follows: Section 6.2 describes the problem formulation and the estimation approaches. Section 6.3 discusses the findings from applying the estimation approaches. Section 6.4 includes the conclusions of the chapter.

6.2 Problem Formulation and Estimation Approaches

First, Section 6.2.1 formulates the research problem using a state-space model. Then, three different estimation approaches are described: the PF (Section 6.2.2.1), the KF (Section 6.2.2.2) and the AKF (Section 6.2.2.3).

6.2.1 State-Space Model

The state-space model is represented by a state equation and a measurement equation. The state equation describes how the system behaves and provides a prior knowledge of

the estimation. The measurement equation is used to help correct and improve the prior estimation. In this chapter, the goal is to estimate the number of vehicles on signalized links using only CV data, as depicted in Figure 6.1, where CVs are the vehicles that have the connection icon (e.g., the first vehicle on the left). The only information that is needed in practice is as follows: (1) the traffic flow of CVs observed at the tested link's entrance and exit. (2) the travel time of each CV. Vehicle-to-Infrastructure (V2I) communication can provide this information to the traffic signal controller.

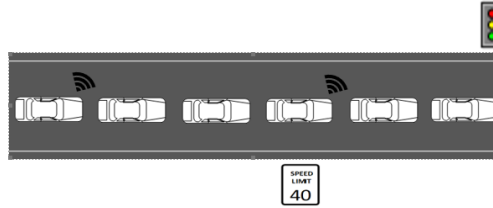


Figure 6.1: Tested link section includes connected vehicles (CVs) and non-CVs.

The model is formulated using the derived state-space equations in [42]. The state equation, Equation (6.1), is based on the continuity equation of traffic flow; whereas the measurement equation, Equation (6.2), is based on the traffic flow hydrodynamic relationship, based on measurements of the average travel time of CVs. In Equation (6.1), the number of vehicles is computed by continuously adding the difference of the number of vehicles that enter and exit the tested section to the cumulative number of vehicles traveling along the section previously computed.

$$N(t) = N(t - \Delta t) + u(t) \quad (6.1)$$

$$TT(t) = H(t) \times N(t) \quad (6.2)$$

where $N(t)$ is the number of vehicles traversing the link at time t , $N(t - \Delta t)$ is the number of vehicles traversing the link in the preceding time interval, and $u(t)$ is the system inputs, as described in Equation (6.3).

$$u(t) = \frac{\Delta t [q^{in}(t) - q^{out}(t)]}{\max(\rho^{actual}, \rho^{min})} \quad (6.3)$$

where q^{in} and q^{out} represent the flow of CVs entering and exiting the link, respectively, during

Δt . ρ is the CVs' LMP, defined as the ratio of CV count to total vehicle count. In the state equation, the ρ variable is set to be the maximum number of the actual ρ (ρ_{actual}) and a predefined minimum value of ρ (ρ_{min}). ρ_{actual} can be obtained from historical data. ρ_{min} is introduced to avoid producing large errors in the state equation since a single ρ value is used to approximate the two ρ values (upstream and downstream of the tested link) [42]. In this chapter, ρ_{min} is set to be equal to 0.5; more details about the system state representation can be found in [42]. It should be noted that the ρ variable is the main noise source in the system, and thus, there is an urgent need to develop the measurement equation to fix these errors. In Equation (6.2), TT is the average vehicle travel time, $H(t)$ is a vector that transforms the vehicle counts to travel times. $H(t)$ is derived from the hydrodynamic relationship between the macroscopic traffic parameters (flow, density, and space-mean speed), as presented in Equation (6.4).

$$H(t) = \frac{1}{\bar{q}(t)} = \frac{2 \times \rho_{actual}}{q^{in}(t) + q^{out}(t)} \quad (6.4)$$

6.2.2 Estimation Approaches

As mentioned earlier, the KF and the AKF are considered linear estimators that can efficiently handle linear state-space systems. However, in the proposed state-space equations, we suspect some nonlinearity coming from the ρ variable, which raises the question, would a nonlinear filter improve the estimation performance? For this purpose, this chapter develops a nonlinear PF approach to estimate the vehicle counts along the signalized link. This section presents the formulation of the three approaches used to estimate the vehicle counts using only CV data along signalized approaches. The three techniques are the proposed PF, the KF [42], and the AKF [50].

6.2.2.1 The PF Approach

The PF approach is used to solve nonlinear state-space systems with no form restrictions on the initial state and noise distributions. For instance, the PF can deal with any arbitrary PDF distribution [31]. The PF approach is used to estimate the posterior PDF of the state vehicle count variable (N) given some measurements of CV travel times (TT) by assigning k number of particles (samples). Each particle has a certain relative weight (w). When a new measurement is received, the particles' locations and weights are updated. It should be noted that the particles with low relative weight values are replaced with new particles (resampling) so that the system keeps only the important particles. The estimates are then calculated using the average value of the remaining particles. The following steps are used to implement the proposed PF approach:

1. Initialization: $t = 0$; where t is the time interval.

(a) $\hat{N}^+(0)$, R , V , and l ,

where $\hat{N}^+(0)$ is the initial vehicle count estimate; R is the measurement's covariance error; and V is the variance of the initial vehicle count estimate, which is used to randomly generate the initial particles' locations around $\hat{N}^+(0)$.

(b) Generate l particles' locations randomly, from 1 to L , from the initial prior Gaussian distribution $P(N_0)$.

$$N^l(0) \sim P(N_0) \quad (6.5)$$

2. For $t = 1 : T$.

(a) Update the locations ($N^l(t)$), measurements ($TT^l(t)$), and weights ($w^l(t)$) of the particles.

$$N^l(t) = N^l(t - \Delta t) + u(t) \quad (6.6)$$

$$TT^l(t) = H(t) \times N^l(t) \quad (6.7)$$

$$w^l(t) = \frac{1}{\sqrt{2\pi R}} e^{-(TT - TT^l(t))^2 / 2R} \quad (6.8)$$

where TT is the observed measurement from the CVs. The weights are then normalized using the following equation, $\hat{w}^l(t) = w^l(t) / \sum_{l=1}^L w^l(t)$.

- (b) Replace the low-weighted particles with new particles (resampling [31]). After a few iterations in the PF process, the weight will focus on a few particles only and most particles will have insignificant weights, resulting in sample degeneracy [119]. The resampling process is therefore used to tackle the degeneracy problem. It should be noted that the highly weighted particles are used to compute the PF posterior estimate.
- (c) Compute the PF posterior estimate: The PF posterior estimate is computed as the average value of the remaining particles (particles with high weights), as shown in Equation (6.9).

$$\hat{N}^+(t) = \frac{1}{L} \sum_{l=1}^L N^l(t) \quad (6.9)$$

- (d) Next time step ($t + \Delta t$): When 5 new CVs traverse the link, return to step 2a.

6.2.2.2 The KF Approach

The KF approach is a linear quadratic estimator. It has been proven to be the best for estimating linear systems with Gaussian noise [120]. The KF estimation approach can be solved using the following steps:

1. Initialization: $t = 0$; where t is the time interval.

- (a) $\hat{N}^+(0)$, R , and $\hat{P}^+(0)$,

where $\hat{P}^+(0)$ is the initial posterior error covariance estimate for the state system.

2. For $t = 1 : T$.

(a) Prior estimates:

$$\hat{N}^{-}(t) = \hat{N}^{+}(t - \Delta t) + u(t) \quad (6.10)$$

$$\hat{T}T(t) = H(t) \times \hat{N}^{-}(t) \quad (6.11)$$

$$\hat{P}^{-}(t) = \hat{P}^{+}(t - \Delta t) \quad (6.12)$$

where \hat{N}^{-} is an estimate of a priori vehicle count, $\hat{T}T$ is the estimated average travel time, and \hat{P}^{-} is the a priori covariance estimate for the state system.

(b) Correction: The correction uses the prior estimate and the new measurement (i.e., the CV average travel time) to compute the Kalman gain (G).

$$G(t) = \hat{P}^{-}(t)H(t)^T [H(t)\hat{P}^{-}(t)H(t)^T + R]^{-1} \quad (6.13)$$

(c) Posterior state estimates:

$$\hat{N}^{+}(t) = \hat{N}^{-}(t) + G(t) [TT(t) - T\hat{T}(t)] \quad (6.14)$$

$$\hat{P}^{+}(t) = \hat{P}^{-}(t) \times [1 - H(t)G(t)] \quad (6.15)$$

where \hat{N}^{+} is the posterior vehicle count estimate, and \hat{P}^{+} is the posterior error covariance estimate.

(d) Next time step ($t + \Delta t$): When 5 new CVs traverse the link, return to step 2a.

6.2.2.3 The AKF Approach

The AKF approach is presented to estimate the total number of vehicles, using real-time noise error estimates in the state and measurement systems (i.e., mean and variance values). It should be noted that the KF and the AKF approaches use the same equations, but the AKF approach dynamically estimates the noise statistical parameters every estimation step. The vehicle count estimates can be obtained using the following steps:

1. Initialization: $t = 0$; where t is the time interval.

(a) $\hat{N}^{+}(0)$, $m(0)$, and $\hat{P}^{+}(0)$,

where $m(0)$ is the mean of the noise for the state system.

2. For $t = 1 : T$

(a) Prior estimates:

$$\hat{N}^-(t) = \hat{N}^+(t - \Delta t) + u(t) + m(t - \Delta t) \quad (6.16)$$

$$\hat{P}^-(t) = \hat{P}^+(t - \Delta t) + M(t - \Delta t) \quad (6.17)$$

(b) Estimation of noise statistics for the measurement system:

$$\hat{T}T(t) = H(t) \times \hat{N}^-(t) \quad (6.18)$$

$$r = \frac{1}{n} \sum_{t=1}^n [TT(t) - \hat{T}T(t)] \quad (6.19)$$

$$R = \frac{1}{n-1} \sum_{t=1}^n [(r(t) - r).(r(t) - r)^T - (\frac{n-1}{n})H(t)\hat{P}^-(t)H^T(t)] \quad (6.20)$$

where r and R are the mean and covariance of the measurement noise, respectively, and n is the number of state noise samples.

(c) Correction:

$$G(t) = \hat{P}^-(t)H(t)^T [H(t)\hat{P}^-(t)H(t)^T + R(t)]^{-1} \quad (6.21)$$

(d) Posterior state estimates:

$$\hat{N}^+(t) = \hat{N}^-(t) + G(t) [TT(t) - \hat{T}T(t) - r(t)] \quad (6.22)$$

$$\hat{P}^+(t) = \hat{P}^-(t) \times [1 - H(t)G(t)] \quad (6.23)$$

(e) Estimation of noise statistics for the state system:

$$m = \frac{1}{n} \sum_{t=1}^n [\hat{N}^+(t) - \hat{N}^+(t - \Delta t) - u(t) + m(t - \Delta t)] \quad (6.24)$$

$$M = \frac{1}{n-1} \sum_{t=1}^n [(m(t) - m).(m(t) - m)^T - (\frac{n-1}{n})\hat{P}^+(t - \Delta t) - \hat{P}^+(t)] \quad (6.25)$$

where m and M are the mean and covariance of the state noise, respectively.

(f) Next time step ($t + \Delta t$): When 5 new CVs traverse the link, return to step 2a.

6.3 Results and Discussion

This section evaluates and compares the three estimation approaches. The simulated data were generated for a signalized link under an oversaturation condition in which the traffic demand exceeds the link capacity. The free-flow speed is 40 km/h; the saturation flow rate is 1800 veh/h/lane, resulting in a traffic capacity of 855 veh/h given the cycle length and traffic signal's green times; the speed-at-capacity is 32 km/h; and the jam density is 160 veh/km/lane. The traffic signal is operated at a cycle length of 120 s and a phase split of 50:50. The amber and all-red intervals are 3 s. To test the accuracy of the estimation approaches, the INTEGRATION microscopic traffic assignment and simulation software was used [89, 98]. The relative root mean square error (RRMSE), presented in Equation (6.26), was used to evaluate the proposed estimation approaches.

$$RRMSE(\%) = 100 \sqrt{S \sum_{s=1}^S [\hat{N}^+(s) - N(s)]^2} / \sum_{s=1}^S N(S) \quad (6.26)$$

where $\hat{N}^+(s)$ represents the estimated count of vehicles, $N(s)$ represents the actual count of vehicles, and S is the overall number of estimations.

6.3.1 Performance of Estimation Approaches

The simulations were conducted with the same predefined initial conditions to obtain a fair comparison. The initial conditions are described in Table 6.1. It should be noted that each estimator requires specific initial variables. For instance, $\hat{N}^+(0)$, R , and $\hat{P}^+(0)$ are required for the KF approach. For all estimation approaches, the first estimate begins with an erroneous initial estimate of vehicle count ($\hat{N}^+(0) = 5$ veh), whereas the actual vehicle count is zero [23, 42].

The three estimation approaches were evaluated using different CV LMPs, including 1%, 3%, 5%, 8%, 10%, 15%, 20%, 30%, 40%, 50%, 60%, 70%, 80% and 90%. For each LMP scenario,

Table 6.1: Initial conditions for the KF, AKF, and PF approaches.

| Initial Conditions | KF | AKF | PF |
|------------------------------------|-----------|------------|-----------|
| $\hat{N}^+(0)$ (veh) | 5 | 5 | 5 |
| R (sec ²) | 20 | – | 20 |
| V (veh ²) | – | – | 5 |
| L (# of part.) | – | – | 200 |
| $\hat{P}^+(0)$ (veh ²) | 5 | 5 | – |
| m (veh) | – | 5 | – |

100 random samples from the full data set were created using a Monte Carlo simulation. Table 6.2 presents the RRMSE values of the KF, AKF, and the PF approaches. The table indicates that estimation errors decrease with increasing LMP for all estimation approaches. The table also demonstrates that the KF outperforms the AKF and the PF approaches. For instance, for the scenario of 1% LMP, the vehicle count estimates were off by 30%, 48% and 64% using KF, AKF and PF, respectively.

The PF approach produces high RRMSE values at low LMPs (LMP < 40%), while for the high-LMP scenarios, the PF produces RRMSE values close to the values obtained from the KF. Moreover, the AKF approach produces high errors, especially at very low LMPs (LMP < 10%) and high LMPs (LMP ≥ 70%). This demonstrates that the real-time estimates of the statistical noise values obtained from the AKF are not needed for the high-LMP scenarios, and the user may proceed with predefined statistical values due to low errors in the vehicle count estimates (low error in the ρ value). It was found that the high RRMSE error values produced from the AKF and PF approaches are mainly caused from assigning an inappropriate initial vehicle count estimate, as discussed in the next section.

Figure 6.2 presents the KF, AKF, and PF estimation outcomes with regard to the actual values at different LMPs (i.e., 10% to 90% with an increase of 10%). In each subfigure, three plots are generated to display the estimation approaches' outcomes with regard to the actual values; the top one displays the PF outcomes, the middle one presents the KF outcomes, and the bottom one displays the AKF outcomes. The actual curve is represented by the dotted

Table 6.2: RRMSE of KF, AKF, and PF approaches for different LMPs.

| LMPs % | RRMSE (%) | | |
|--------|-----------|-----|----|
| | KF | AKF | PF |
| 1 | 30 | 48 | 64 |
| 3 | 25 | 34 | 60 |
| 5 | 23 | 32 | 56 |
| 8 | 23 | 28 | 52 |
| 10 | 19 | 24 | 48 |
| 15 | 19 | 24 | 42 |
| 20 | 18 | 23 | 40 |
| 30 | 18 | 19 | 30 |
| 40 | 18 | 18 | 22 |
| 50 | 18 | 17 | 18 |
| 60 | 14 | 16 | 15 |
| 70 | 12 | 17 | 12 |
| 80 | 9 | 17 | 9 |
| 90 | 6 | 17 | 7 |

curve. In conclusion, the KF approach is recommended, as it produces the most accurate estimates in addition to its simplicity and applicability in the field. The next section will discuss the impact of the initial conditions on the performance of the various estimation approaches.

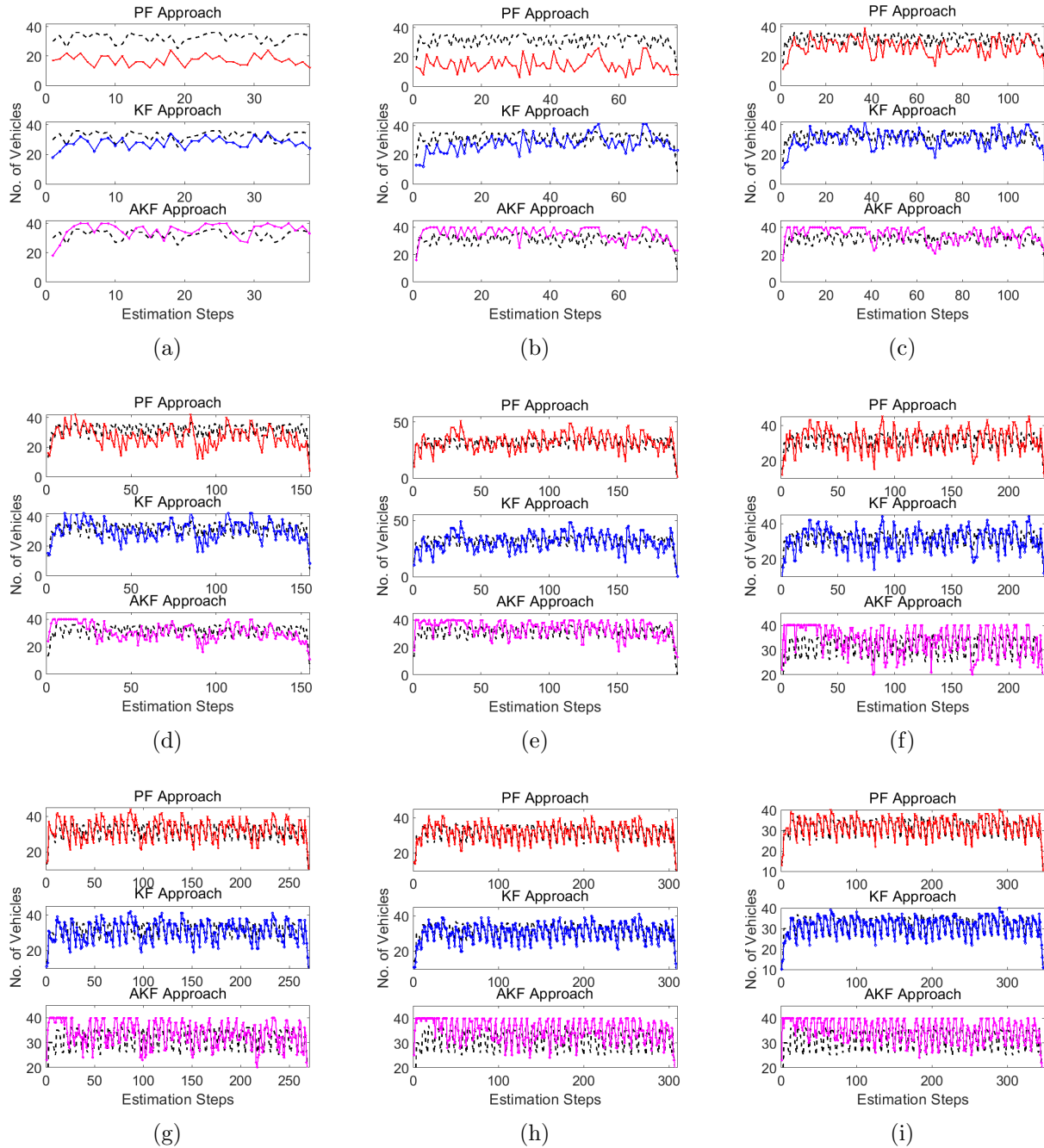


Figure 6.2: Actual and estimated vehicle counts at different LMP scenarios: (a) 10%, (b) 20%, (c) 30%, (d) 40%, (e) 50%, (f) 60%, (g) 70%, (h) 80% and (i) 90%.

6.3.2 Impact of Initial Conditions

This section examines the effect of the choice of the initial conditions on the performance of the estimators, such as the initial vehicle count estimate $\hat{N}^+(0)$ and the l number of particles in the PF approach. First, different $\hat{N}^+(0)$ values were tested, from 0 to 25 at increments of 5, at different LMP scenarios, as presented in Tables 6.3 and 6.4. Table 6.3 presents the RRMSE values when the $\hat{N}^+(0)$ is set to equal 0, 5, and 10 vehicles. Table 6.4 displays the RRMSE for the $\hat{N}^+(0)$ values of 15, 20, and 25 vehicles. The tables demonstrate that the RRMSE values are sensitive to the changes of the $\hat{N}^+(0)$ values. The tables also show that the PF is the most sensitive estimator to $\hat{N}^+(0)$ for all LMP scenarios. For instance, for the scenario of 1% LMP, the RRMSE is 81% when the simulation starts with 0 veh, while the RRMSE is 17% when $\hat{N}^+(0)$ is equal to 25. Therefore, starting the simulations with an appropriate initial estimate close to the truth value significantly improves the estimation accuracy since this helps the PF to quickly converge. In addition, the AKF seems to be sensitive to the $\hat{N}^+(0)$ with low LMP scenarios (LMP \leq 10%), while the choice of $\hat{N}^+(0)$ has a slight effect on the estimation accuracy for the scenarios with medium and high LMPs. For instance, for the scenario of 1% LMP, the RRMSE is 71% when the simulation starts with 0 veh, while the RRMSE is 21% when $\hat{N}^+(0)$ is equal to 25. Lastly, the tables show that the KF is the least-sensitive estimator to the $\hat{N}^+(0)$ value. Figure 6.3 summarizes the RRMSE values for nine LMP scenarios presented in Tables 6.3 and 6.4.

Table 6.3: RRMSE values for the KF, AKF, and PF approaches using different initial vehicle count estimates (i.e., 0, 5, and 10) for different LMPs.

| LMPs % | $\hat{N}^+(0) = 0$ | | | $\hat{N}^+(0) = 5$ | | | $\hat{N}^+(0) = 10$ | | |
|--------|--------------------|-----|----|--------------------|-----|----|---------------------|-----|----|
| | KF | AKF | PF | KF | AKF | PF | KF | AKF | PF |
| 1 | 34 | 71 | 81 | 30 | 48 | 64 | 27 | 36 | 51 |
| 3 | 28 | 49 | 78 | 25 | 34 | 60 | 23 | 26 | 47 |
| 5 | 26 | 45 | 73 | 23 | 32 | 56 | 23 | 27 | 44 |
| 8 | 24 | 33 | 69 | 23 | 28 | 52 | 23 | 27 | 41 |
| 10 | 19 | 33 | 62 | 19 | 24 | 48 | 20 | 24 | 37 |
| 15 | 21 | 29 | 55 | 19 | 24 | 42 | 20 | 23 | 37 |
| 20 | 20 | 24 | 47 | 18 | 23 | 40 | 19 | 23 | 35 |
| 30 | 19 | 21 | 34 | 18 | 19 | 30 | 19 | 19 | 27 |
| 40 | 18 | 20 | 24 | 18 | 18 | 22 | 19 | 18 | 19 |
| 50 | 19 | 17 | 18 | 18 | 17 | 18 | 17 | 17 | 22 |
| 60 | 14 | 17 | 14 | 14 | 16 | 15 | 15 | 16 | 19 |
| 70 | 12 | 18 | 12 | 12 | 17 | 12 | 12 | 17 | 17 |
| 80 | 9 | 18 | 9 | 9 | 17 | 9 | 9 | 17 | 15 |
| 90 | 6 | 17 | 6 | 6 | 17 | 7 | 7 | 17 | 14 |

Table 6.4: RRMSE values for the KF, AKF, and PF approaches using different initial vehicle count estimates (i.e., 15, 20, and 25) for different LMPs.

| LMPs % | $\hat{N}^+(\mathbf{0}) = 15$ | | | $\hat{N}^+(\mathbf{0}) = 20$ | | | $\hat{N}^+(\mathbf{0}) = 25$ | | |
|--------|------------------------------|-----|----|------------------------------|-----|----|------------------------------|-----|----|
| | KF | AKF | PF | KF | AKF | PF | KF | AKF | PF |
| 1 | 23 | 32 | 36 | 20 | 23 | 24 | 19 | 21 | 17 |
| 3 | 22 | 26 | 33 | 20 | 25 | 24 | 20 | 24 | 19 |
| 5 | 21 | 25 | 31 | 20 | 23 | 26 | 19 | 24 | 20 |
| 8 | 21 | 27 | 33 | 22 | 26 | 26 | 21 | 26 | 23 |
| 10 | 20 | 24 | 30 | 20 | 24 | 27 | 19 | 26 | 22 |
| 15 | 19 | 23 | 30 | 19 | 24 | 26 | 19 | 23 | 18 |
| 20 | 19 | 23 | 30 | 19 | 23 | 30 | 19 | 23 | 16 |
| 30 | 19 | 19 | 21 | 19 | 19 | 21 | 19 | 19 | 26 |
| 40 | 19 | 18 | 20 | 19 | 18 | 20 | 19 | 18 | 44 |
| 50 | 18 | 17 | 33 | 18 | 17 | 47 | 18 | 17 | 33 |
| 60 | 15 | 16 | 32 | 15 | 16 | 32 | 15 | 16 | 32 |
| 70 | 12 | 17 | 30 | 12 | 17 | 30 | 12 | 17 | 30 |
| 80 | 9 | 17 | 30 | 9 | 17 | 30 | 9 | 17 | 30 |
| 90 | 7 | 17 | 29 | 7 | 17 | 44 | 7 | 17 | 29 |

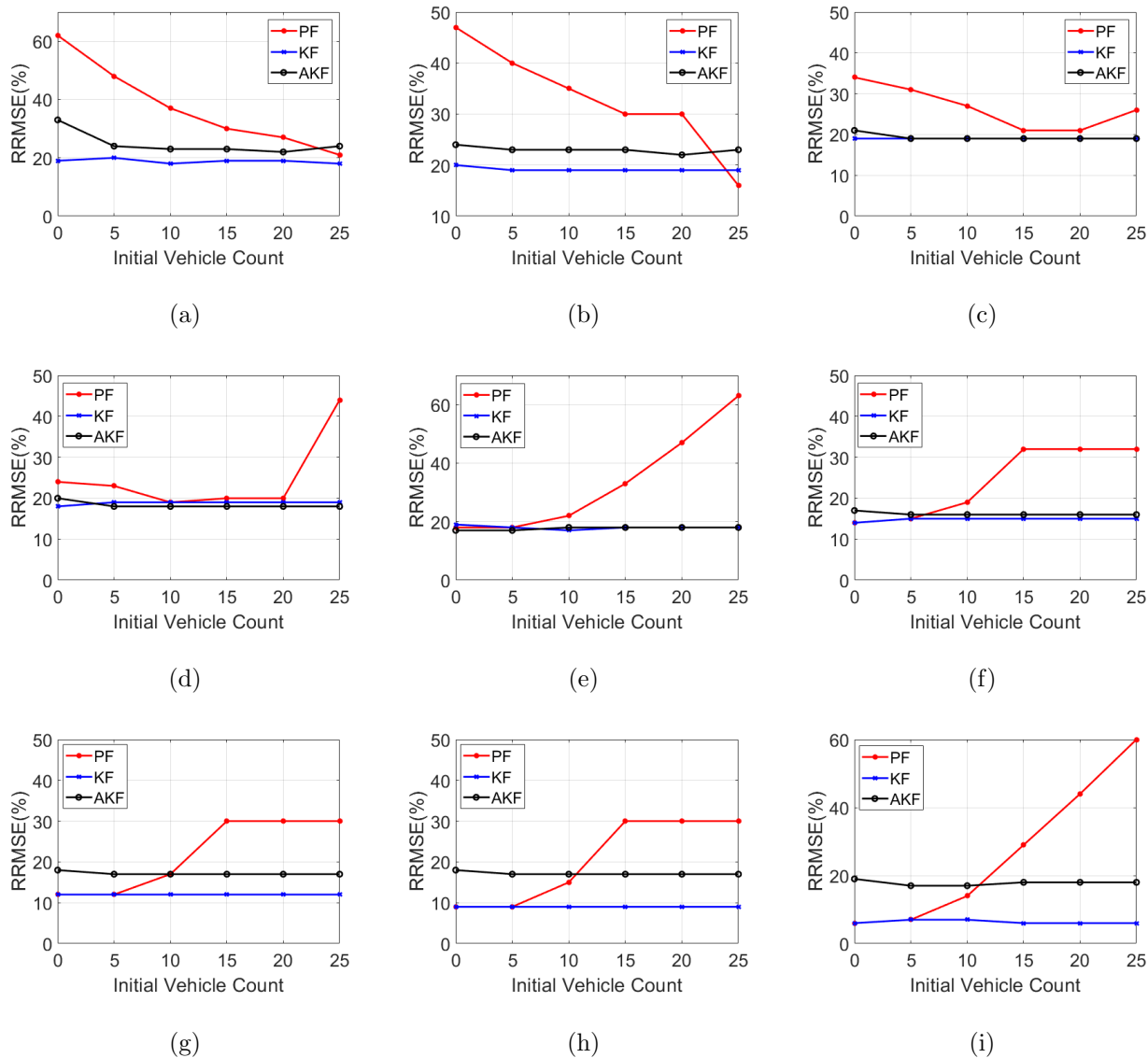


Figure 6.3: RRMSE values using various initial vehicle count estimates at different LMP scenarios: (a) 10%, (b) 20%, (c) 30%, (d) 40%, (e) 50%, (f) 60%, (g) 70%, (h) 80% and (i) 90%.

This chapter also examined the choice of the number of particles, l , on the PF performance (i.e., $l = 10, 100, 200, 1000$, and 2000), as presented in Table 6.5. The findings show that the estimation accuracy increases as the number of particles increases, especially at low LMPs. However, increasing the number of particles is associated with additional computational time. The PF is implemented in MATLAB R2019a on a Dell PC with 8.0 GB RAM. The

computation time ranges between 0.2 and 1.6 s, with 10 particles for various LMPs; 1.1 and 3.0 s with 100 particles; 1.3 and 6.8 sec with 200 particles; 1.3 and 73 s with 1000 particles; 4 and 256 s with 2000 particles. The results in Table 6.5 show that the use of 1000 and 2000 particles slightly reduces the RRMSE values compared to the use of 200 particles; however, this comes at a very high computational cost. Therefore, the use of 200 particles is recommended in the PF approach.

Table 6.5: RRMSE values using different number of particles in the PF for different LMPs.

| LMPs % | RRMSE (%) | | | | |
|--------|-----------|-----------|-----------|------------|------------|
| | $l = 10$ | $l = 100$ | $l = 200$ | $l = 1000$ | $l = 2000$ |
| 1 | 72 | 66 | 64 | 61 | 59 |
| 3 | 69 | 62 | 60 | 57 | 56 |
| 5 | 66 | 59 | 56 | 53 | 52 |
| 8 | 60 | 54 | 52 | 48 | 47 |
| 10 | 56 | 50 | 48 | 46 | 44 |
| 15 | 48 | 44 | 42 | 40 | 40 |
| 20 | 44 | 41 | 40 | 38 | 36 |
| 30 | 34 | 30 | 30 | 30 | 30 |
| 40 | 22 | 22 | 22 | 22 | 22 |
| 50 | 19 | 18 | 18 | 18 | 17 |
| 60 | 16 | 15 | 15 | 14 | 14 |
| 70 | 13 | 12 | 12 | 12 | 11 |
| 80 | 11 | 9 | 9 | 9 | 9 |
| 90 | 9 | 7 | 7 | 6 | 6 |

6.4 Summary and Conclusions

The chapter developed a nonlinear PF estimation approach to estimate the number of vehicles approaching a traffic signal based solely on CV data, with the aim of improving the estimation accuracy of linear state-of-the-art estimation approaches. This chapter introduced two linear approaches, KF and AKF, as benchmarks, to be compared with the proposed nonlinear PF approach. The results show that the KF produces the least error and accurately estimates the vehicle counts compared with the AKF and PF approaches. Consequently,

to address the research problem appropriately, it is recommended to deploy the linear KF approach rather than the more complex AKF and PF approaches because of its simplicity and high-performance accuracy. In addition, the chapter investigated the sensitivity of the developed approaches to different factors, including the LMP of CVs, the initial vehicle count estimates, and the number of particles used in the PF approach. The results indicate that the estimation errors decrease as the LMP increases. Furthermore, the chapter investigated the effect of the choice of the number of particles on the performance of the PF and showed that the PF estimation accuracy increases as the number of particles increases. However, this comes at the expense of significantly longer computational times. This can significantly impact the performance of the PF, requiring longer time to converge. The results demonstrate that the KF approach is the least sensitive to the initial vehicle count estimate, while the PF approach is the most sensitive to the initial vehicle count estimate and thus is the most suitable for the proposed application.

Chapter 7

Development of Data-Driven Approaches

This chapter is an edited version of: Mohammad A. Aljamal, Mohamed Farag, and Hesham A. Rakha (2020), "Developing Data-Driven Approaches for Traffic Density Estimation using Connected Vehicle Data," in review, *IEEE Access Journal*.

This chapter introduces novel approaches for the estimation of the traffic stream density. First, an artificial neural network (ANN) data-driven approach is developed to estimate the level of market penetration (LMP) of connected vehicles at two fixed locations. Then, the estimated values are used as inputs to a Kalman filter (KF) approach to estimate the vehicle count between these two locations. Second, three data-driven approaches are developed to directly estimate the vehicle count using only connected vehicle data, an ANN, a k-nearest neighbor (k-NN), and a random forest (RF). A congested signalized roadway in downtown Blacksburg, Virginia, is used to test and compare the performance of the estimation approaches. Results demonstrate that the ANN approach produces reasonable errors in estimating the LMPs; however, integrating the ANN with the KF results in larger errors than the errors produced from using the KF with a predefined average value obtained from the

actual LMPs. The results also demonstrate that the data-driven approaches provide accurate vehicle count estimates, with the ANN being the most accurate of the three approaches. Lastly, the chapter compares the three developed data-driven approaches with model-driven approaches (i.e., KF), showing that the ANN outperforms all other approaches. However, taking into consideration the computational time needed to train the ANN, the large amount of data needed, and the uncertainty in the performance when new traffic behaviors are observed (e.g., incidents), the use of the KF approach is highly recommended in the estimation of traffic stream density due to its simplicity and applicability in the field.

7.1 Introduction

people wasted around 166 billion hours in traffic congestion in 2017, including around 3.8 billion gallons of fuel [121]. Traffic engineers and researchers are working to provide solutions for the traffic congestion problem. One efficient solution is to deploy Intelligent Transportation System (ITS) applications with the aim of increasing the capacity of the existing traffic infrastructure [122]. One ITS application is the use of connected vehicle (CV) technology, which can allow information exchange between two CVs (V2V communication) and also between any CV and the traffic infrastructure (V2I communication). In the case of traffic congestion, traffic infrastructures such as the traffic signal controller can send early messages to the surrounding CVs to find alternative routes, leading to a reduction in trip travel times.

Traffic congestion can be represented by the macroscopic traffic stream density (the number of vehicles that traverse a specific roadway segment divided by the length of that segment). Traffic density is considered a spatial rather than a temporal measurement. Consequently, the temporal traffic occupancy measurements, obtained from loop detectors, cannot be used to estimate the traffic density for the entire link unless multiple loop detectors are installed, which results in high costs. A more efficient way to estimate the traffic density is to exploit CV technology with the ability to share real-time information, such as the vehicle's location and speed, anywhere inside the link.

To estimate the number of vehicles, researchers have developed different estimation approaches such as model-driven (filtering techniques) and data-driven (machine learning). In addition, different data sources have been used to implement the proposed estimation approaches, such as the data from fixed sensors (e.g., loop detectors), data from two different detection sources (fusion data), and CV data.

7.1.1 Model-Driven Estimation Approaches

For the use of fixed sensors, the input-output approach has been widely used to develop model-driven approaches. One study developed a Kalman filter (KF) approach to estimate the vehicle counts on a signalized link using at least three loop detectors (two at the boundaries of the tested link and the third one in the middle of the link) [23]. Another study [33] employed data from four loop detectors to estimate the number of vehicles, resulting in accurate estimates. Traffic flow and occupancy data, measured from six loop detectors, were utilized to provide accurate estimates for the vehicle counts in an on-ramp segment [35]. However, these studies have a high implementation cost due to the necessity of installing multiple fixed sensors. Moreover, it was found that fixed sensors always produce some noise in their data [28]. Thus, there is an urgent need to use additional data sources to reduce the noise.

Fusion data has been given more attention following the introduction of advanced technologies such as CVs. Recently, researchers have started using fixed sensors together with CV data for seeking better estimation accuracy. A study attempted to provide accurate estimates of traffic density using mobile sensors and loop detector data [71], showing that the estimation accuracy using fusion data outperformed the loop detector data. A recent study utilized CVs and cameras to estimate traffic density in a 500 m highway segment. The model developments were based on the assumption that the average speed of CVs is approximately equal the average speed of traditional vehicles [69]. In that study, a KF model was developed under the consideration of having a linear parameter-varying system with known parameters. The state equation was based on the traffic flow continuity equation, while the measurement equation was based on the average speed of CVs. Wright et al. [41] developed a particle filter (PF) using fusion loop and CV measurements to estimate the number of vehicles in a freeway section, demonstrating that the use of fusion data resulted in improving the estimation accuracy. Another study [70] developed a KF approach using fused loop and CV data to estimate the number of vehicles in a signalized link.

Recently, a few studies have attempted to estimate the number of vehicles on signalized links using CV data only. In those studies, the KF, adaptive KF (AKF), and PF model-driven approaches were developed to provide accurate estimates [42, 50, 79, 111].

7.1.2 Data-Driven Approaches

Machine learning techniques require considerable amounts of data to build mathematical models that draw the relationship between the model's inputs and outputs, and thus machine learning is considered a data-driven technique. Data-driven approaches have been employed to estimate traffic state variables such as traffic stream density and speed [50, 72, 73, 75, 76, 77, 78]. In previous studies, the proposed estimation approaches have relied on different detection techniques such as fixed sensors and the fusion data.

Artificial neural network (ANN) and k-nearest neighbor (k-NN) data-driven approaches were developed to produce reliable estimates of vehicle counts [78]. In that study, authors relied on fixed sensors to obtain traffic speed and flow measurements to build and train the ANN and the k-NN approaches. Fulari et. al [72] developed an ANN approach to estimate the number of vehicles using video and Bluetooth data. It was found that the ANN approach performs well if a good quantity of training data is accessible. Fused loop and CV data were used to develop support vector machine and k-NN approaches, with the aim of estimating the level of traffic congestion in a freeway segment [74]. Another study [77] deployed data from fixed sensors and CVs to build different data-driven estimation approaches such as ANN, k-NN, and random forest (RF) to estimate the hourly traffic volumes. In that study, the ANN was found to outperform the other approaches. Aljamal et al. [50] developed an ANN approach to estimate the level of market penetration (LMP) rate of the CVs. In that study, the ANN approach provides the AKF approach with real-time values of the LMPs, resulting in improving the vehicle count estimation accuracy. The LMP represents the percentage of the CVs to the total number of vehicles.

In summary, studies have shown the benefits of using data-driven approaches in addressing

different aspects of the traffic state estimation problem. Therefore, the research described in this chapter aims to develop data-driven approaches in the application of traffic stream density estimation (vehicle counts). One commonality among the related studies is that they all estimated the vehicle counts using data from fixed sensors or using fused source data (e.g., loop with CV data).

The research described in this chapter aims to develop different data-driven estimation techniques to estimate the vehicle counts using only CV data. The proposed estimation approaches are applied to test a signalized link in downtown Blacksburg, Virginia. The proposed research extends the state-of-the-art in vehicle count estimation by making three major contributions:

1. This chapter develops three data-driven estimation approaches to estimate the vehicle counts in signalized links. The three data-driven approaches are developed using only CV data.
2. This chapter develops a data-driven approach to estimate the LMP for the CVs at the entrance and the exit of the link.
3. This chapter compares the three proposed data-driven approaches with state-of-the-art model-driven estimation approaches.

The chapter is organized as follows: Section 7.2 demonstrates the development of the simulation data. Section 7.3 presents the proposed estimation approaches. Section 7.4 shows the findings of the estimation approaches. Section 7.5 presents the conclusions of the chapter.

7.2 Development of Simulation Data

A congested link in downtown Blacksburg, Virginia, was selected to evaluate the proposed estimation approaches. The link falls between two traffic signals, as shown in Figure 7.1. The link length is 97 meters. The INTEGRATION microscopic traffic assignment and simulation

software [89, 98, 123, 124] was used to simulate the network in Figure 7.1. The INTEGRATION software tracks vehicle longitudinal motion using the Rakha–Pasumarthy–Adjerid collision-free car-following model, also known as the RPA model [125]. The RPA model captures vehicle steady-state car-following behavior using the Van Aerde model [126, 127]. Movement from one steady state to another is constrained by a vehicle dynamics model described in [128, 129]. Vehicle lateral motion is modeled using lane-changing models described in [124]. The model estimates of vehicle delay were validated in [130], while vehicle stop estimation procedures were described and validated in [131]. The traffic origin-destination (O-D) values for the network were calibrated using real count data. The speed limit of the tested link is 40 km/h, the speed-at-capacity is 32 km/h, the jam density is 160 veh/km/ln, and the saturation flow rate is 1800 veh/h/lane.

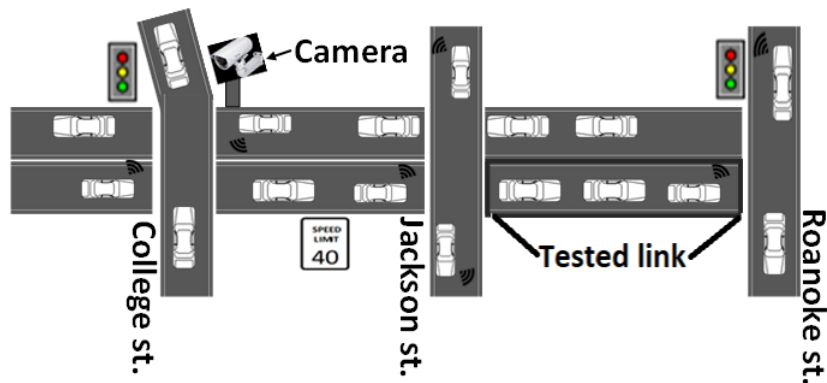


Figure 7.1: Tested link section in downtown Blacksburg, VA.

7.2.1 Generation of the Training Data Set

Training data are needed to develop machine learning estimation approaches. The INTEGRATION simulation software was used to generate the CV data given that empirical CV data are costly to gather. A total of 400 scenarios were simulated, using different scaling factors of the base O-D table and right-turn traffic volumes that exit Main Street toward Jackson Street. For right-turn traffic volumes, 20 different demand scaling factors were gen-

erated from a uniform distribution, ranging from 0.8 to 1.2; for instance, a scenario with a 0.82 O-D demand scaling factor and 1.05 right-turn volume demand scaling factor. In addition, 25 scenarios with different random seeds were considered for each LMP, which resulted in having a total of 1000 scenarios ($20 \times 20 \times 25$) to build the training data. The INTEGRATION simulation software generates an output time-space file that includes real-time information about the CVs, such as the vehicle's location and speed. In section 7.3, more details are provided about the inputs and outputs that are considered in the training data set.

7.3 Methodology

In this section, three research approaches are presented: (1) model-driven approaches, (2) integrating data-driven and model-driven approaches, and (3) data-driven approaches. In the first research approach, linear and nonlinear filtering approaches are used to estimate the vehicle counts. The second approach first develops a data-driven approach to estimate the ratio of the number of CVs (N_{cv}) to the total number of vehicles (N_T), and then combines the data-driven approach with the most accurate model-driven approach to finally estimate the vehicle counts. The third approach develops data-driven approaches to directly estimate the vehicle counts.

7.3.1 First Approach: Model-Driven Approaches

Linear and nonlinear filtering approaches are presented in this section, namely: 1) KF, 2) AKF, and (3) PF. These filtering techniques are always used to solve state-space models. A state-space model is represented by: (1) a state, and (2) a measurement system. The filtering techniques are mainly used to provide posterior estimates given some measurements with the aim of minimizing the errors in the a priori estimates.

In this chapter, the state-space model presented in [42] is used to estimate the vehicle counts. The state and measurement equations are presented in Equations (7.1) and (7.3), respec-

tively.

$$N(t) = N(t - \Delta t) + u(t) \quad (7.1)$$

$$u(t) = \frac{\Delta t [q^{in}(t) - q^{out}(t)]}{\max(\rho, \rho_{min})} \quad (7.2)$$

$$TT(t) = H(t) \times N(t) \quad (7.3)$$

$$H(t) = \frac{2 \times \rho}{q^{in}(t) + q^{out}(t)} \quad (7.4)$$

where $N(t)$ is the number of vehicles crossing the link at time t , $N(t - \Delta t)$ is the number of vehicles crossing the link in the preceding time interval, ρ is the CVs' LMP, defined as the ratio of the CV counts to the total vehicle counts. In this research approach. the ρ is computed from historical data and assumed to remain constant for the entire simulation. For instance, if a scenario of 10% LMP is evaluated, the ρ value is assumed to be 10%. q^{in} and q^{out} represent the flow of CVs entering and exiting the link, respectively, during Δt . The Δt is updated when 5 CVs traversed the tested link [42]. TT is the average travel time for CVs.

The following subsections present three filtering techniques to solve the described state-space model.

7.3.1.1 The KF Approach

The KF is a linear filtering technique and can be implemented using the following equations:

$$\hat{N}^-(t) = \hat{N}^+(t - \Delta t) + u(t) \quad (7.5)$$

$$\hat{TT}(t) = H(t) \times \hat{N}^-(t) \quad (7.6)$$

$$\hat{P}^-(t) = \hat{P}^+(t - \Delta t) \quad (7.7)$$

$$G(t) = \hat{P}^-(t)H(t)^T [H(t)\hat{P}^-(t)H(t)^T + R]^{-1} \quad (7.8)$$

$$\hat{N}^+(t) = \hat{N}^-(t) + G(t) [TT(t) - \hat{TT}(t)] \quad (7.9)$$

$$\hat{P}^+(t) = \hat{P}^-(t) \times [1 - H(t)G(t)] \quad (7.10)$$

where \hat{N}^- and \hat{N}^+ are the priori and the posterior vehicle count estimates, $T\hat{T}$ is the estimated average travel time, \hat{P}^- and \hat{P}^+ are the priori and posterior covariance estimates for the state system, G is the Kalman gain, and R is the error covariance in the measurement system. For more details, readers can refer to [42].

7.3.1.2 The AKF Approach

The linear AKF dynamically estimates the noise error values for the state and measurement systems every estimation step. The AKF approach can be solved using the following equations:

$$\hat{N}^-(t) = \hat{N}^+(t - \Delta t) + u(t) + m(t - \Delta t) \quad (7.11)$$

$$T\hat{T}(t) = H(t) \times \hat{N}^-(t) \quad (7.12)$$

$$\hat{P}^-(t) = \hat{P}^+(t - \Delta t) + M(t - \Delta t) \quad (7.13)$$

$$r = \frac{1}{n} \sum_{t=1}^n [TT(t) - T\hat{T}(t)] \quad (7.14)$$

$$R = \frac{1}{n-1} \sum_{t=1}^n [(r(t) - r).(r(t) - r)^T - (\frac{n-1}{n})H(t)\hat{P}^-(t)H^T(t)] \quad (7.15)$$

$$G(t) = \hat{P}^-(t)H(t)^T [H(t)\hat{P}^-(t)H(t)^T + R(t)]^{-1} \quad (7.16)$$

$$\hat{N}^+(t) = \hat{N}^-(t) + G(t) [TT(t) - T\hat{T}(t) - r(t)] \quad (7.17)$$

$$\hat{P}^+(t) = \hat{P}^-(t) \times [1 - H(t)G(t)] \quad (7.18)$$

$$m = \frac{1}{n} \sum_{t=1}^n [\hat{N}^+(t) - \hat{N}^+(t - \Delta t) - u(t) + m(t - \Delta t)] \quad (7.19)$$

$$M = \frac{1}{n-1} \sum_{t=1}^n [(m(t) - m).(m(t) - m)^T - (\frac{n-1}{n})\hat{P}^+(t - \Delta t) - \hat{P}^+(t)] \quad (7.20)$$

where r and R are the mean and covariance of the measurement noise, n is the number of state noise samples, and m and M are the mean and covariance of the state noise.

7.3.1.3 The PF Approach

The PF is a nonlinear filtering technique. First, the PF generates different particles with unique relative weights. In every estimation step, the system removes the particles with low relative weights and replaces them with new particles (resampling), thus preserving only the important particles. To compute the posterior value, an average value of the remaining important particles are calculated. The PF approach can be implemented using the following steps:

- Initialization: $t = 0$
 - $\hat{N}^+(0)$, R , V , and l .
 - Generate particles:

$$N^l(0) \sim P(N_0) \quad (7.21)$$

- For $t = 1 : T$

$$N^l(t) = N^l(t - \Delta t) + u(t) \quad (7.22)$$

$$TT^l(t) = H(t) \times N^l(t) \quad (7.23)$$

$$w^l(t) = \frac{1}{\sqrt{2\pi R}} e^{-(TT - TT^l(t))^2 / 2R} \quad (7.24)$$

$$\hat{w}^l(t) = w^l(t) / \sum_{l=1}^L w^l(t) \quad (7.25)$$

After normalizing the weights using Equation (7.25), the low-weighted particles are replaced with new particles (resampling [31]). After a few iterations in the PF process, the weight will focus on a few particles only and most particles will have insignificant weights, resulting in sample degeneracy [119]. The resampling process is therefore used to tackle the degeneracy problem.

$$\hat{N}^+(t) = \frac{1}{L} \sum_{l=1}^L N^l(t) \quad (7.26)$$

where V is the variance of the initial vehicle count estimate, N^l is the particles' locations from 1 to L , and TT is the observed measurement from the CVs. More details can be found in [111].

7.3.2 Second Approach: Integrating Data-Driven and Model-Driven Approaches

In our state-space equations, the ρ variable is found to be the main source of noise in the state-space model [42]. Unlike the first research approach described in 7.3.1, two ρ variables, instead of one ρ variable, are used in the state-space equations, namely: 1) ρ_{in} , and 2) ρ_{out} . ρ_{in} and ρ_{out} are observed at the entrance and exit of the link, respectively. The ρ_{in} and the ρ_{out} are displayed in Equations (7.27) and (7.28), respectively. A_{cv} , A_T , D_{cv} , and D_T are the number of CV arrivals, total number of arrivals, number of CV departures, and total number of departures, respectively. Equations (7.29) and (7.30) present the new formulation of the $u(t)$ and $H(t)$ using the two ρ variables.

$$\rho_{in}(t) = A_{cv}/AT \quad (7.27)$$

$$\rho_{out}(t) = D_{cv}/DT \quad (7.28)$$

$$u(t) = \Delta t \left[\frac{q^{in}(t)}{\rho_{in}(t)} - \frac{q^{out}(t)}{\rho_{out}(t)} \right] \quad (7.29)$$

$$H(t) = \frac{2}{\frac{q^{in}(t)}{\rho_{in}(t)} + \frac{q^{out}(t)}{\rho_{out}(t)}} \quad (7.30)$$

It should be noted that the two variables can be measured if two fixed sensors (e.g., cameras) are installed in the entry and exit of the tested link; however, the installation cost is high, thus making this approach undesirable. A more-efficient approach is to employ estimation techniques such as machine learning without the need to add to the existing infrastructure. Hence, in this research approach, an ANN is developed to estimate the ρ_{in} and ρ_{out} variables.

7.3.2.1 ANN Approach

The ANN data-driven model is a combination of simple units (nodes) that are connected by links. The ANN aims to recognize relationships between enormous amounts of data by adding certain number of neurons in the assigned hidden layers. The ANN contains three layers: the input layer, the hidden layer, and the output layer [100]. The mechanism behind the ANN is that every node receives/sends signals from incoming/outgoing links by performing computations. The links that connect the nodes in the network have certain weight values, and these weights determine the strength of connection between the nodes.

ANN Inputs and Outputs

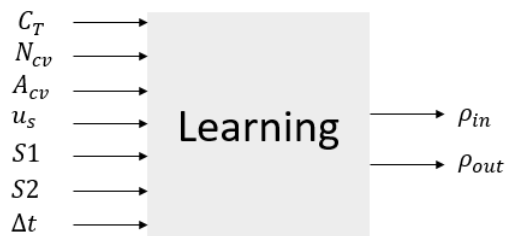
In this section, the aim was to use the nearest existing fixed sensor with the CV data to build the ANN model. As seen in Figure 7.1, an existing camera is located upstream of the tested link (at the intersection of College Street). The camera in the field measures the total traffic counts at the intersection. Consequently, the total traffic count variable is used as an input for the ANN model. In addition, CVs are used to generate the inputs of the ANN model as their ability to provide measurements at any location inside the network.

Seven inputs are used to build the ANN approach, as follows:

1. The total traffic counts obtained from the camera (C_T),
2. The number of CVs on the tested link (N_{cv}),
3. The number of CVs at the entrance of the link (A_{cv}),
4. The space-mean speed of CVs (u_s),
5. The average speed for CVs at link entrance ($S1$),
6. The average speed for CVs at link exit ($S2$), and

7. The estimation interval time (Δt).

Figure 7.2 displays the ANN inputs and outputs. To build a strong ANN approach, the inputs must relate to the outputs, which allows the ANN to define the relationship between the inputs and the outputs. For instance, a high traffic volume (C_T , N_{cv} , and A_{cv}) means that we have more vehicles in the link, which results in having large values in the denominator in Equations (7.27) and (7.28). The speed factor (u_s , $S1$, and $S2$) is also an important indicator of the level of congestion. A congested link can also result in having large values in the denominator in the two equations. It should be noted that the Δt variable strongly relates to the output variables. Remember that Δt is not a constant value and is updated when new 5 CVs are observed at the end of the link. A high Δt value means that the number of CVs is low, which results in low output values. The ANN output variables are ρ_{in} and ρ_{out} . In reality, the ρ output values vary between 0 and 1; 0 means that no CVs are observed, while the value of 1 means that the number of CVs is equal to the total number of vehicles.

Figure 7.2: Estimating the ρ_{in} and ρ_{out} variables.

The developed ANN consists of single hidden layer with 10 neurons, with the use of a transfer function of hyperbolic tangent sigmoid and the Levenberg-Marquardt (LM) optimization method.

After developing and training the ANN approach, the estimated values for ρ_{in} and ρ_{out} are used in our most accurate model-driven approach to estimate the main research goal, which is the vehicle count.

7.3.3 Third Approach: Data-Driven Approaches

The third research approach aims to directly estimate the vehicle counts by developing different data-driven estimation approaches, namely: (1) ANN, (2) k-NN, and (3) RF. The data-driven approaches were developed using CV data only without the need to use data from the camera. Six inputs were considered to train and build the data-driven approaches, as shown in Figure 7.3.

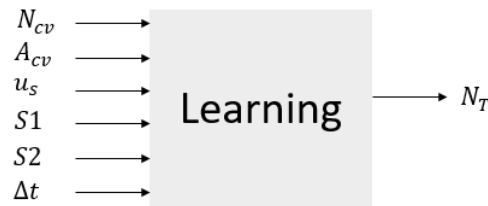


Figure 7.3: Estimating the vehicle counts (N_T) on the tested link.

7.3.3.1 ANN Approach

To estimate the vehicle counts using the ANN approach, the structure of the ANN consists of single hidden layer with 10 neurons, with the use of a transfer function of hyperbolic tangent sigmoid and the LM optimization method.

7.3.3.2 k-NN Approach

The k-NN [132] is used for classification and regression applications. The k-NN does not build a model but requires storing the entire data set. To estimate a new value using the k-NN, the following information is required: (1) having access to the training records, (2) defining the distance metric to compute the distance between the records, and (3) identifying the value of the number of nearest neighbors (k). The results section will test different k values to find the optimal k value for the k-NN approach. The new estimated value is computed by taking the average value of the nearest neighbors.

7.3.3.3 RF Approach

The RF [133] is a supervised learning technique and can be used in classification and regression. The RF is a set of decision trees. Each decision tree is constructed using a subset of inputs. The desired estimation values are given based on the majority votes from all trees. The advantage of using the RF is the ability to handle a large data set without the need to create dummy variables. For the purpose of this chapter, 100 trees were used to develop the RF.

7.4 Results and Discussion

This section tests the accuracy of the three research approaches on a signalized link in downtown Blacksburg, Virginia. The relative root mean square error (RRMSE) and the root mean square error (RMSE) are used to evaluate and compare the proposed estimation approaches. The RRMSE and RMSE can be computed using Equations (7.31) and (7.32), respectively.

$$\text{RRMSE (\%)} = 100 \sqrt{S \sum_{s=1}^S [\hat{N}^+(s) - N(s)]^2 / \sum_{s=1}^S N(S)} \quad (7.31)$$

$$\text{RMSE (veh)} = \sqrt{\sum_{s=1}^S [\hat{N}^+(s) - N(s)]^2 / S} \quad (7.32)$$

where $N(s)$ is the actual vehicle count, $\hat{N}^+(s)$ is the estimated vehicle count value, and S is the total number of estimations.

7.4.1 First Research Approach

This section evaluates the three estimation model-driven approaches: 1) KF, 2) AKF, and 3) PF, using data from CVs only. The three approaches are used to estimate the number of vehicles crossing the tested link. Table 7.1 presents the RRMSE and RMSE values at

different LMPs; 1, 3, 5, 8, 10, 15, 20, 30, 40, 50, 60, 70, 80, and 90%. For most of the LMP scenarios, the KF approach produces the lowest error values, while the PF approach outperforms the KF and the AKF for a few scenarios (1, 70, 80, and 90%). However, the nonlinear PF requires more computational time [111]. Consequently, the use of the linear KF approach is highly recommended due to its simplicity and high-performance accuracy.

Table 7.1: RRMSE and RMSE values of KF, AKF, and PF approaches for different LMPs.

| LMPs % | RRMSE (%), RMSE (veh) | | |
|--------|-----------------------|---------|---------|
| | KF | AKF | PF |
| 1 | 44, 3.2 | 58, 4.3 | 37, 2.8 |
| 3 | 39, 3.0 | 48, 3.6 | 39, 3.0 |
| 5 | 37, 2.8 | 44, 3.2 | 38, 2.9 |
| 8 | 36, 2.8 | 40, 3.0 | 37, 2.9 |
| 10 | 36, 2.8 | 38, 2.9 | 37, 2.9 |
| 15 | 36, 2.8 | 40, 3.0 | 39, 3.0 |
| 20 | 37, 2.8 | 39, 3.0 | 39, 3.0 |
| 30 | 38, 2.9 | 38, 2.9 | 42, 3.2 |
| 40 | 37, 2.9 | 38, 2.9 | 39, 3.0 |
| 50 | 37, 2.8 | 38, 2.9 | 37, 2.8 |
| 60 | 31, 2.4 | 38, 2.9 | 31, 2.4 |
| 70 | 26, 2.0 | 32, 2.5 | 25, 1.9 |
| 80 | 23, 1.8 | 31, 2.4 | 20, 1.5 |
| 90 | 20, 1.5 | 30, 2.2 | 14, 1.1 |

7.4.2 Second Research Approach

First, the ANN approach is developed to estimate the percentage of the CVs to the total number of vehicles at the entry and the exit of the tested link, ρ_{in} and ρ_{out} , respectively. Table 7.2 presents the RRMSE values for estimating the two variables. The results demonstrate that the ANN produces reasonable error values; the errors for estimating ρ_{in} vary between

14 and 25%, while the error values are between 10 and 23% for ρ_{out} .

Table 7.2: RRMSE of ρ_{in} and ρ_{out} at different LMPs.

| LMPs % | RRMSE (%) | |
|--------|-------------|--------------|
| | ρ_{in} | ρ_{out} |
| 10 | 14 | 19 |
| 20 | 18 | 23 |
| 30 | 22 | 22 |
| 40 | 25 | 21 |
| 50 | 25 | 19 |
| 60 | 24 | 16 |
| 70 | 24 | 14 |
| 80 | 25 | 12 |
| 90 | 24 | 10 |

After that, the estimated ρ values are used as inputs to the KF to estimate the vehicle counts on the tested link. A new approach, named KFNN, was developed based on integrating the KF and the ANN approaches. Remember that the KF approach uses an average one value from the actual ρ values in its equations, while the KFNN approach uses real-time values for ρ_{in} and ρ_{out} in the KF equations at every estimation step. Table 7.3 shows the RRMSE values for estimating the vehicle counts using the KF and KFNN approaches. The table demonstrates that the KF approach outperforms the KFNN approach. Investigations were undertaken to find the reason. The investigations found that the ANN may over-estimate ρ_{in} and under-estimate ρ_{out} or vice versa for the same estimation step, resulting in large errors in the state equation compared to the errors from using the average ρ . Such large errors make the error corrections from the KF difficult. In conclusion, the use of one single ρ value in the state-space equations is sufficient to produce accurate estimates.

In next section, data-driven approaches are developed to directly estimate the vehicle counts without the need for model-driven approaches.

Table 7.3: RRMSE of KF and KFNN approaches at different LMPs.

| LMPs % | RRMSE (%) | |
|--------|-----------|------|
| | KF | KFNN |
| 10 | 36 | 64 |
| 20 | 37 | 50 |
| 30 | 38 | 52 |
| 40 | 37 | 54 |
| 50 | 37 | 58 |
| 60 | 31 | 59 |
| 70 | 26 | 57 |
| 80 | 23 | 52 |
| 90 | 20 | 35 |

7.4.3 Third Research Approach

This section utilizes the three data-driven approaches to estimate the number of vehicles traversing the tested link. The data source used to train and build the three approaches was only CV data without the need of the camera data.

First, different neighbors (k) were tested to calibrate and train the k-NN approach, as shown in Table 7.4. The optimal k was found to be 14, with an RRMSE of 18.47%.

After calibrating the data-driven estimation approaches, external data were used to test and evaluate the performance of the estimation approaches. Table 7.5 presents the RRMSE and RMSE values using the three data-driven estimation approaches: ANN, k-NN, and RF. The results demonstrate that the ANN outperforms the k-NN and the RF for all LMP scenarios.

Next, the chapter compares the performance of the model-driven approaches (KF, AKF, and PF) and the data-driven approaches (ANN, k-NN, and RF) for the application to traffic stream density. Table 7.6 summarizes the RRMSE and RMSE values using the six esti-

Table 7.4: RRMSE of k-NN approach using different k values.

| k | RRMSE (%) |
|-----------|------------------|
| 1 | 24.63 |
| 2 | 21.63 |
| 3 | 20.47 |
| 4 | 19.91 |
| 5 | 19.49 |
| 6 | 19.27 |
| 7 | 19.07 |
| 8 | 18.88 |
| 9 | 18.81 |
| 10 | 18.68 |
| 11 | 18.54 |
| 12 | 18.58 |
| 13 | 18.48 |
| 14 | 18.47 |
| 15 | 18.47 |

mation approaches. The table demonstrates that the ANN approach produces the most accurate estimates compared with the other approaches. However, it is worth mentioning the difficulties of applying this approach in the field due to the huge amount of data needed to train and build the ANN approach, especially for a large network (e.g., Los Angeles, CA). Moreover, sudden changes in traffic behaviors (e.g., incidents) would not always ensure accurate estimates and thus might lead to worsen the performance of the traffic signal controller. Consequently, we recommend using the KF approach for traffic density estimation due to its simplicity and applicability in the field.

7.5 Summary and Conclusions

The chapter presents three estimation research approaches to estimate the number of vehicles along signalized links. The first research approach presents three model-driven approaches

Table 7.5: RRMSE and RMSE values using data-driven approaches.

| LMPs % | RRMSE (%), RMSE (veh) | | |
|--------|-----------------------|---------|---------|
| | ANN | k-NN | RF |
| 1 | 27, 2.1 | 40, 3.1 | 42, 3.2 |
| 3 | 29, 2.2 | 37, 2.8 | 42, 3.2 |
| 5 | 29, 2.2 | 37, 2.8 | 38, 2.8 |
| 8 | 28, 2.1 | 36, 2.7 | 38, 2.8 |
| 10 | 27, 2.1 | 35, 2.8 | 38, 2.8 |
| 15 | 25, 1.9 | 33, 2.4 | 36, 2.7 |
| 20 | 24, 1.8 | 33, 2.4 | 36, 2.7 |
| 30 | 22, 1.7 | 30, 2.3 | 34, 2.6 |
| 40 | 20, 1.5 | 27, 2.1 | 30, 2.3 |
| 50 | 17, 1.3 | 24, 1.8 | 26, 2.0 |
| 60 | 14, 1.1 | 22, 1.6 | 23, 1.7 |
| 70 | 11, 0.9 | 20, 1.5 | 21, 1.6 |
| 80 | 9, 0.7 | 18, 1.4 | 19, 1.5 |
| 90 | 8, 0.6 | 17, 1.3 | 17, 1.3 |

(KF, AKF, and PF) using solely CV data. The first approach uses a single average ρ value, obtained from the actual LMPs, in the state-space equations. The second research approach develops an ANN to estimate two ρ variables, ρ_{in} and ρ_{out} , to be used in the state-space equations. Fused CV and camera data are utilized to build the ANN. After that, the second approach integrates the ANN with the KF approach (KFNN approach) to estimate the number of vehicles on signalized links. The third research approach develops three data-driven approaches (ANN, k-NN, and RF) to directly estimate the number of vehicles using only CV data. The three research approaches were applied on a signalized link in downtown Blacksburg, Virginia. The main findings and conclusions of the chapter are summarized as follows:

- The use of CV data is sufficient to provide accurate vehicle count estimates.

Table 7.6: RRMSE and RMSE values using model- and data-driven approaches.

| LMPs % | Model-Driven Approaches | | | Data-Driven Approaches | | |
|--------|-------------------------|---------|---------|------------------------|---------|---------|
| | KF | AKF | PF | ANN | k-NN | RF |
| 1 | 44, 3.2 | 58, 4.3 | 37, 2.8 | 27, 2.1 | 40, 3.1 | 42, 3.2 |
| 3 | 39, 3.0 | 48, 3.6 | 39, 3.0 | 29, 2.2 | 37, 2.8 | 42, 3.2 |
| 5 | 37, 2.8 | 44, 3.2 | 38, 2.9 | 29, 2.2 | 37, 2.8 | 38, 2.8 |
| 8 | 36, 2.8 | 40, 3.0 | 37, 2.9 | 28, 2.1 | 36, 2.7 | 38, 2.8 |
| 10 | 36, 2.8 | 38, 2.9 | 37, 2.9 | 27, 2.1 | 35, 2.8 | 38, 2.8 |
| 15 | 36, 2.8 | 40, 3.0 | 39, 3.0 | 25, 1.9 | 33, 2.4 | 36, 2.7 |
| 20 | 37, 2.8 | 39, 3.0 | 39, 3.0 | 24, 1.8 | 33, 2.4 | 36, 2.7 |
| 30 | 38, 2.9 | 38, 2.9 | 42, 3.2 | 22, 1.7 | 30, 2.3 | 34, 2.6 |
| 40 | 37, 2.9 | 38, 2.9 | 39, 3.0 | 20, 1.5 | 27, 2.1 | 30, 2.3 |
| 50 | 37, 2.8 | 38, 2.9 | 37, 2.8 | 17, 1.3 | 24, 1.8 | 26, 2.0 |
| 60 | 31, 2.4 | 38, 2.9 | 31, 2.4 | 14, 1.1 | 22, 1.6 | 23, 1.7 |
| 70 | 26, 2.0 | 32, 2.5 | 25, 1.9 | 11, 0.9 | 20, 1.5 | 21, 1.6 |
| 80 | 23, 1.8 | 31, 2.4 | 20, 1.5 | 9, 0.7 | 18, 1.4 | 19, 1.5 |
| 90 | 20, 1.5 | 30, 2.2 | 14, 1.1 | 8, 0.6 | 17, 1.3 | 17, 1.3 |

- The use of two estimated variable values in the state-space equations is not recommended as it may produce undesired large errors in the state equation. It was found that the ANN approach may over-estimate the first variable and under-estimate the second variable or vice versa for the same estimation step. Consequently, the second research approach is not recommended.
- The ANN is the most accurate estimation approach. However, taking into consideration the huge amount of data needed to train and build the ANN, the long computational time needed to build the ANN, and the constraints on keeping the traffic behavior the same as the behavior in the training data set, the use of the KF approach is highly recommended for the application of traffic density due to its simplicity and applicability in the field.

Chapter 8

Summary and Conclusions

This chapter presents the main findings of the dissertation and recommended future work.

8.1 Summary and Conclusions

In this dissertation, the presented research develops model-driven and data-driven approaches for real-time estimation of the traffic stream density on signalized approaches. The main findings in this dissertation are summarized as follows:

1. The work done in this dissertation demonstrated the importance of having a variable estimation time interval and its benefits on the estimation accuracy, especially when dealing with low levels of market penetration (LMPs) of connected vehicles (CVs). Fixed estimation intervals were shown to produce Not a Number (NaN) values due to the lack of CVs within the polling interval. Consequently, treating the estimation time interval as a variable would always ensure a sufficient number of CV observations.
2. Chapter 3 developed a linear Kalman filter (KF) estimation approach using only CV data, with the use of the expected (mean) ρ value (obtained from historical data) in the state-space equations. For instance, for the scenario of 10% LMP, the ρ value used in the state and measurement equations remains 0.1 for the entire simulations. It was found that the use of the average value in the state equation may produce large errors especially at low LMPs (LMP = 10%). The chapter also evaluated the KF approach considering two traffic signal timing scenarios, namely: a fixed-time plan and an adaptive phase split optimizer. The results demonstrated that the KF works better for the fixed plan at lower traffic demand levels. Alternatively, the KF works better for the adaptive traffic signal controller for high link traffic demand levels. This was a result of extending the green times for the higher traffic demand links, which produced shorter estimation intervals, as n CVs traversed the link in shorter time periods. Finally, the chapter investigated the sensitivity of the KF approach's accuracy when adding some trucks to the traffic flow, showing that the estimation accuracy decreased as the percentage of trucks increased.
3. Chapter 4 developed a linear adaptive KF (AKF) approach using only CV data. The

AKF dynamically provides real-time estimates of the noise in the state and measurement systems. The state-space equations used in the AKF are the same for the KF presented in Chapter 3. Results demonstrated the ability of the AKF to reduce the large errors that were observed in the developed KF approach in Chapter 3. Moreover, Chapter 4 introduced a novel approach that combines the AKF with an artificial neural network (AKFNN) to enhance the traffic density estimates, where the neural network is employed to provide real-time estimates of the CV LMP (ρ values). The AKFNN approach fuses loop and CV data. Results indicated that the estimation accuracy is significantly improved using the AKFNN approach.

4. Chapter 5 proposed a new formulation of the state equation to prevent the state equation from producing large errors. The ρ factor in the state equation was set to be the maximum of the average ρ value and a lower bound (ρ_{min}), taken to be 0.5 in the analysis after examining different ρ_{min} values. Using the new formulation of the state equation, the KF was evaluated using empirical and simulated data. Results showed that the KF approach produced accurate estimates using solely CV data. In addition, the chapter investigated the sensitivity of the KF estimation approach to traffic demand levels, showing that the KF approach worked better at higher demand levels given that more CVs exist for the same LMP.
5. Chapter 6 first developed the nonlinear Particle filter (PF) estimation approach using CV data only. The chapter then compared the performance of the PF to the linear KF and AKF approaches. Results demonstrated that the KF is the most accurate estimation approach. A sensitivity of the estimation approaches to various factors including the LMP of CVs, the initial conditions, and the number of particles in the PF was also presented. As expected, the chapter demonstrated that the accuracy of the PF estimation increased as the number of particles increased. Furthermore, the accuracy of the density estimate increased as the level of CV market penetration increased. The results indicated that the KF is least sensitive to the initial condition,

while the PF is most sensitive to the initial condition. In conclusion, the chapter demonstrated that the simple linear KF estimation approach is best suited for the proposed application.

6. Chapter 7 first developed three data-driven estimation approaches; namely, the artificial neural network (ANN), the k-nearest neighbor (k-NN), and the random forest (RF). Results demonstrated that the three data-driven approaches provide accurate estimates, with the ANN being the most accurate of the three approaches. After that, the chapter compared the three developed data-driven approaches with the three model-driven approaches, showing that the ANN approach outperformed all other approaches. However, taking into consideration the computational time needed to train the ANN approach, the huge amount of data needed, and the uncertainty in the performance when new traffic behaviors are observed (e.g., incidents), the use of the KF approach was highly recommended in the application of traffic density estimation due to its simplicity and applicability in the field.

8.2 Recommendations for Future Work

Proposed future work entails the following:

1. Develop techniques to estimate the CV LMP using historical and real-time information.
2. Study the impact of biased CV samples (e.g. CVs are trucks) on the algorithm performance.
3. Enhance the algorithms to deal with low CV LMPs.
4. Develop on-line learning techniques, to estimate the traffic density, by adapting dynamically to local traffic conditions.
5. Develop recommendations on the optimum locations and number of additional sources of data (e.g. stationary sensor data) for fusion with the CV data to provide better

traffic stream density estimates.

6. Integrate the KF and other estimation approaches with an adaptive traffic signal controller to quantify the impact of inaccuracies in the traffic stream density estimates on the traffic signal controller performance.
7. Consider and evaluate the impact of communication delays (V2V and V2I) on the estimation performance.

Bibliography

- [1] Statista. Number of motor vehicles registered in the united states from 1990 to 2016 (in 1,000's). <https://www.statista.com/statistics/183505/number-of-vehicles-in-the-united-states-since-1990/>, May 2018.
- [2] David Schrank, Bill Eisele, Tim Lomax, and Jim Bak. 2015 urban mobility scorecard. 2015.
- [3] Robert L Bertini, CM Monsere, and T Yin. Benefits of intelligent transportation systems technologies in urban areas: A literature review. *Portland State University Center for Transportation Studies*, 2005.
- [4] H Rakha and M Van Aerde. Realtran: an off-line emulator for estimating the effects of scoot. *Transportation research record*, pages 124–128, 1995.
- [5] Hossam M Abdelghaffar, Hao Yang, and Hesham A Rakha. A novel game theoretic decentralized traffic signal controller: Model development and testing. Technical report, 2018.
- [6] Hossam M Abdelghaffar, Hao Yang, and Hesham A Rakha. Isolated traffic signal control using nash bargaining optimization. *Global Journal of Research In Engineering*, 2017.
- [7] Hesham Ahmed Rakha. A simulation approach for modeling real-time traffic signal controls. *Transportation Research Part A*, 1(30):74, 1996.

- [8] R. P. Roess, E. S. Prassas, and W. R. McShane. Traffic engineering. *Hoboken, NJ, USA Pearson Education, Inc.*, 2011.
- [9] FV Webster. Traffic signals. *Road research technical paper*, 56, 1966.
- [10] WB Cronje. Analysis of existing formulas for delay, overflow, and stops. Technical report, 1983.
- [11] Kevin N Balke, Hassan A Charara, and Ricky Parker. Development of a traffic signal performance measurement system (tspms). Technical report, Texas Transportation Institute, Texas A & M University System College , 2005.
- [12] Fo Vo Webster. Traffic signal settings. Technical report, 1958.
- [13] Denos C Gazis. Optimum control of a system of oversaturated intersections. *Operations Research*, 12(6):815–831, 1964.
- [14] Gordon Frank Newell. Approximation methods for queues with application to the fixed-cycle traffic light. *Siam Review*, 7(2):223–240, 1965.
- [15] DH Green. Control of oversaturated intersections. *Journal of the Operational Research Society*, 18(2):161–173, 1967.
- [16] Panos G Michalopoulos and George Stephanopoulos. Oversaturated signal systems with queue length constraintsi: Single intersection. *Transportation Research*, 11(6):413–421, 1977.
- [17] Carlos Daganzo and CF Daganzo. *Fundamentals of transportation and traffic operations*, volume 30. Pergamon Oxford, 1997.
- [18] Yizhe Wang, Xiaoguang Yang, Hailun Liang, and Yangdong Liu. A review of the self-adaptive traffic signal control system based on future traffic environment. *Journal of Advanced Transportation*, 2018, 2018.

- [19] Johanna Zmud, Ginger Goodin, Maarit Moran, Nidhi Kalra, and Eric Thorn. Advancing automated and connected vehicles: policy and planning strategies for state and local transportation agencies. 2017.
- [20] R. A. Anand, L. Vanajakshi, and S. C. Subramanian. Traffic density estimation under heterogeneous traffic conditions using data fusion. In *Intelligent Vehicles Symposium (IV), IEEE*, pages 31–36, 2011.
- [21] A. Anand, G. Ramadurai, and L. Vanajakshi. Data fusion-based traffic density estimation and prediction. *Journal of Intelligent Transportation Systems*, 18:367–378, 2014.
- [22] Brian E Badillo, Hesham Rakha, Thomas W Rioux, and Marc Abrams. Queue length estimation using conventional vehicle detector and probe vehicle data. In *2012 15th International IEEE Conference on Intelligent Transportation Systems*, pages 1674–1681. IEEE, 2012.
- [23] G. Vigos, M. Papageorgiou, and Y. Wang. Real-time estimation of vehicle-count within signalized links. *Transportation Research Part C: Emerging Technologies*, 16:18–35, 2008.
- [24] Sing Yiu Cheung, Sinem Coleri, Baris Dundar, Sumitra Ganesh, Chin-Woo Tan, and Pravin Varaiya. Traffic measurement and vehicle classification with single magnetic sensor. *Transportation research record*, 1917(1):173–181, 2005.
- [25] Gongbin Qian, Jinwoo Lee, and Edward Chung. Algorithm for queue estimation with loop detector of time occupancy in off-ramps on signalized motorways. *Transportation research record*, 2278(1):50–56, 2012.
- [26] Markos Papageorgiou and Georgios Vigos. Relating time-occupancy measurements to space-occupancy and link vehicle-count. *Transportation Research Part C: Emerging Technologies*, 16(1):1–17, 2008.

- [27] David L Gerlough and Matthew J Huber. Traffic flow theory. Technical report, 1976.
- [28] Luz Elena Y Mimbela and Lawrence A Klein. Summary of vehicle detection and surveillance technologies used in intelligent transportation systems. 2000.
- [29] Jonathan Lee, Marcial Hernandez, and Arne Stoschek. Camera system for a vehicle and method for controlling a camera system, July 10 2012. US Patent 8,218,007.
- [30] R. E. Kalman. A new approach to linear filtering and prediction problems. *Journal of basic Engineering*, 82:35–45, 1960.
- [31] Jun S Liu and Rong Chen. Sequential monte carlo methods for dynamic systems. *Journal of the American statistical association*, 93(443):1032–1044, 1998.
- [32] Branko Ristic, Sanjeev Arulampalam, and Neil Gordon. *Beyond the Kalman filter: Particle filters for tracking applications*. Artech house, 2003.
- [33] D. Ghosh and C. Knapp. Estimation of traffic variables using a linear model of traffic flow. *Transportation Research*, 12:395–402, 1978.
- [34] A. Kurkjian, S. B. Gershwin, P. K. Houpt, A. S. Willsky, E. Chow, and C. Greene. Estimation of roadway traffic density on freeways using presence detector data. *Transportation Science*, 14:232–261, 1980.
- [35] N. Bhouri, H. H. Salem, M. Papageorgiou, and J. M. Blosseville. Estimation of traffic density on motorways. In *IFAC/IFIP/IFORS International Symposium (AIPAC'89)*, pages 579–583, 1989.
- [36] S Beucher, JM Blosseville, and F Lenoir. Traffic spatial measurements using video image processing. In *Intelligent Robots and Computer Vision VI*, volume 848, pages 648–655. International Society for Optics and Photonics, 1988.
- [37] Anurag Kanungo, Ayush Sharma, and Chetan Singla. Smart traffic lights switching and traffic density calculation using video processing. In *2014 Recent Advances in Engineering and Computational Sciences (RAECS)*, pages 1–6. IEEE, 2014.

- [38] Erhan Bas, A Murat Tekalp, and F Sibel Salman. Automatic vehicle counting from video for traffic flow analysis. In *2007 IEEE Intelligent Vehicles Symposium*, pages 392–397. Ieee, 2007.
- [39] Paul BC van Erp, Victor L Knoop, and Serge P Hoogendoorn. Estimating the vehicle accumulation: Data-fusion of loop-detector flow and floating car speed data. In *97th TRB Annual Meeting, Washington DC*, 2018.
- [40] T. Qiu, X.-Y. Lu, A. Chow, and S. Shladover. Estimation of freeway traffic density with loop detector and probe vehicle data. *Transportation Research Record: Journal of the Transportation Research Board*, pages 21–29, 2010.
- [41] Matthew Wright and Roberto Horowitz. Fusing loop and gps probe measurements to estimate freeway density. *IEEE Transactions on Intelligent Transportation Systems*, 17(12):3577–3590, 2016.
- [42] Mohammad A Aljamal, Hossam M Abdelghaffar, and Hesham A Rakha. Real-time estimation of vehicle counts on signalized intersection approaches using probe vehicle data. *IEEE Transactions on Intelligent Transportation Systems*, 2020.
- [43] Enrique Castillo, José María Menéndez, and Santos Sánchez-Cambronero. Predicting traffic flow using bayesian networks. *Transportation Research Part B: Methodological*, 42(5):482–509, 2008.
- [44] Aude Hoeffleitner, Ryan Herring, Pieter Abbeel, and Alexandre Bayen. Learning the dynamics of arterial traffic from probe data using a dynamic bayesian network. *IEEE Transactions on Intelligent Transportation Systems*, 13(4):1679–1693, 2012.
- [45] Pierre Del Moral. Non-linear filtering: interacting particle resolution. *Markov processes and related fields*, 2(4):555–581, 1996.
- [46] Hao Chen and Hesham A Rakha. Real-time travel time prediction using particle

- filtering with a non-explicit state-transition model. *Transportation Research Part C: Emerging Technologies*, 43:112–126, 2014.
- [47] Yibing Wang and Markos Papageorgiou. Real-time freeway traffic state estimation based on extended kalman filter: a general approach. *Transportation Research Part B: Methodological*, 39(2):141–167, 2005.
- [48] Lyudmila Mihaylova and René Boel. A particle filter for freeway traffic estimation. In *2004 43rd IEEE Conference on Decision and Control (CDC)(IEEE Cat. No. 04CH37601)*, volume 2, pages 2106–2111. IEEE, 2004.
- [49] Lyudmila Mihaylova, René Boel, and Andreas Hegyi. Freeway traffic estimation within particle filtering framework. *Automatica*, 43(2):290–300, 2007.
- [50] Mohammad A Aljamal, Hossam M Abdelghaffar, and Hesham A Rakha. Developing a neural–kalman filtering approach for estimating traffic stream density using probe vehicle data. *Sensors*, 19(19):4325, 2019.
- [51] Y. Wang and M. Papageorgiou. Real-time freeway traffic state estimation based on extended kalman filter: a general approach. *Transportation Research Part B: Methodological*, 39:141–167, 2005.
- [52] H. M. Abdelghaffar, C. A. Woolsey, and H. A. Rakha. Comparison of three approaches to atmospheric source localization. In *Journal of Aerospace Information Systems*, volume 14, pages 40–52, 2017.
- [53] Simon J Julier and Jeffrey K Uhlmann. New extension of the kalman filter to nonlinear systems. In *Signal processing, sensor fusion, and target recognition VI*, volume 3068, pages 182–193. International Society for Optics and Photonics, 1997.
- [54] Y Zhai and M Yeary. Implementing particle filters with metropolis-hastings algorithms. In *Region 5 Conference: Annual Technical and Leadership Workshop, 2004*, pages 149–152. IEEE, 2004.

- [55] Hao Chen, Hesham A Rakha, and Shereef Sadek. Real-time freeway traffic state prediction: A particle filter approach. In *2011 14th International IEEE Conference on Intelligent Transportation Systems (ITSC)*, pages 626–631. IEEE, 2011.
- [56] Zhirui Ye, Yunlong Zhang, and Dan R Middleton. Unscented kalman filter method for speed estimation using single loop detector data. *Transportation research record*, 1968(1):117–125, 2006.
- [57] Jianhua Guo, Jingxin Xia, and Brian L Smith. Kalman filter approach to speed estimation using single loop detector measurements under congested conditions. *Journal of Transportation Engineering*, 135(12):927–934, 2009.
- [58] Peng Cheng, Zhijun Qiu, and Bin Ran. Particle filter based traffic state estimation using cell phone network data. In *2006 IEEE Intelligent Transportation Systems Conference*, pages 1047–1052. IEEE, 2006.
- [59] Lianyu Chu, S Oh, and Will Recker. Adaptive kalman filter based freeway travel time estimation. In *84th TRB Annual Meeting, Washington DC*. Citeseer, 2005.
- [60] Joyoung Lee, Byungkyu Park, and Ilsoo Yun. Cumulative travel-time responsive real-time intersection control algorithm in the connected vehicle environment. *Journal of Transportation Engineering*, 139(10):1020–1029, 2013.
- [61] Jiann-Shiou Yang. Travel time prediction using the gps test vehicle and kalman filtering techniques. In *Proceedings of the 2005, American Control Conference, 2005.*, pages 2128–2133. IEEE, 2005.
- [62] Iwao Okutani and Yorgos J Stephanedes. Dynamic prediction of traffic volume through kalman filtering theory. *Transportation Research Part B: Methodological*, 18(1):1–11, 1984.
- [63] Jianhua Guo, Wei Huang, and Billy M Williams. Adaptive kalman filter approach

- for stochastic short-term traffic flow rate prediction and uncertainty quantification. *Transportation Research Part C: Emerging Technologies*, 43:50–64, 2014.
- [64] Muhammet Balcilar and A Coskun Sonmez. Extracting vehicle density from background estimation using kalman filter. In *2008 23rd International Symposium on Computer and Information Sciences*, pages 1–5. IEEE, 2008.
- [65] Majid Rostami Shahrabaki, Ali Akbar Safavi, Markos Papageorgiou, and Ioannis Papamichail. A data fusion approach for real-time traffic state estimation in urban signalized links. *Transportation research part C: emerging technologies*, 92:525–548, 2018.
- [66] Denos Gazis and Chiu Liu. Kalman filtering estimation of traffic counts for two network links in tandem. *Transportation Research Part B: Methodological*, 37(8):737–745, 2003.
- [67] T Ajitha, L Vanajakshi, and SC Subramanian. Real-time traffic density estimation without reliable side road data. *Journal of Computing in Civil Engineering*, 29(2):04014033, 2013.
- [68] Ameena Padiath, Lelitha Vanajakshi, Shankar C Subramanian, and Harishreddy Manda. Prediction of traffic density for congestion analysis under indian traffic conditions. In *2009 12th International IEEE Conference on Intelligent Transportation Systems*, pages 1–6. IEEE, 2009.
- [69] Nikolaos Bekiaris-Liberis, Claudio Roncoli, and Markos Papageorgiou. Highway traffic state estimation with mixed connected and conventional vehicles. *IEEE Transactions on Intelligent Transportation Systems*, 17(12):3484–3497, 2016.
- [70] Xuan Di, Henry X Liu, and Gary A Davis. Hybrid extended kalman filtering approach for traffic density estimation along signalized arterials: Use of global positioning system data. *Transportation research record*, 2188(1):165–173, 2010.

- [71] Juan C Herrera and Alexandre M Bayen. Traffic flow reconstruction using mobile sensors and loop detector data, 2008.
- [72] Shrikant Fulari, Lelitha Vanajakshi, and Shankar C Subramanian. Artificial neural network-based traffic state estimation using erroneous automated sensor data. *Journal of Transportation Engineering, Part A: Systems*, 143(8):05017003, 2017.
- [73] Constantinos Antoniou and Haris N Koutsopoulos. Estimation of traffic dynamics models with machine-learning methods. *Transportation research record*, 1965(1):103–111, 2006.
- [74] Sakib Mahmud Khan, Kakan C Dey, and Mashrur Chowdhury. Real-time traffic state estimation with connected vehicles. *IEEE Transactions on Intelligent Transportation Systems*, 18(7):1687–1699, 2017.
- [75] Thanés Wassantachatt, Zhidong Li, Jing Chen, Yang Wang, and Evan Tan. Traffic density estimation with on-line svm classifier. In *2009 Sixth IEEE International Conference on Advanced Video and Signal Based Surveillance*, pages 13–18. IEEE, 2009.
- [76] Arash Jahangiri, Hesham A Rakha, and Thomas A Dingus. Adopting machine learning methods to predict red-light running violations. In *2015 IEEE 18th International Conference on Intelligent Transportation Systems*, pages 650–655. IEEE, 2015.
- [77] Przemysław Sekuła, Nikola Marković, Zachary Vander Laan, and Kaveh Farokhi Sadabadi. Estimating historical hourly traffic volumes via machine learning and vehicle probe data: A maryland case study. *Transportation Research Part C: Emerging Technologies*, 97:147–158, 2018.
- [78] Jithin Raj, Hareesh Bahuleyan, and Lelitha Devi Vanajakshi. Application of data mining techniques for traffic density estimation and prediction. *Transportation Research Procedia*, 17:321–330, 2016.

- [79] Mohammad A Aljamal, Hossam M Abdelghaffar, and Hesham A Rakha. Kalman filter-based vehicle count estimation approach using probe data: A multi-lane road case study. In *2019 IEEE Intelligent Transportation Systems Conference (ITSC)*, pages 4374–4379. IEEE, 2019.
- [80] S. Beucher, J. Blosseville, and F. Lenoir. Traffic spatial measurements using video image processing. In *Intelligent Robots and Computer Vision VI*, pages 648–656, 1988.
- [81] M. R. Shahrababaki, A. A. Safavi, M. Papageorgiou, and I. Papamichail. A data fusion approach for real-time traffic state estimation in urban signalized links. *Transportation research part C: emerging technologies*, 92:525–548, 2018.
- [82] Z. Ye, Y. Zhang, and D. Middleton. Unscented kalman filter method for speed estimation using single loop detector data. *Transportation Research Record: Journal of the Transportation Research Board*, pages 117–125, 2006.
- [83] J. Guo, J. Xia, and B. L. Smith. Kalman filter approach to speed estimation using single loop detector measurements under congested conditions. *Journal of Transportation Engineering*, 135:927–934, 2009.
- [84] J. Lee, B. Park, and I. Yun. Cumulative travel-time responsive real-time intersection control algorithm in the connected vehicle environment. *Journal of Transportation Engineering*, 139, 2013.
- [85] L. Chu, S. Oh, and W. Recker. Adaptive kalman filter based freeway travel time estimation. In *84th TRB Annual Meeting, Washington DC*, 2005.
- [86] Samah EI-Tantawy and Baher Abdulhai. An agent-based learning towards decentralized and coordinated traffic signal control. In *Annual Conference on Intelligent Transportation Systems*, Madeira Island, Portugal, September 2010.
- [87] C. Daganzo. *Fundamentals of Transportation and Traffic Operations*. 1997.

- [88] Stan Teply. *Highlights of the Canadian capacity guide for signalized intersections*. TRB, 1985.
- [89] M. Van Aerde and Hesham A. Rakha. Integration release 2.40 for windows: User's guide-volume ii: Advanced model features. Technical report.
- [90] Hossam M Abdelghaffar and Hesham A Rakha. A novel decentralized game-theoretic adaptive traffic signal controller: large-scale testing. *Sensors*, 19(10):2282, 2019.
- [91] S James Press and James S Press. *Bayesian statistics: principles, models, and applications*. Wiley New York, 1989.
- [92] Mei Chen and Steven IJ Chien. Dynamic freeway travel-time prediction with probe vehicle data: Link based versus path based. *Transportation Research Record*, 1768(1):157–161, 2001.
- [93] Kenneth Myers and BD Tapley. Adaptive sequential estimation with unknown noise statistics. *IEEE Transactions on Automatic Control*, 21(4):520–523, 1976.
- [94] Francois Dion, Hesham Rakha, and Youn-Soo Kang. Comparison of delay estimates at under-saturated and over-saturated pre-timed signalized intersections. *Transportation Research Part B: Methodological*, 38(2):99–122, 2004.
- [95] Hesham Rakha, Youn-Soo Kang, and François Dion. Estimating vehicle stops at undersaturated and oversaturated fixed-time signalized intersections. *Transportation Research Record*, 1776(1):128–137, 2001.
- [96] Edward Chamberlayne, Hesham Rakha, and Douglas Bish. Modeling the capacity drop phenomenon at freeway bottlenecks using the integration software. *Transportation Letters*, 4(4):227–242, 2012.
- [97] H Rakha, P Pasumarthy, and S Adjerid. The integration framework for modeling longitudinal vehicle motion. In *TRANSTEC*. 2004.

- [98] Mohammad A Aljamal, Hesham A Rakha, Jianhe Du, and Ihab El-Shawarby. Comparison of microscopic and mesoscopic traffic modeling tools for evacuation analysis. In *2018 21st International Conference on Intelligent Transportation Systems (ITSC)*, pages 2321–2326. IEEE, 2018.
- [99] Hesham Rakha and Yihua Zhang. Integration 2.30 framework for modeling lane-changing behavior in weaving sections. *Transportation Research Record*, 1883(1):140–149, 2004.
- [100] Simon Haykin. *Neural networks: a comprehensive foundation*. Prentice Hall PTR, 1994.
- [101] Sam Roweis. Levenberg-marquardt optimization. *Notes, University Of Toronto*, 1996.
- [102] Ron Kohavi et al. A study of cross-validation and bootstrap for accuracy estimation and model selection. In *Ijcai*, volume 14, pages 1137–1145. Montreal, Canada, 1995.
- [103] Hossam M Abdelghaffar and Hesham A Rakha. Development and testing of a novel game theoretic de-centralized traffic signal controller. *IEEE Transactions on Intelligent Transportation Systems*, 2019.
- [104] Hossam M Abdelghaffar, Hao Yang, and Hesham A Rakha. Developing a de-centralized cycle-free nash bargaining arterial traffic signal controller. In *2017 5th IEEE International Conference on Models and Technologies for Intelligent Transportation Systems (MT-ITS)*, pages 544–549. IEEE, 2017.
- [105] N.Y.C.DOT. Traffic signals. <http://www.nyc.gov/html/dot/html/infrastructure/signals.shtml/>, 2011.
- [106] Karric Kwong, Robert Kavaler, Ram Rajagopal, and Pravin Varaiya. Real-time measurement of link vehicle count and travel time in a road network. *IEEE Transactions on Intelligent Transportation Systems*, 11(4):814–825, 2010.
- [107] Adolf D May. *Traffic flow fundamentals*.

- [108] M Van Aerde and H Rakha. Integration© release 2.30 for windows: Users guide—volume ii: Advanced model features. 2007, m. *Van Aerde & Assoc., Ltd.: Blacksburg*, 41.
- [109] Jianhe Du, Hesham A Rakha, Ahmed Elbery, and Matthew Klenk. Microscopic simulation and calibration of a large-scale metropolitan network: Issues and proposed solutions. Technical report, 2018.
- [110] Ahmed Elbery, Youssef Bichiou, Hesham A Rakha, Jianhe Du, Filip Dvorak, and Matthew Klenk. City-level agent-based multi-modal modeling of transportation networks: Model development and preliminary testing. In *Smart Cities, Green Technologies and Intelligent Transport Systems*, pages 279–303. Springer, 2018.
- [111] Mohammad A Aljamal, Hossam M Abdelghaffar, and Hesham A Rakha. Estimation of traffic stream density using connected vehicle data: Linear and nonlinear filtering approaches. *Sensors*, 20(15):4066, 2020.
- [112] Yiheng Feng, K Larry Head, Shayan Khoshmashgham, and Mehdi Zamanipour. A real-time adaptive signal control in a connected vehicle environment. *Transportation Research Part C: Emerging Technologies*, 55:460–473, 2015.
- [113] Lyudmila Mihaylova, Andreas Hegyi, Amadou Gning, and René K Boel. Parallelized particle and gaussian sum particle filters for large-scale freeway traffic systems. *IEEE Transactions on Intelligent Transportation Systems*, 13(1):36–48, 2012.
- [114] TL Pan, Agachai Sumalee, Ren-Xin Zhong, and Nakorn Indra-Payoong. Short-term traffic state prediction based on temporal–spatial correlation. *IEEE Transactions on Intelligent Transportation Systems*, 14(3):1242–1254, 2013.
- [115] Andreas Hegyi, Daniela Girimonte, Robert Babuska, and Bart De Schutter. A comparison of filter configurations for freeway traffic state estimation. In *2006 IEEE Intelligent Transportation Systems Conference*, pages 1029–1034. IEEE, 2006.

- [116] Hossam M Abdelghaffar, Maha Elouni, Youssef Bichiou, and Hesham A Rakha. Development of a connected vehicle dynamic freeway sliding mode variable speed controller. *IEEE Access*, 2020.
- [117] Alvaro J. Calle-Laguna, Jianhe Du, and Hesham A. Rakha. Computing optimum traffic signal cycle length considering vehicle delay and fuel consumption. *Transportation Research Interdisciplinary Perspectives*, 3:100021, 2019.
- [118] E. S.; McShane W. R. Roess, R.P.; Prassas. *Traffic engineering - Fifth Edition*. Pearson Education: Hoboken, NJ, USA, 2019.
- [119] Tiancheng Li, Tariq Pervez Sattar, and Shudong Sun. Deterministic resampling: unbiased sampling to avoid sample impoverishment in particle filters. *Signal Processing*, 92(7):1637–1645, 2012.
- [120] Peter S Maybeck. The kalman filter: An introduction to concepts. In *Autonomous robot vehicles*, pages 194–204. Springer, 1990.
- [121] Texas AM Transportation Institute. Commuters waste about 54 hours a year in traffic, and it’s not just during rush hour. https://www.nwitimes.com/news/national/commuters-waste-about-hours-a-year-in-traffic-and-it/collection_eac664b9-5300-55bf-bffe-3dbcb68a8483.html, 2019.
- [122] Fei-Yue Wang. Parallel control and management for intelligent transportation systems: Concepts, architectures, and applications. *IEEE Transactions on Intelligent Transportation Systems*, 11(3):630–638, 2010.
- [123] M. Van Aerde and Hesham A. Rakha. Integration release 2.40 for windows: User’s guide-volume i: Fundamental model features. Technical report.
- [124] Hesham A Rakha and Yihua Zhang. The integration 2.30 framework for modeling lane-changing behavior in weaving sections. *Transportation Research Record: Journal of the Transportation Research Board*, 1883(140-149), 2004.

- [125] Hesham A Rakha, Praveen Pasumarthy, and Slimane Adjerid. A simplified behavioral vehicle longitudinal motion model. *Transportation Letters: The International Journal of Transportation Research*, 1(2):95–110, 2009.
- [126] Hesham A Rakha. Validation of van aerdes simplified steady-state car-following and traffic stream model. *Transportation Letters: The International Journal of Transportation Research*, 1(13):227–244, 2009.
- [127] N Wu and Hesham A Rakha. Derivation of van aerde traffic stream model from tandem-queueing theory. *Transportation Research Record: Journal of the Transportation Research Board*, 2124(18-27), 2009.
- [128] Hesham A Rakha, Ivana Lucic, Sergio Demarchi, and Jose Setti. Vehicle dynamics model for predicting maximum truck accelerations. *Journal of Transportation Engineering*, 127(5):418–425, 2001.
- [129] Hesham A Rakha, Matthew Snare, and Francois Dion. Vehicle dynamics model for estimating maximum light duty vehicle acceleration levels. *Transportation Research Record: Journal of the Transportation Research Board*, 1883(40-49), 2004.
- [130] Francois Dion, Hesham A Rakha, and Yoon So Kang. Comparison of delay estimates at under-saturated and over-saturated pre-timed signalized intersections. *Transportation Research, Part B: Methodological*, 38(2):99–122, 2004.
- [131] Hesham A Rakha, Yoon So Kang, and Francois Dion. Estimating vehicle stops at under-saturated and over-saturated fixed-time signalized intersections. *Transportation Research Record*, 1776:128–137, 2001.
- [132] Thomas Cover and Peter Hart. Nearest neighbor pattern classification. *IEEE transactions on information theory*, 13(1):21–27, 1967.
- [133] Leo Breiman. Random forests. *Machine learning*, 45(1):5–32, 2001.